UC Berkeley

UC Berkeley Previously Published Works

Title
Measurement of jet fragmentation in Pb+Pb and pp collisions at sNN=5.02 TeV with the ATLAS detector

Permalink
https://escholarship.org/uc/item/35r1v5rn

Journal
Physical Review C, 98(2)

ISSN
2469-9985

Authors
Aaboud, M
Aad, G
Abbott, B
et al.

Publication Date
2018-08-01

DOI
10.1103/physrevc.98.024908

Copyright Information

Peer reviewed

Measurement of jet fragmentation in Pb+Pb and pp collisions at $\sqrt{s_{\mathrm{NN}}} = 5.02$ TeV with the ATLAS detector

The ATLAS Collaboration

This paper presents a measurement of jet fragmentation functions in 0.49 nb^{-1} of Pb+Pb collisions and 25 pb^{-1} of pp collisions at $\sqrt{s_{\mathrm{NN}}} = 5.02$ TeV collected in 2015 with the ATLAS detector at the LHC. These measurements provide insight into the jet quenching process in the quark–gluon plasma created in the aftermath of ultra-relativistic collisions between two nuclei. The modifications to the jet fragmentation functions are quantified by dividing the measurements in Pb+Pb collisions by baseline measurements in pp collisions. This ratio is studied as a function of the transverse momentum of the jet, the jet rapidity, and the centrality of the collision. In both collision systems, the jet fragmentation functions are measured for jets with transverse momentum between 126 GeV and 398 GeV and with an absolute value of jet rapidity less than 2.1. An enhancement of particles carrying a small fraction of the jet momentum is observed, which increases with centrality and with increasing jet transverse momentum. Yields of particles carrying a very large fraction of the jet momentum are also observed to be enhanced. Between these two enhancements of the fragmentation functions a suppression of particles carrying an intermediate fraction of the jet momentum is observed in Pb+Pb collisions. A small dependence of the modifications on jet rapidity is observed.

arXiv:1805.05424v2 [nucl-ex] 5 Sep 2018

Contents

1 Introduction

Ultra-relativistic nuclear collisions at the Large Hadron Collider (LHC) produce hot dense matter called the quark–gluon plasma (QGP); recent reviews can be found in Refs. [1, 2]. Hard-scattering processes occurring in these collisions produce jets which traverse and interact with the QGP. The study of modifications of jet rates and properties in heavy-ion collisions compared to pp collisions provides information about the properties of the QGP.

The rates of jet production are observed to be reduced by approximately a factor of two in lead–lead (Pb+Pb) collisions at LHC energies compared to expectations from the jet production cross-sections measured in pp interactions scaled by the nuclear overlap function of Pb+Pb collisions [3–5]. Similarly, back-to-back dijet [6–8] and photon–jet pairs [9] are observed to have unbalanced transverse momentum in Pb+Pb collisions compared to pp collisions. Related phenomena were first observed at the Relativistic Heavy Ion Collider where the measurements were made with hadrons rather than reconstructed jets [10–12]. These observations imply that some of the energy of the parton showering process is transferred outside of the jet through its interaction with the QGP. This has been termed "jet quenching".

The distribution of particles within the jet are affected by this mechanism of energy loss. Several related observables sensitive to the properties of the medium can be constructed. Measurements of the jet shape [13] and the fragmentation functions were made in 2.76 TeV Pb+Pb collisions [14–16]. In Ref. [16], jet fragmentation functions are measured as a function of both the charged-particle transverse momentum, p_T, and the charged-particle longitudinal momentum fraction relative to the jet,

$$z \equiv p_T \cos \Delta R \, / \, p_T^{\text{jet}}. \tag{1}$$

The fragmentation functions are defined as:

$$D(z) \equiv \frac{1}{N_{\text{jet}}} \frac{dn_{\text{ch}}}{dz},$$

2

and

$$D(p_\mathrm{T}) \equiv \frac{1}{N_\mathrm{jet}} \frac{dn_\mathrm{ch}}{dp_\mathrm{T}},$$

where $p_\mathrm{T}^\mathrm{jet}$ is the transverse momentum of the jet, n_ch is the number of charged particles in the jet, N_jet is the number of jets under consideration, and $\Delta R = \sqrt{(\Delta\eta)^2 + (\Delta\phi)^2}$ with $\Delta\eta$ and $\Delta\phi$ defined as the differences between the jet axis and the charged-particle direction in pseudorapidity and azimuth,[1] respectively. In order to quantify differences between Pb+Pb and pp collisions at the same collision energy, the ratios of the fragmentation functions are measured:

$$R_{D(z)} \equiv \frac{D(z)_\mathrm{PbPb}}{D(z)_{pp}},$$

and

$$R_{D(p_\mathrm{T})} \equiv \frac{D(p_\mathrm{T})_\mathrm{PbPb}}{D(p_\mathrm{T})_{pp}}.$$

Relative to jets in pp collisions, it was found in Ref. [16] that jets in Pb+Pb collisions have an excess of particles with transverse momentum below 4 GeV and an excess of particles carrying a large fraction of the jet transverse momentum. At intermediate charged-particle p_T, there is a suppression of the charged-particle yield. At the same time, an excess of low-p_T particles is observed for particles in a wide region around the jet cone [17, 18]. These observations may indicate that the energy lost by jets through the jet quenching process is being transferred to soft particles within and around the jet [19, 20]; measurements of these soft particles have the potential to constrain the models describing such processes. A possible explanation for the enhancement of particles carrying a large fraction of the jet momentum is that it is related to the gluon-initiated jets losing more energy than quark-initiated jets. This leads to a higher quark-jet fraction in Pb+Pb collisions than in pp collisions. The change in flavor composition, combined with the different shapes of the quark and gluon fragmentation functions [21] then lead to the observed excess.

Proton–nucleus collisions, which do not generate a large amount of QGP, are used to differentiate between initial- and final-state effects due to the QGP formed in Pb+Pb collisions. Fragmentation functions in p+Pb collisions show no evidence of modification when compared with those in pp collisions [22]. Thus, any modifications observed in Pb+Pb collisions can be attributed to the presence of the QGP rather than to effects arising from the presence of the large nucleus.

The rapidity dependence of jet observables in Pb+Pb collisions is of great interest, in part because at fixed $p_\mathrm{T}^\mathrm{jet}$ the fraction of quark jets increases with increasing $|y^\mathrm{jet}|$ (see, for example, Refs. [21, 23]). This makes the rapidity dependence of jet observables potentially sensitive to the different interactions of quarks and gluons with the QGP. Previous measurements of the rapidity dependence of jet fragmentation functions at $\sqrt{s_\mathrm{NN}} = 2.76$ TeV in Pb+Pb collisions found a rapidity dependence of the fragmentation function modification with limited significance [16].

In this paper, the fragmentation functions and the $R_{D(z)}$ and $R_{D(p_\mathrm{T})}$ ratios are measured in Pb+Pb and pp collisions at 5.02 TeV using 0.49 nb^{-1} of Pb+Pb collisions and 25 pb^{-1} of pp collisions collected in 2015.

---

[1] ATLAS uses a right-handed coordinate system with its origin at the nominal interaction point (IP) in the center of the detector and the z-axis along the beam pipe. The x-axis points from the IP to the center of the LHC ring, and the y-axis points upward. Cylindrical coordinates (r, ϕ) are used in the transverse plane, ϕ being the azimuthal angle around the beam pipe. The pseudorapidity is defined in terms of the polar angle θ as $\eta = -\ln\tan(\theta/2)$. The rapidity is defined as $y = 0.5\ln[(E + p_z)/(E - p_z)]$ where E and p_z are the energy and the component of the momentum along the beam direction.

Jets are measured over a rapidity range of $|y^{\text{jet}}| < 2.1$ using the anti-k_t reconstruction algorithm [24] with radius parameter $R = 0.4$. The measurement is presented in intervals of $p_{\text{T}}^{\text{jet}}$, y^{jet}, and collision centrality. These data extend the previous studies at $\sqrt{s_{\text{NN}}} = 2.76$ TeV in two ways. First, an increase in the peak energy density of the medium is expected. Second, the Pb+Pb integrated luminosity in the current dataset is 3.5 times the integrated luminosity available at 2.76 TeV, and the increase in the collision energy also increases the jet cross-sections. These two factors allow a measurement of the dependence of jet fragmentation functions on the transverse momentum of the jet over a wider range than was previously possible.

2 Experimental setup

The measurements presented in this paper were performed using the ATLAS inner detector, calorimeter, trigger and data acquisition systems [25]. The calorimeter system consists of a sampling liquid argon (LAr) electromagnetic (EM) calorimeter covering $|\eta| < 3.2$, a steel/scintillator sampling hadronic calorimeter covering $|\eta| < 1.7$, LAr hadronic calorimeters covering $1.5 < |\eta| < 3.2$, and two LAr forward calorimeters (FCal) covering $3.1 < |\eta| < 4.9$ [25]. The EM calorimeters are segmented longitudinally in shower depth into three layers with an additional presampler layer. They have segmentation in ϕ and η that varies with layer and pseudorapidity. The hadronic calorimeters have three sampling layers longitudinal in shower depth.

The inner detector measures charged particles within the pseudorapidity interval $|\eta| < 2.5$ using a combination of silicon pixel detectors, silicon microstrip detectors (SCT), and a straw-tube transition radiation tracker (TRT), all immersed in a 2 T axial magnetic field [25]. Each of the three detectors is composed of a barrel and two symmetric endcap sections. The pixel detector is composed of four layers: the "insertable B-layer" [26, 27] and three layers with a pixel size of 50 μm $\times$ 400 μm. The SCT barrel section contains four layers of modules with 80 μm pitch sensors on both sides and each endcap consists of nine layers of double-sided modules with radial strips having a mean pitch of 80 μm. The two sides of each SCT layer in both the barrel and the endcaps have a relative stereo angle of 40 mrad. The TRT contains up to 73 (160) layers of staggered straws interleaved with fibres in the barrel (endcap).

The zero-degree calorimeters (ZDCs) are located symmetrically at $z = \pm140$ m and cover $|\eta| > 8.3$. They are constructed from tungsten absorber plates and Čerenkov light is transmitted via quartz fibers. In Pb+Pb collisions the ZDCs primarily measure "spectator" neutrons, i.e. neutrons that do not interact hadronically when the incident nuclei collide. A ZDC coincidence trigger is implemented by requiring the pulse height from each ZDC to be above a threshold set to accept the single-neutron peak.

A two-level trigger system is used to select the Pb+Pb and pp collisions. The first trigger level (L1) is hardware-based and implemented with custom electronics. The second level is the software-based high-level trigger (HLT) and is used to further reduce the accepted event rate. Minimum-bias Pb+Pb events are recorded using a trigger defined by the logical OR of a L1 total energy trigger and the ZDC coincidence trigger. The total energy trigger required the total transverse energy measured in the calorimeter system to be greater than 50 GeV in Pb+Pb collisions. Jet events are selected by the HLT, after requiring the identification of a jet by the L1 jet trigger in pp collisions or the total energy trigger with a threshold of 50 GeV in Pb+Pb collisions. The L1 jet trigger utilized in pp collisions required a jet with transverse momentum greater than 20 GeV. The HLT jet trigger used a jet reconstruction algorithm similar to that used in the offline analysis (the offline jet reconstruction is discussed in Section 4). It selected events containing jets with transverse energy of at least 75 GeV in Pb+Pb collisions and at least 85 GeV in

pp collisions. In *pp* collisions, the 85 GeV threshold jet trigger sampled the full delivered luminosity. The 75 GeV threshold jet trigger used in Pb+Pb collisions was prescaled[2] in a small part of the Pb+Pb data-taking period; however, the trigger sampled more than 99% of the total integrated luminosity. The measurement is performed in the jet transverse momentum region where the triggers are fully efficient.

3 Data sets and event selection

The Pb+Pb and *pp* data used in this analysis were recorded in 2015. The data samples consist of 25 pb^{-1} of $\sqrt{s}$ = 5.02 TeV *pp* data and 0.49 nb^{-1} of $\sqrt{s_{\mathrm{NN}}}$ = 5.02 TeV Pb+Pb data. In Pb+Pb and *pp* collisions, events are required to have a reconstructed vertex within 150 mm of the nominal interaction point along the beam axis. Only events taken during stable beam conditions and satisfying detector and data-quality requirements, which include the calorimeters and inner tracking detectors being in nominal operation, are considered.

In Pb+Pb collisions, the event centrality reflects the overlap area of the two colliding nuclei and is characterized by $\Sigma E_{\mathrm{T}}^{\mathrm{FCal}}$, the total transverse energy deposited in the FCal [28]. The centrality intervals used in this analysis are defined according to successive percentiles of the $\Sigma E_{\mathrm{T}}^{\mathrm{FCal}}$ distribution obtained from minimum-bias triggered Pb+Pb events ordered from the most central (highest $\Sigma E_{\mathrm{T}}^{\mathrm{FCal}}$) to the most peripheral collisions (lowest $\Sigma E_{\mathrm{T}}^{\mathrm{FCal}}$): 0–10%, 10–20%, 20–30%, 30–40%, 40–60%, 60–80%.

In addition to the jet-triggered sample, a separate Pb+Pb data sample was recorded with the minimum-bias trigger and two total transverse-energy triggers requiring 1.5 TeV and 6.5 TeV to enhance the rate of more central Pb+Pb events. This data sample is used to produce a Pb+Pb Monte Carlo (MC) events with conditions that match those registered while the data were recorded.

The performance of the detector and of the analysis procedure in Pb+Pb collisions is evaluated using 1.8×10^7 5.02 TeV MC events. These were produced from minimum-bias Pb+Pb data events overlaid with hard-scattering dijet *pp* events generated with Powheg+Pythia8 [29, 30] using a set of tuned parameters called the A14 tune [31] and the NNPDF23LO parton distribution function (PDF) set [32]. The detector response was simulated using Geant4 [33, 34] and the simulated hits were combined with those from the data event. A weight is assigned to each MC event such that the event sample obtained from the minimum-bias trigger has the same centrality distribution as the sample collected by the jet trigger. A separate sample of 1.8×10^7 simulated 5.02 TeV Pythia8 *pp* hard-scattering events, generated with the same tune and PDFs as for the Pb+Pb MC sample, is used to evaluate the performance for measuring fragmentation functions in the *pp* data. The contribution from additional collisions in the same bunch crossing is not included in the MC simulation. A sample of Pb+Pb events generated with HIJING version 1.38b [35] is also used to evaluate the performance of the track reconstruction.

4 Jet and track selection

The jet reconstruction, underlying event (UE) determination, and subtraction procedures closely follow those used by ATLAS for jet measurements in *pp* and Pb+Pb collisions at $\sqrt{s_{\mathrm{NN}}}$ = 2.76 TeV [4]. The anti-k_t algorithm is first run in four-momentum recombination mode, on $\Delta\eta \times \Delta\phi = 0.1 \times 0.1$ calorimeter

---

[2] The prescale indicates which fraction of events that passed the trigger selection was selected for recording by the data acquisition system.

towers with the anti-k_t radius parameter $R = 0.2$ and $R = 0.4$. The energies in the towers are obtained by summing the energies of calorimeter cells at the electromagnetic energy scale within the tower boundaries. Then, an iterative procedure is used to estimate the η-dependent UE transverse energy density on an event-by-event basis using the energy measurements in all calorimeter towers in the event while excluding the regions populated by jets. The resulting UE transverse energy density is modulated taking into account the presence of the azimuthal anisotropy of particle production [36]. The modulation includes contributions of the second-, third-, and fourth-order azimuthal anisotropy harmonics. Higher-order harmonics introduce negligible variation of the reconstructed jet energy. The UE transverse energy is subtracted from each calorimeter cell within the towers included in the reconstructed jet, and the four-momentum of the jet is updated accordingly. Then, a jet η- and p_{T}-dependent correction factor to the $p_{\mathrm{T}}^{\mathrm{jet}}$ derived from the simulation samples is applied to correct for the calorimeter energy response [37]. An additional correction based on *in situ* studies of jets recoiling against photons, Z bosons, and jets in other regions of the calorimeter is applied [38, 39]. The same jet reconstruction procedure without the azimuthal modulation of the UE is also applied to pp collisions.

Jets are required to have a rapidity within $|y^{\mathrm{jet}}| < 2.1$ so that all $R = 0.4$ jet cones are contained within the inner detector's acceptance. To prevent neighboring jets from distorting the measurement of the fragmentation functions, jets are rejected if there is another jet with higher $p_{\mathrm{T}}^{\mathrm{jet}}$ anywhere within a distance $\Delta R < 1.0$. A correction is applied to reduce the effects of the broadening of the jet direction measurement for $R = 0.4$ jets due to the UE. The correction uses jets reconstructed with a smaller distance parameter, $R = 0.2$ since their angular resolution evaluated in MC studies is found to be less affected by the UE fluctuations than that of larger-R jets. The jet direction is redefined as that of the closest $R = 0.2$ jet with $p_{\mathrm{T}}^{\mathrm{jet}} > 35$ GeV and matching the original jet direction within $\Delta R = 0.3$ of the $R = 0.4$ jet, when such a matching jet is found. If no matching $R = 0.2$ jet is found the axis remains unchanged.

Charged-particle tracks are reconstructed from hits in the inner detector using the track reconstruction algorithm with settings optimized for the high hit density in heavy-ion collisions [40]. Tracks used in this analysis are required to have a total of at least 9 (11) hits in the silicon pixel and microstrip detectors for charged particles with pseudorapidity $|\eta^{\mathrm{ch}}| \leq 1.65$ ($|\eta^{\mathrm{ch}}| > 1.65$). At least one hit is required in one of the two innermost pixel layers. If the track trajectory passed through an active module in the innermost layer, then a hit in this layer is required. Furthermore, a track must have no more than two holes in the Pixel and SCT detectors together, where a hole is defined by the absence of a hit predicted by the track trajectory. All charged-particle tracks used in this analysis are required to have reconstructed transverse momentum $p_{\mathrm{T}}^{\mathrm{ch}} > 1$ GeV. In order to suppress the contribution from secondary particles, the distance of closest approach of the track to the primary vertex in the transverse plane is required to be less than a value which varies from 0.45 mm at $p_{\mathrm{T}}^{\mathrm{ch}} = 4$ GeV to 0.2 mm at $p_{\mathrm{T}}^{\mathrm{ch}} = 20$ GeV, and at that point the track must be less than 1.0 mm from the primary vertex in the longitudinal direction.

The efficiency, $\varepsilon(p_{\mathrm{T}}^{\mathrm{truth}}, p_{\mathrm{T}}^{\mathrm{jet}}, y^{\mathrm{jet}})$, for reconstructing charged particles within jets in Pb+Pb and pp collisions is evaluated from the matching of reconstructed tracks to generator-level primary particles[3] using MC samples described above. The matching is based on contributions of generator-level particles to the hits in the detector layers. A reconstructed track is matched to a generator-level particle if it contains hits produced primarily by this particle [34]. The efficiency is evaluated separately in four $|y^{\mathrm{jet}}|$ intervals and each interval of reconstructed $p_{\mathrm{T}}^{\mathrm{jet}}$ used in the measurement. Furthermore, the efficiency is evaluated separately for each centrality interval in the case of Pb+Pb collisions. The charged-particle reconstruction efficiencies as a function of the generator-level primary particle transverse momentum, $p_{\mathrm{T}}^{\mathrm{truth}}$, are shown

---

[3] Primary particles are defined as particles with a mean lifetime $\tau > 0.3 \times 10^{-10}$ s either directly produced in pp interactions or from subsequent decays of particles with a shorter lifetime. All other particles are considered to be secondary.
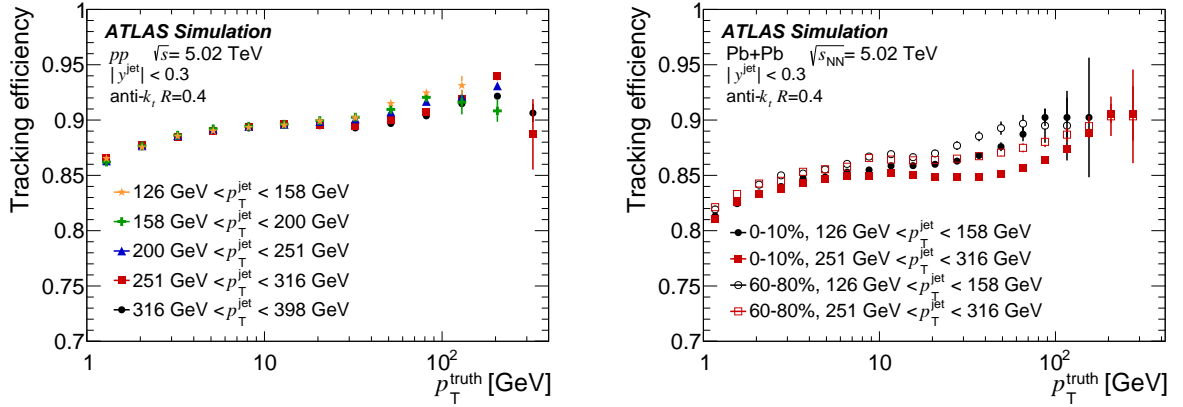
Figure 1: Tracking efficiency, ε, smoothed using a third-order polynomial in $\ln(p_T^{truth})$ as a function of p_T^{truth} in pp collisions in five different jet-p_T intervals (left) and in Pb+Pb collisions (right) in two different jet-p_T intervals and for 0–10% and 60–80% centrality intervals. In both plots the efficiency is evaluated for tracks within jets with $|y^{jet}| < 0.3$.

in Figure 1 for jets with $|y^{jet}| < 0.3$ in pp and Pb+Pb collisions. In order to remove fluctuations in the efficiency due to the limited MC sample size, the p_T^{truth} dependence of the efficiencies is parameterized and smoothed using a third-order polynomial in $\log(p_T^{truth})$ that gives a good description of the efficiency in the full range of p_T^{truth}. The efficiencies shown in Figure 1 exhibit only a modest variation with p_T^{truth}, centrality, and p_T^{jet}. A small almost continuous increase of the efficiency with the increasing p_T^{truth} is observed. The efficiency over the 20–100 GeV p_T^{truth} range is smaller for high p_T^{jet} compared to low p_T^{jet} by about 2% and 5% in pp and Pb+Pb collisions, respectively. This behavior is attributed to the higher probability to lose tracks in the dense core of high-p_T jets than to lose tracks that are more isolated [41]. The efficiency is lower in more central Pb+Pb collisions due to the higher hit density. The efficiency exhibits only a small variation with y^{jet} in the region $|y^{jet}| < 1.2$, and it decreases by approximately 10% in the most forward y^{jet} interval.

The contribution of reconstructed tracks which are not be matched to a generated primary particle in the MC samples of pp collision events produced without data overlay, along with the residual contribution of tracks matched to secondary particles, are together considered "fake" tracks. The fraction of fake tracks is less than 2% over the full kinematic range of this measurement. A possible degradation of the tracking performance at high occupancy is checked in the sample of Pb+Pb collision events simulated with the HIJING MC. No significant dependence of the rate of fake tracks on centrality is observed. The correction for the fake contribution is discussed in Section 5.

5 Analysis procedure

The analysis procedure closely follows the one used in the measurement of jet fragmentation at $\sqrt{s_{NN}} = 2.76$ TeV [16]. Reconstructed tracks are associated with a reconstructed jet if they fall within $\Delta R = 0.4$ of the jet axis and for each of these particles the longitudinal momentum fraction, z, is calculated. The

measured track yields, $dn_{\mathrm{ch}}^{\mathrm{meas}}/dz$ or $dn_{\mathrm{ch}}^{\mathrm{meas}}/dp_{\mathrm{T}}^{\mathrm{ch}}$, are constructed as:

$$\frac{dn_{\mathrm{ch}}^{\mathrm{meas}}}{dz} = \frac{\Delta N_{\mathrm{ch}}(z, y^{\mathrm{jet}}, p_{\mathrm{T}}^{\mathrm{jet}})}{\Delta z}$$

and

$$\frac{dn_{\mathrm{ch}}^{\mathrm{meas}}}{dp_{\mathrm{T}}^{\mathrm{ch}}} = \frac{\Delta N_{\mathrm{ch}}(p_{\mathrm{T}}^{\mathrm{ch}}, y^{\mathrm{jet}}, p_{\mathrm{T}}^{\mathrm{jet}})}{\Delta p_{\mathrm{T}}^{\mathrm{ch}}},$$

where the quantities $\Delta N_{\mathrm{ch}}(z)$ and $\Delta N_{\mathrm{ch}}(p_{\mathrm{T}}^{\mathrm{ch}})$ represent the number of associated tracks within the given z or $p_{\mathrm{T}}^{\mathrm{ch}}$ range, respectively corrected for the track reconstruction efficiency. The efficiency correction is applied as a $1/\varepsilon(p_{\mathrm{T}}^{\mathrm{ch}}, p_{\mathrm{T}}^{\mathrm{jet}}, y^{\mathrm{jet}})$ weight on a track-by-track basis, assuming $p_{\mathrm{T}}^{\mathrm{ch}} = p_{\mathrm{T}}^{\mathrm{truth}}$. While that assumption is not strictly valid, the efficiency varies sufficiently slowly with $p_{\mathrm{T}}^{\mathrm{truth}}$ that the error introduced by this assumption is less than 1%.

Tracks which are not correlated with the jet need to be subtracted from the measured distributions; these tracks come from both fake tracks and the UE. In Pb+Pb collisions, contributions to the fragmentation functions from the charged particles originating from the UE in Pb+Pb collisions are subtracted. This contribution is evaluated as a function of charge particle z or $p_{\mathrm{T}}^{\mathrm{ch}}$, y^{jet}, $p_{\mathrm{T}}^{\mathrm{jet}}$, and the collision centrality. Additionally, the measured track yields in *pp* and Pb+Pb collisions are corrected for the presence of fake tracks.

The UE contribution is determined for each measured jet using a grid of $R = 0.4$ cones spanning the full coverage of the inner detector and following the method introduced in Ref. [14]. The method is applied to events containing jets included in the analysis. The cones have a fixed distance between their centers chosen such that the inner detector acceptance is uniformly covered while avoiding overlaps. Any cone having a charged particle with $p_{\mathrm{T}}^{\mathrm{ch}} > 10$ GeV or overlapping with a reconstructed jet with $p_{\mathrm{T}}^{\mathrm{jet}} > 90$ GeV is assumed to be associated with a hard process and is excluded from the UE estimation to avoid biasing it. The parameters defining the exclusion regions are evaluated in MC studies and are subjected to variations as part of the estimation of systematic uncertainties. The resulting UE charged-particle yields, $dn_{\mathrm{ch}}^{\mathrm{UE}}/dz$ or $dn_{\mathrm{ch}}^{\mathrm{UE}}/dp_{\mathrm{T}}^{\mathrm{ch}}$, are evaluated over $1 < p_{\mathrm{T}}^{\mathrm{ch}} < 10$ GeV according to:

$$\frac{dn_{\mathrm{ch}}^{\mathrm{UE}}}{dz} = \frac{1}{N_{\mathrm{cone}}} \frac{1}{\varepsilon(p_{\mathrm{T}}^{\mathrm{ch}}, \eta^{\mathrm{ch}})} \left. \frac{\Delta N_{\mathrm{ch}}^{\mathrm{cone}}(z, p_{\mathrm{T}}^{\mathrm{jet}}, y^{\mathrm{jet}})}{\Delta z} \right|_{z = p_{\mathrm{T}}^{\mathrm{ch}} \cos \Delta R / p_{\mathrm{T}}^{\mathrm{jet}}},$$

$$\frac{dn_{\mathrm{ch}}^{\mathrm{UE}}}{dp_{\mathrm{T}}^{\mathrm{ch}}} = \frac{1}{N_{\mathrm{cone}}} \frac{1}{\varepsilon(p_{\mathrm{T}}^{\mathrm{ch}}, \eta^{\mathrm{ch}})} \frac{\Delta N_{\mathrm{ch}}^{\mathrm{cone}}(p_{\mathrm{T}}^{\mathrm{ch}}, p_{\mathrm{T}}^{\mathrm{jet}}, y^{\mathrm{jet}})}{\Delta p_{\mathrm{T}}^{\mathrm{ch}}}.$$

Here N_{cone} is the number of background cones used in the UE determination of a given jet, $\Delta N_{\mathrm{ch}}^{\mathrm{cone}}$ represents the number of charged particles summed over all background cones, and ΔR represents the distance between the center of a cone and the direction of a given charged particle. The term $\varepsilon(p_{\mathrm{T}}^{\mathrm{ch}}, \eta^{\mathrm{ch}})$ is the efficiency for reconstructing charged particles, estimated as a function of $p_{\mathrm{T}}^{\mathrm{ch}}$ and η^{ch} without requiring track-to-jet matching.

The estimated contribution from the UE in each cone is corrected for the difference in the average yield of UE charged particles at a given $p_{\mathrm{T}}^{\mathrm{ch}}$ between the η position of the cone and η position of the jet. This correction is based on the centrality-, $p_{\mathrm{T}}^{\mathrm{ch}}$-, and η-dependent distribution of charged-particle yields in minimum-bias data events. An additional correction is applied to the charged-particle UE estimate to

account for the difference in the azimuthal particle density, due to elliptic flow, between the ϕ angle of the cone and the ϕ angle of the jet. This utilizes a centrality- and p_T^{ch}-dependent parameterization of the measured elliptic flow coefficients [36].

The UE contribution is further corrected for the correlation between the actual UE charged particle yield underneath the jet and the jet energy resolution [14]; in regions where the UE has an upward fluctuation, the jet energy resolution is worse. The smearing due to jet energy resolution leads to a net migration of jets from lower p_T^{jet} to higher p_T^{jet} values. The effect of the migration causes the actual UE contribution underneath the jet to be larger than that estimated from the procedure described above. This effect is corrected for by applying multiplicative correction factors, depending on p_T^{ch} or z, y^{jet}, p_T^{jet}, and collision centrality. The correction is estimated as a ratio of the UE charged particle yield evaluated by two different methods using the Pb+Pb MC samples. The first estimate uses the cone method discussed above. The second method calculates the UE contribution in the data overlay MC samples from tracks, within the area of a jet, that do not have an associated generated primary particle. The size of the correction is less than 2% at low z or p_T^{ch} where the UE has the largest impact, and has only a small dependence on p_T^{jet}.

The contribution from fake tracks to the fragmentation functions is estimated from the MC samples without minimum-bias interactions overlaid. The fraction of these tracks is found to be below 2% of the tracks that pass the selection in all track and jet kinematic regions in this analysis.

The UE distributions corrected for the additive contribution of fake tracks, $d\tilde{n}_{\text{ch}}^{\text{UE+fake}}/dp_T^{\text{ch}}$ and $d\tilde{n}_{\text{ch}}^{\text{UE+fake}}/dz$, are then subtracted from the measured distributions, and the subtracted charged-particle yields and fragmentation functions are evaluated:

$$
\frac{dn_{\text{ch}}^{\text{sub}}}{dz} = \frac{dn_{\text{ch}}^{\text{meas}}}{dz} - \frac{d\tilde{n}_{\text{ch}}^{\text{UE+fake}}}{dz},
$$

$$
D^{\text{sub}}(z) = \frac{1}{N_{\text{jet}}^{\text{meas}}} \frac{dn_{\text{ch}}^{\text{sub}}}{dz},
$$

and

$$
\frac{dn_{\text{ch}}^{\text{sub}}}{dp_T^{\text{ch}}} = \frac{dn_{\text{ch}}^{\text{meas}}}{dp_T^{\text{ch}}} - \frac{d\tilde{n}_{\text{ch}}^{\text{UE+fake}}}{dp_T^{\text{ch}}},
$$

$$
D^{\text{sub}}(p_T^{\text{ch}}) = \frac{1}{N_{\text{jet}}^{\text{meas}}} \frac{dn_{\text{ch}}^{\text{sub}}}{dp_T^{\text{ch}}},
$$

where $N_{\text{jet}}^{\text{meas}}$ is the total number of measured jets in a given p_T^{jet} interval. The signal-to-background ratio, $n_{\text{ch}}^{\text{sub}}/n_{\text{ch}}^{\text{UE}}$, strongly depends on the collision centrality and p_T^{ch}. Figure 2 shows the distributions prior to the UE and fake-track subtraction, $\dfrac{dn_{\text{ch}}^{\text{meas}}}{dp_T^{\text{ch}}}$, divided by the distributions after the subtraction, $\dfrac{dn_{\text{ch}}^{\text{sub}}}{dp_T^{\text{ch}}}$, as a function of p_T^{ch} for three centrality selections. In 0–10% central collisions, the distributions prior to subtraction are over ten times larger than the subtracted distributions for the most extreme case of 1 GeV charged particles. This ratio is reduced to approximately 2 in peripheral collisions at the same charged-particle p_T. The fake-track contribution to the fragmentation functions is subtracted from the measured fragmentation functions in both the pp and Pb+Pb collisions; the UE subtraction is performed
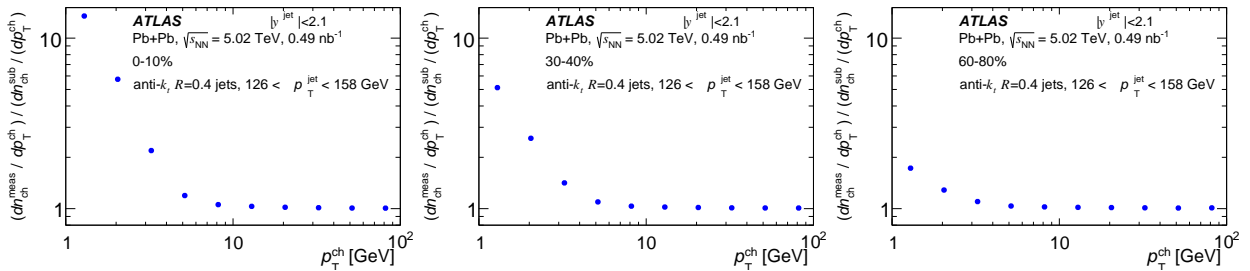
Figure 2: Ratio of the measured charged-particle distributions before and after the subtraction of the UE and fake tracks as a function of $p_{\mathrm{T}}^{\mathrm{ch}}$ for $p_{\mathrm{T}}^{\mathrm{jet}}$ in the range 126–158 GeV for 0–10% (left), 30-40% (middle), and 60–80% (right) centrality. The uncertainties are smaller than the marker size in all cases for which there is a significant UE.

only for the Pb+Pb measurement as the UE contribution is negligible in the pp collisions (less than 2% over the entire kinematic range measured).

To remove the effects of bin migration due to the jet energy and track momentum resolution, the subtracted $dn_{\mathrm{ch}}^{\mathrm{sub}}/dz$ and $dn_{\mathrm{ch}}^{\mathrm{sub}}/dp_{\mathrm{T}}^{\mathrm{ch}}$ distributions are corrected by using a two-dimensional Bayesian unfolding procedure [42] in z or p_{T} and $p_{\mathrm{T}}^{\mathrm{jet}}$ as implemented in the RooUnfold package [43]. Two-dimensional unfolding is used because the calorimetric jet energy response depends on the fragmentation pattern of the jet [44]. Using MC samples, four-dimensional response matrices are created using the generator-level and reconstructed $p_{\mathrm{T}}^{\mathrm{jet}}$, and the generator-level and reconstructed charged-particle z or p_{T}. Separate unfolding matrices are constructed for pp data and each centrality interval in Pb+Pb collisions. A separate one-dimensional Bayesian unfolding is used to correct the measured $p_{\mathrm{T}}^{\mathrm{jet}}$ spectra which are used to normalize the unfolded unnormalized fragmentation functions, $dn_{\mathrm{ch}}^{\mathrm{unfolded}}/dp_{\mathrm{T}}$ and $dn_{\mathrm{ch}}^{\mathrm{unfolded}}/dz$. To achieve better agreement with the data, the MC jet spectra and fragmentation functions are reweighted to match the shapes in the reconstructed data. The Bayesian procedure requires a choice in the number of iterations. Additional iterations reduce the sensitivity to the choice of prior, but may amplify statistical fluctuations in the distributions. After four iterations for both the one-dimensional and two-dimensional unfoldings the fragmentation functions are stable for both the Pb+Pb and pp data. The final, particle-level corrected distributions are defined as:

$$D(z) \;=\; \frac{1}{N_{\mathrm{jet}}^{\mathrm{unfolded}}} \frac{dn_{\mathrm{ch}}^{\mathrm{unfolded}}}{dz},$$

$$D(p_{\mathrm{T}}) \;=\; \frac{1}{N_{\mathrm{jet}}^{\mathrm{unfolded}}} \frac{dn_{\mathrm{ch}}^{\mathrm{unfolded}}}{dp_{\mathrm{T}}},$$

where $N_{\mathrm{jet}}^{\mathrm{unfolded}}$ is the unfolded number of jets in a given $p_{\mathrm{T}}^{\mathrm{jet}}$ interval.

The performance of the analysis procedure is tested by dividing the MC events in half and using one half to generate response matrices with which the other half is unfolded and the ratio of unfolded to generator-level fragmentation functions[4] is evaluated. This procedure tests all the analysis corrections and the unfolding procedure. Good recovery of the generator-level (truth) MC distributions is observed for the unfolded events. The deviations from the exact recovery of the generator-level MC distributions, the non-closure, are included in the systematic uncertainties. The ratios of $D^{\mathrm{sub}}(z)$ and $D^{\mathrm{sub}}(p_{\mathrm{T}}^{\mathrm{ch}})$ distributions

---

[4] The generator-level fragmentation functions are constructed using generator-level jets and primary charged particles.
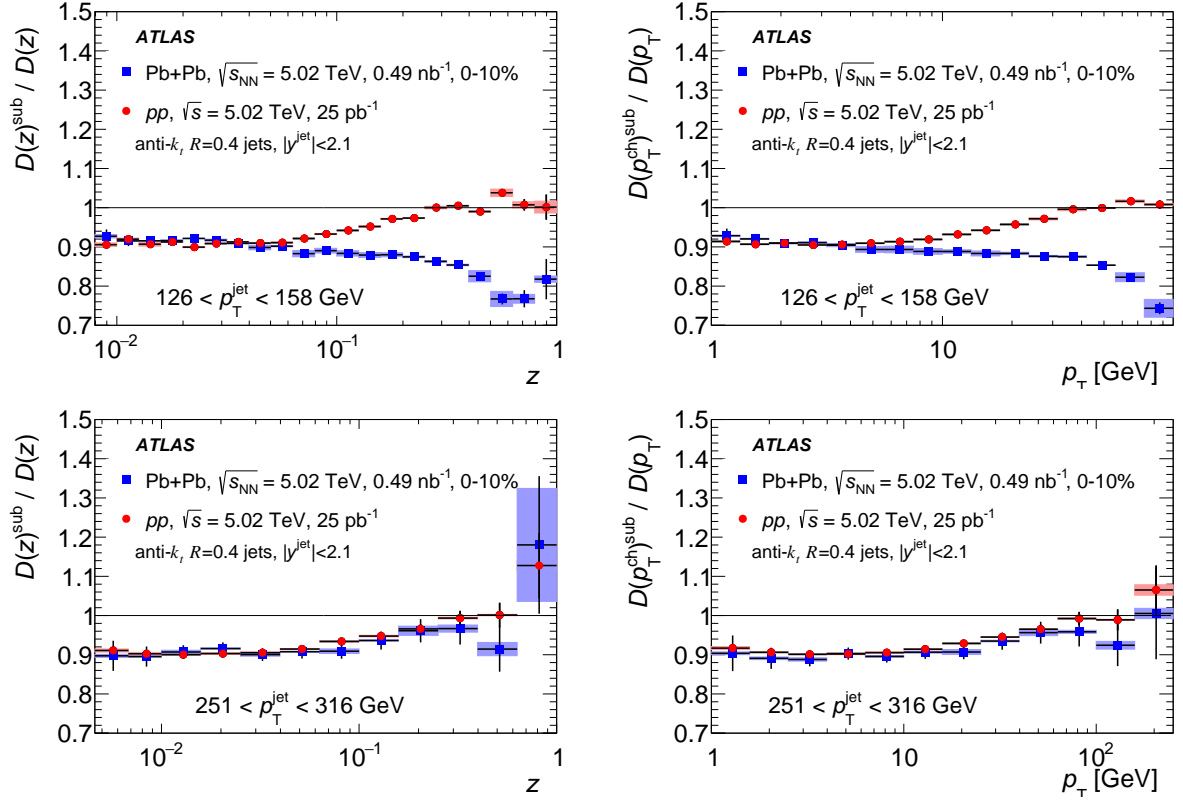
Figure 3: Ratios $D^{\mathrm{sub}}(z)/D(z)$ (left) and $D^{\mathrm{sub}}(p_{\mathrm{T}}^{\mathrm{ch}})/D(p_{\mathrm{T}})$ (right) for pp and 0–10% central Pb+Pb collisions for $126 < p_{\mathrm{T}}^{\mathrm{jet}} < 158$ GeV (top) and $251 < p_{\mathrm{T}}^{\mathrm{jet}} < 316$ GeV (bottom) for $|y^{\mathrm{jet}}| < 2.1$. The error bars show the statistical uncertainties and the boxes show the systematic uncertainties in the unfolding procedure.

to the unfolded $D(z)$ and $D(p_{\mathrm{T}})$ distributions are shown in Figure 3 for pp collisions and 0–10% central Pb+Pb collisions. The magnitude of the unfolding effect varies as a function of $p_{\mathrm{T}}^{\mathrm{jet}}$, $p_{\mathrm{T}}^{\mathrm{ch}}$, and centrality. The effect of the unfolding is similar in pp and Pb+Pb collisions at low z and p_{T}, but for higher-momentum particles within the jet, the effect of the unfolding in pp and Pb+Pb collisions differs by up to 25% between the two collision systems for $126 < p_{\mathrm{T}}^{\mathrm{jet}} < 158$ GeV. This difference is due to UE fluctuations, which lead to poorer jet energy resolution in Pb+Pb collisions than in pp collisions. With increasing $p_{\mathrm{T}}^{\mathrm{jet}}$, the effect of UE fluctuations decreases; for $251 < p_{\mathrm{T}}^{\mathrm{jet}} < 316$ GeV the effect of the unfolding is similar in Pb+Pb and pp collisions at all value of z and p_{T}. The effect of the unfolding is larger at high z and p_{T} due to the steepness of the fragmentation function near $z = 1$. The shaded boxes in Figure 3 show the size of systematic uncertainties associated with the unfolding which originate from the sensitivity of the unfolding to the shape of input MC distributions, as described in the next section.

6 Systematic uncertainties

The following sources of systematic uncertainty are considered: the jet energy scale (JES), the jet energy resolution (JER), the sensitivity of the unfolding to the prior, the residual non-closure of the analysis

procedure, UE contribution, and tracking-related uncertainties. For each variation accounting for a source of systematic uncertainty, the fragmentation functions and ratios of $D(z)$ and $D(p_T)$ distributions in Pb+Pb and pp collisions are re-evaluated. The difference between the varied and nominal distributions is used as an estimate of the resulting uncertainty.

The systematic uncertainty due to the JES in Pb+Pb collisions is composed of two parts: a centrality-independent baseline component and a centrality-dependent component. Only the centrality-independent baseline component is used in pp collisions; it is determined from *in situ* studies of the calorimeter response [37, 45, 46], and studies of the relative energy scale difference between the jet reconstruction procedure in heavy-ion collisions [45] and the procedure in pp collisions [37]. The centrality-dependent uncertainty reflects a modification of parton showers by the Pb+Pb environment. It is evaluated by comparing calorimeter p_T^{jet} and the sum of p_T of tracks within the jet in data and MC simulation. The size of the centrality-dependent uncertainty in the JES reaches 0.5% in the most central collisions. Each component that contributes to the JES uncertainty is varied separately by ±1 standard deviation for each interval in p_T^{jet}, and the response matrix is recomputed accordingly. The data are unfolded with these matrices. The resulting uncertainty on the fragmentation functions increases with increasing z and particle p_T at fixed p_T^{jet} and decreases with increasing p_T^{jet}.

The uncertainty in the fragmentation functions due to the JER is evaluated by repeating the unfolding procedure with modified response matrices, where an additional contribution is added to the resolution of the reconstructed p_T^{jet} using a Gaussian smearing procedure. The smearing factor is evaluated using an *in situ* technique in 13 TeV pp data involving studies of dijet energy balance [47, 48]. An additional uncertainty is included to account for differences between the heavy-ion-style jet reconstruction and that used in analyses of 13 TeV pp data. The size of the resulting uncertainty on the fragmentation functions due to the JER typically reaches 10% for the highest charged-particle z and p_T bins and decreases with decreasing charged-particle z and p_T at fixed p_T^{jet}. The positive and negative uncertainties from the JER are symmetrized.

The unfolding uncertainty is estimated by generating the response matrices from the MC distributions without reweighting in p_T^{jet}, $D(z)$, and $D(p_T)$. An additional uncertainty is assigned for the non-closure of the unfolded distributions in simulations, as described in Section 5. The magnitude of the uncertainty due to the unfolding and the non-closure is typically below 2% and 5%, respectively.

The systematic uncertainty associated with the estimation of the UE contribution on the fragmentation functions has two components. First, the parameter that excludes random cones from the estimate is varied. Random cones are assumed to be associated with a hard process and excluded if the centroid of the cone is $\Delta R < 0.8$ from a reconstructed jet with $p_T > 90$ GeV. The exclusion requirement is changed to $\Delta R < 1.2$ to estimate the sensitivity of the UE contributions. The size of the resulting uncertainty on the fragmentation function is everywhere smaller than 3% and it decreases in higher charged-particle z or p_T. The second component of the UE uncertainty arises from a difference when the UE from the cone method is compared with an alternative UE estimation. The UE is alternatively evaluated using an efficiency-corrected differential yield of charged particles $d^4 n_{ch}/d\eta^{ch} d\phi^{ch} dp_T^{ch} d\Delta\Psi$, where $\Delta\Psi$ is the difference in azimuth of the charged particle from the second-order event plane, evaluated in minimum-bias Pb+Pb events. To each event considered, a weight is assigned such that the event sample obtained from the minimum-bias trigger has the same centrality distribution as the sample collected by the jet trigger. The resulting uncertainty on the fragmentation functions is smaller than 10% at low z or p_T and it rapidly decreases in higher charged-particle z or p_T bins.
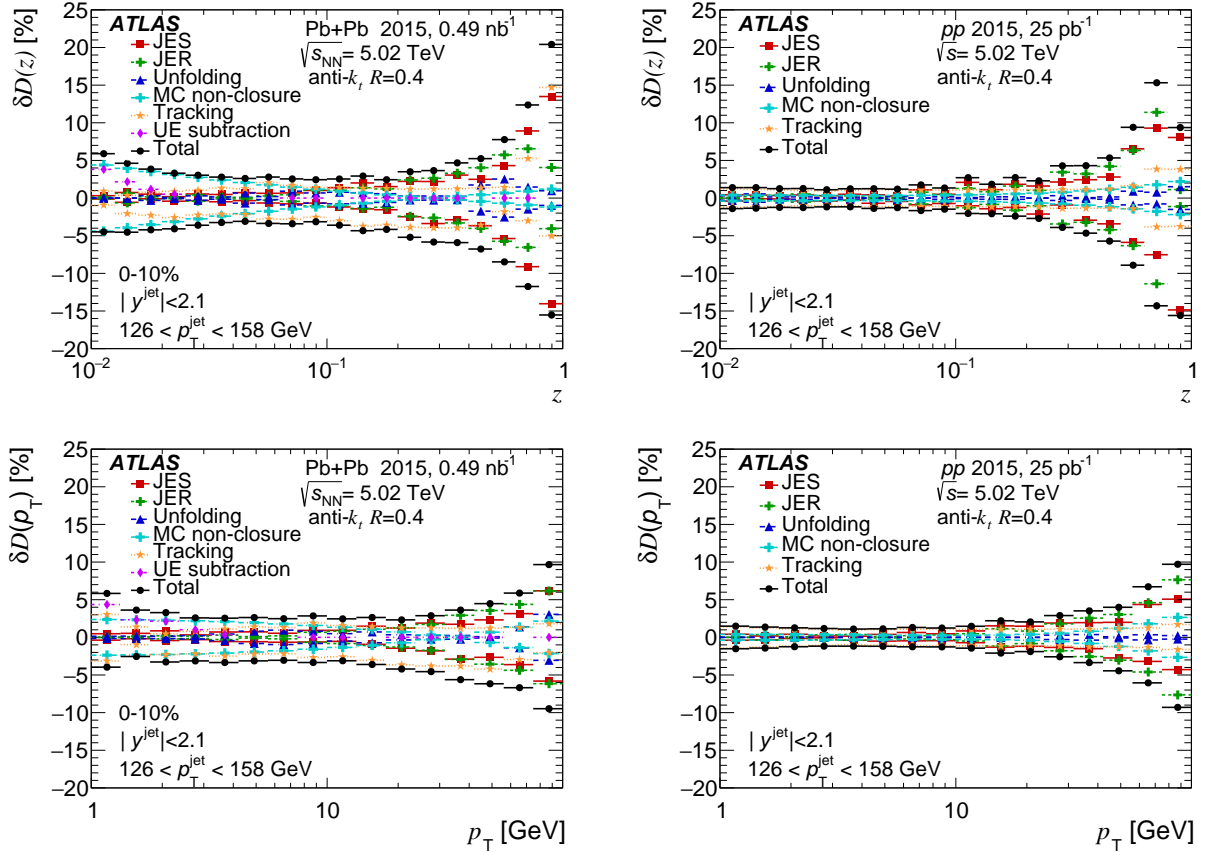
Figure 4: Summary of the systematic uncertainties of the $D(z)$ (top) and $D(p_T)$ (bottom) distributions in 0–10% central Pb+Pb collisions (left) and pp collisions (right) for jets in the 126–158 GeV p_T^{jet} interval. The systematic uncertainties due to JES, JER, unfolding, UE contribution, MC non-closure and tracking are shown along with the total systematic uncertainty from all sources.

The uncertainties related to the track reconstruction and selection originate from several sources. Uncertainties related to the fake rate, the material description in simulation, and the track transverse momentum are obtained from studies in data and simulation described in Ref. [49]. The systematic uncertainty on the fake-track rate is 30% in both collision systems [49]. The contamination of fake tracks is less than 2%, and the resulting uncertainty on the fragmentation functions is at most 0.5%. The sensitivity of the tracking efficiency to the description of the inactive material in the MC samples is evaluated by varying the material description. This resulting uncertainty in the track reconstruction efficiency is between 0.5% and 2% over the track p_T range used in the analysis. An additional uncertainty takes into account a possible residual misalignment of the tracking detectors in pp and Pb+Pb data-taking. The alignment in these data sets is checked *in situ* using $Z \rightarrow \mu^+\mu^-$ events, and a track-p_T dependent uncertainty arises from the finite size of this sample. The resulting uncertainties on the fragmentation functions are typically smaller than 1%, except at large z, where they are as large as 4%. An additional uncertainty on the tracking efficiency due to the high local track density in the core of jets is 0.4% [41] for all p_T^{jet} ranges in this analysis. The uncertainty due to the track selection is evaluated by repeating the analysis with an additional requirement on the significance of the distance of closest approach of the track to the primary vertex. This uncertainty affects the track reconstruction efficiencies, track momentum resolution, and
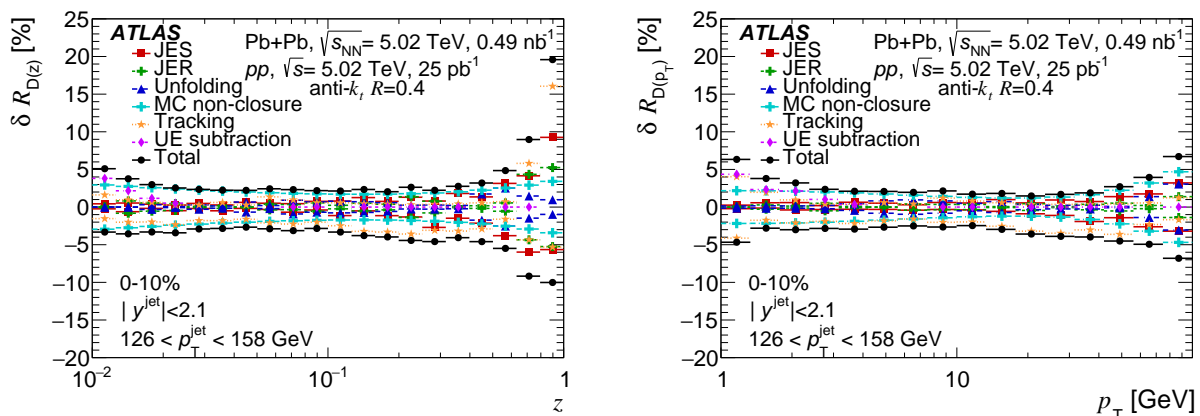
Figure 5: Summary of the systematic uncertainties for 0–10% central $R_{D(z)}$ (left) and $R_{D(p_{\mathrm{T}})}$ (right) ratios, for jets in the 126–158 GeV $p_{\mathrm{T}}^{\mathrm{jet}}$ interval. The systematic uncertainties due to JES, JER, unfolding, UE contribution, MC non-closure and tracking are shown along with the total systematic uncertainty from all sources.

rate of fake tracks. The resulting uncertainty typically varies from 1% at low track p_{T} to 5% at high track p_{T}. Finally, the track-to-particle matching requirements are varied. This variation affects the track reconstruction efficiency, track momentum resolution, and rate of fake tracks. The resulting systematic uncertainty in the fragmentation functions is less than 0.5%.

Example systematic uncertainties on the $D(z)$ and $D(p_{\mathrm{T}})$ distributions for jets in the 126–158 GeV $p_{\mathrm{T}}^{\mathrm{jet}}$ range measured in the two collision systems are presented in Figure 4. All track-related systematic uncertainties are added in quadrature and presented as a total tracking uncertainty. The systematic uncertainties from each source are assumed to be uncorrelated, so they are combined in quadrature to obtain the total systematic uncertainty.

The correlations between the various systematic components are considered in evaluating the ratios of Pb+Pb to pp fragmentation functions. The unfolding and the MC non-closure are each taken to be uncorrelated between the two collision systems. All other uncertainties are taken to be correlated. For the correlated uncertainties, the ratios are re-evaluated by applying the variation to both collision systems; the resulting variations of the ratios from their central values are used as the correlated systematic uncertainty. The uncorrelated uncertainties are added in quadrature. Each systematic uncertainty is assumed to be fully correlated with itself between different rapidity bins. The systematic uncertainty from each source, except the non-closure of the unfolded distributions and the residual misalignment of the tracking detectors, is bin-to-bin correlated. The total systematic uncertainties of the $R_{D(z)}$ and $R_{D(p_{\mathrm{T}})}$ distributions are shown in Figure 5 for one selected $p_{\mathrm{T}}^{\mathrm{jet}}$ range.

7 Results

In this section, results are presented of the measurement of the $D(z)$ and $D(p_{\mathrm{T}})$ distributions for jet p_{T} between 126 and 398 GeV and six centrality intervals in Pb+Pb collisions; the same distributions are presented in pp collisions for the same $p_{\mathrm{T}}^{\mathrm{jet}}$ ranges. In order to study the effects of hot dense matter on the jet fragmentation process, ratios of Pb+Pb fragmentation functions to pp fragmentation functions are evaluated.

The $D(z)$ and $D(p_\text{T})$ distributions in pp collisions are shown in Figure 6. The corresponding distributions in Pb+Pb collisions are shown in Figures 7 through 11.
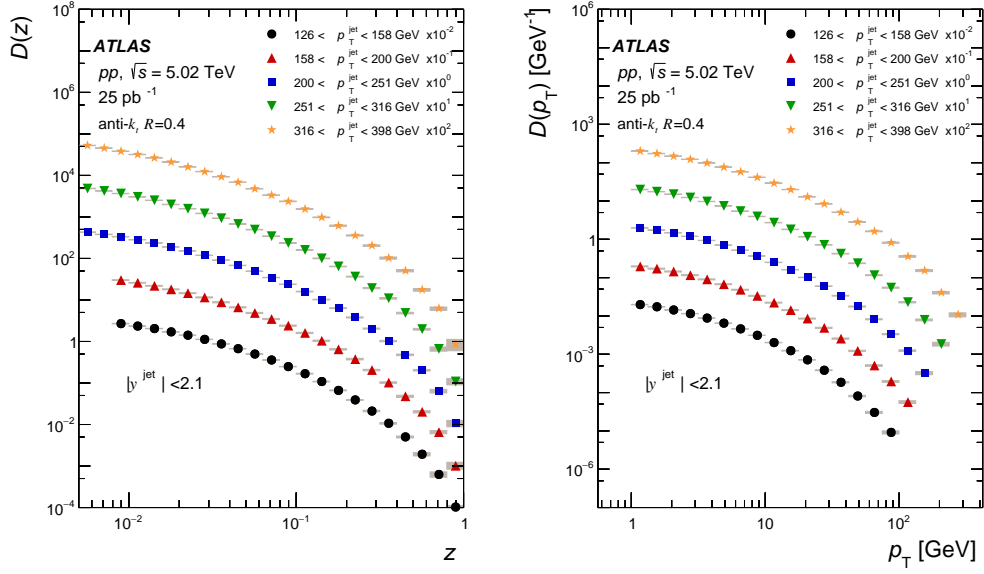
Figure 6: Fragmentation functions, $D(z)$ (left) and $D(p_T)$ (right), in pp collisions measured in five p_T^{jet} ranges from 126 to 398 GeV. The vertical bars on the data points indicate statistical uncertainties, while the shaded bands indicate systematic uncertainties. In most cases, the statistical uncertainties are smaller than the marker size.
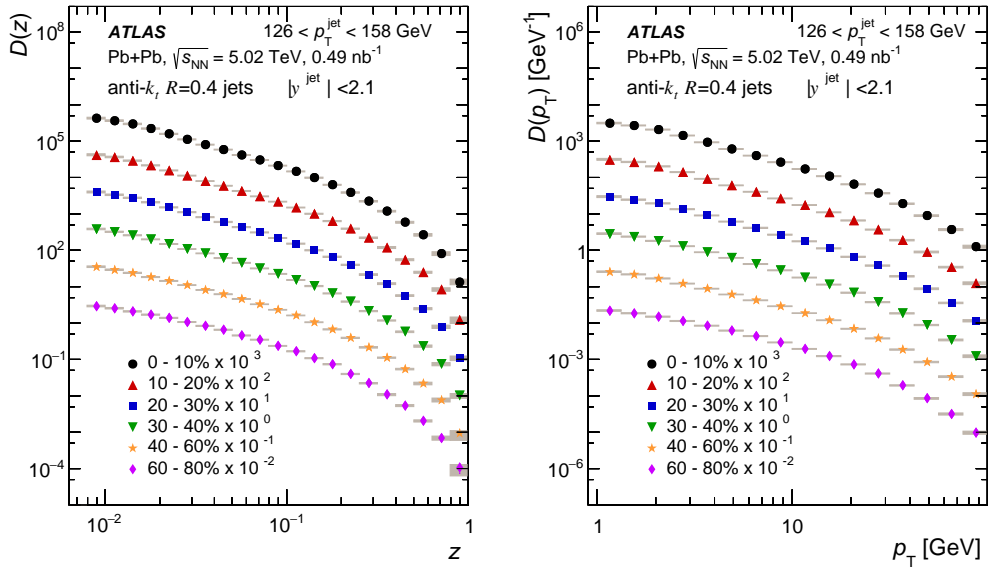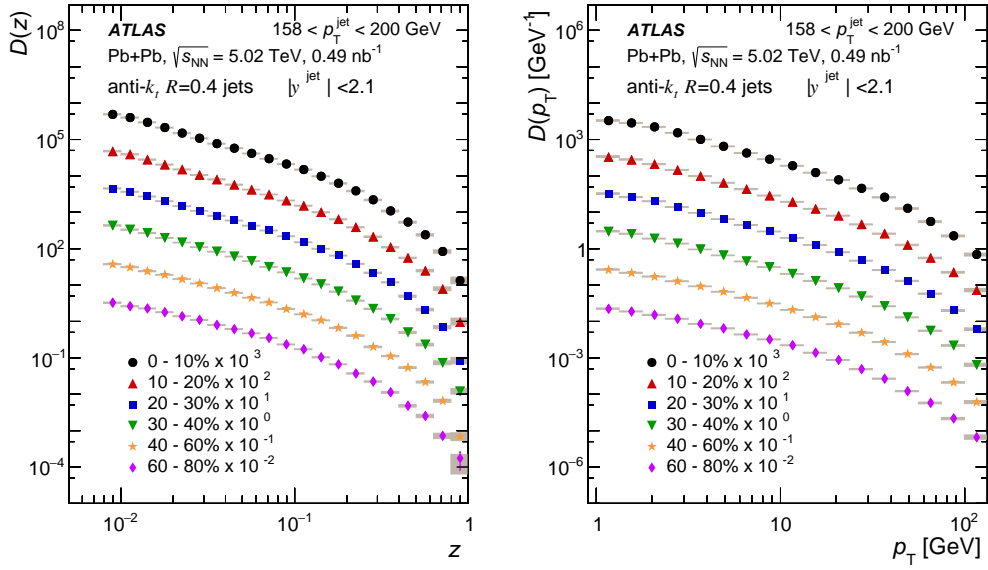

Figure 7: Fragmentation functions, $D(z)$ (left) and $D(p_T)$ (right), in Pb+Pb collisions measured in six different centrality classes for p_T^{jet} of 126 to 158 GeV. The vertical bars on the data points indicate statistical uncertainties, while the shaded bands indicate systematic uncertainties. In most cases, the statistical uncertainties are smaller than the marker size.

Figure 8: Fragmentation functions, $D(z)$ (left) and $D(p_T)$ (right), in Pb+Pb collisions measured in six different centrality classes for p_T^{jet} of 158 to 200 GeV. The vertical bars on the data points indicate statistical uncertainties, while the shaded bands indicate systematic uncertainties. In most cases, the statistical uncertainties are smaller than the marker size.
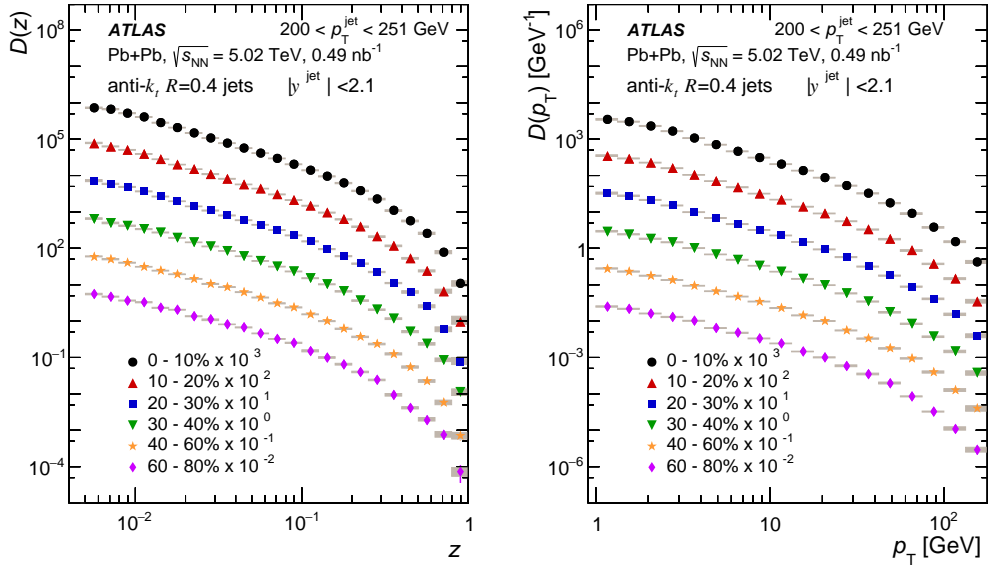

Figure 9: Fragmentation functions, $D(z)$ (left) and $D(p_T)$ (right), in Pb+Pb collisions measured in six different centrality classes for p_T^{jet} of 200 to 251 GeV. The vertical bars on the data points indicate statistical uncertainties, while the shaded bands indicate systematic uncertainties. In most cases, the statistical uncertainties are smaller than the marker size.
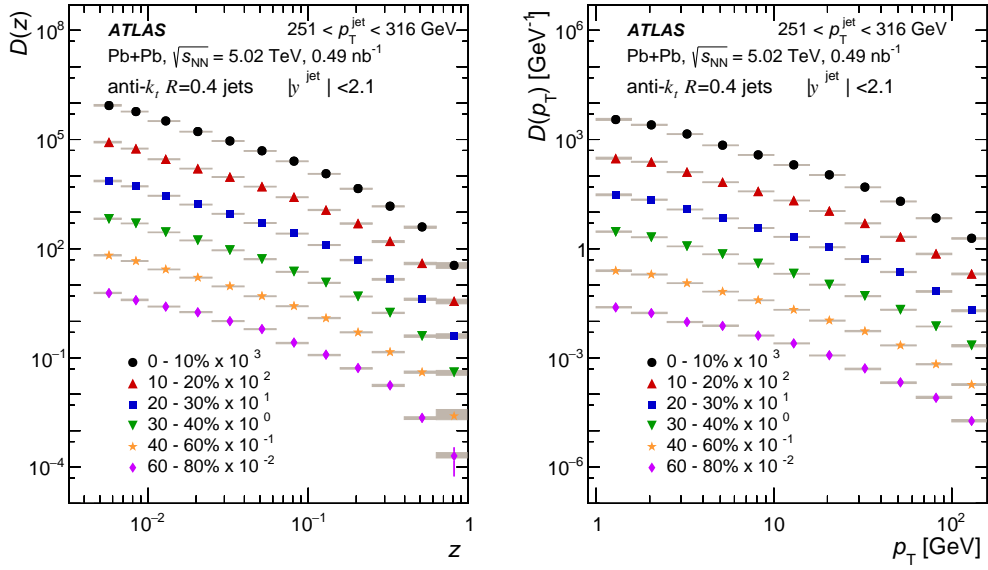
Figure 10: Fragmentation functions, $D(z)$ (left) and $D(p_T)$ (right), in Pb+Pb collisions measured in six different centrality classes for p_T^{jet} of 251 to 316 GeV. The vertical bars on the data points indicate statistical uncertainties, while the shaded bands indicate systematic uncertainties. In most cases, the statistical uncertainties are smaller than the marker size.
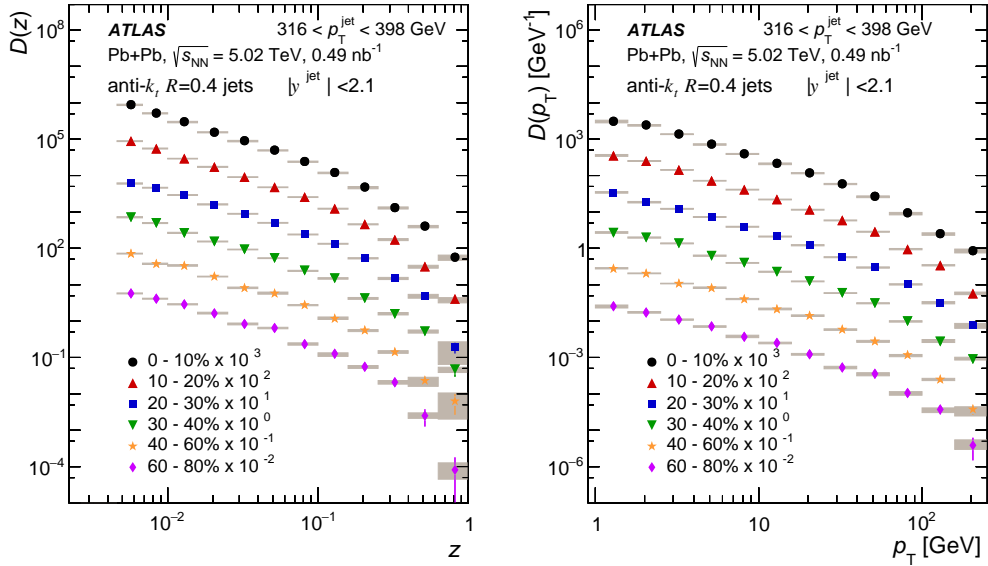

Figure 11: Fragmentation functions, $D(z)$ (left) and $D(p_T)$ (right), in Pb+Pb collisions measured in six different centrality classes for p_T^{jet} of 316 to 398 GeV. The vertical bars on the data points indicate statistical uncertainties, while the shaded bands indicate systematic uncertainties. In most cases, the statistical uncertainties are smaller than the marker size.

In order to quantify the difference in the fragmentation functions between Pb+Pb and pp collisions, the ratios of $D(z)$ and $D(p_T)$ distributions measured in Pb+Pb collisions to those measured in pp collisions, $R_{D(z)}$ and $R_{D(p_T)}$, are shown in Figures 12 and 13, respectively. In each figure, the shaded boxes indicate systematic uncertainties and the vertical bars show the statistical uncertainties.

The shapes of the $R_{D(z)}$ and $R_{D(p_T)}$ distributions are similar for all centralities: inside the jets; the yields of particles with low p_T or z are enhanced; there is a reduction for particles with intermediate p_T or z; and the yields of particles with high p_T or z are enhanced. This is qualitatively consistent with previous measurements of jet fragmentation at $\sqrt{s_{NN}} = 2.76$ TeV [14–16]; a quantitative comparison is provided in Section 8. The magnitudes of the deviations of the ratios from unity decrease with decreasing collision centrality. In the most central collisions, the size of the enhancement is as large as 70% at low p_T or z and 30% at high p_T or z. The depletion of charged-particle yields at intermediate p_T and z is as large as 20%. In some centrality and p_T^{jet} ranges there is a decrease of the fragmentation functions at the highest z values. In this region the statistical and systematic uncertainties are the largest; more precise measurements are needed to determine if a significant decrease exists.

Figures 14 and 15 show the $R_{D(z)}$ distributions for jets in the most central and most forward rapidity intervals, 0.0–0.3 and 1.2–2.1, respectively, for the six centrality intervals used in this analysis and for four p_T^{jet} intervals: 126–158 GeV, 158–200 GeV, 200–251 GeV, and 251–316 GeV. Figures 16 and 17 show $R_{D(p_T)}$ distributions for the same jet rapidity, centrality, and p_T^{jet} ranges. In all rapidity ranges, the $R_{D(z)}$ and $R_{D(p_T)}$ distributions have the same qualitative shape and centrality dependence as the rapidity-inclusive results presented above.
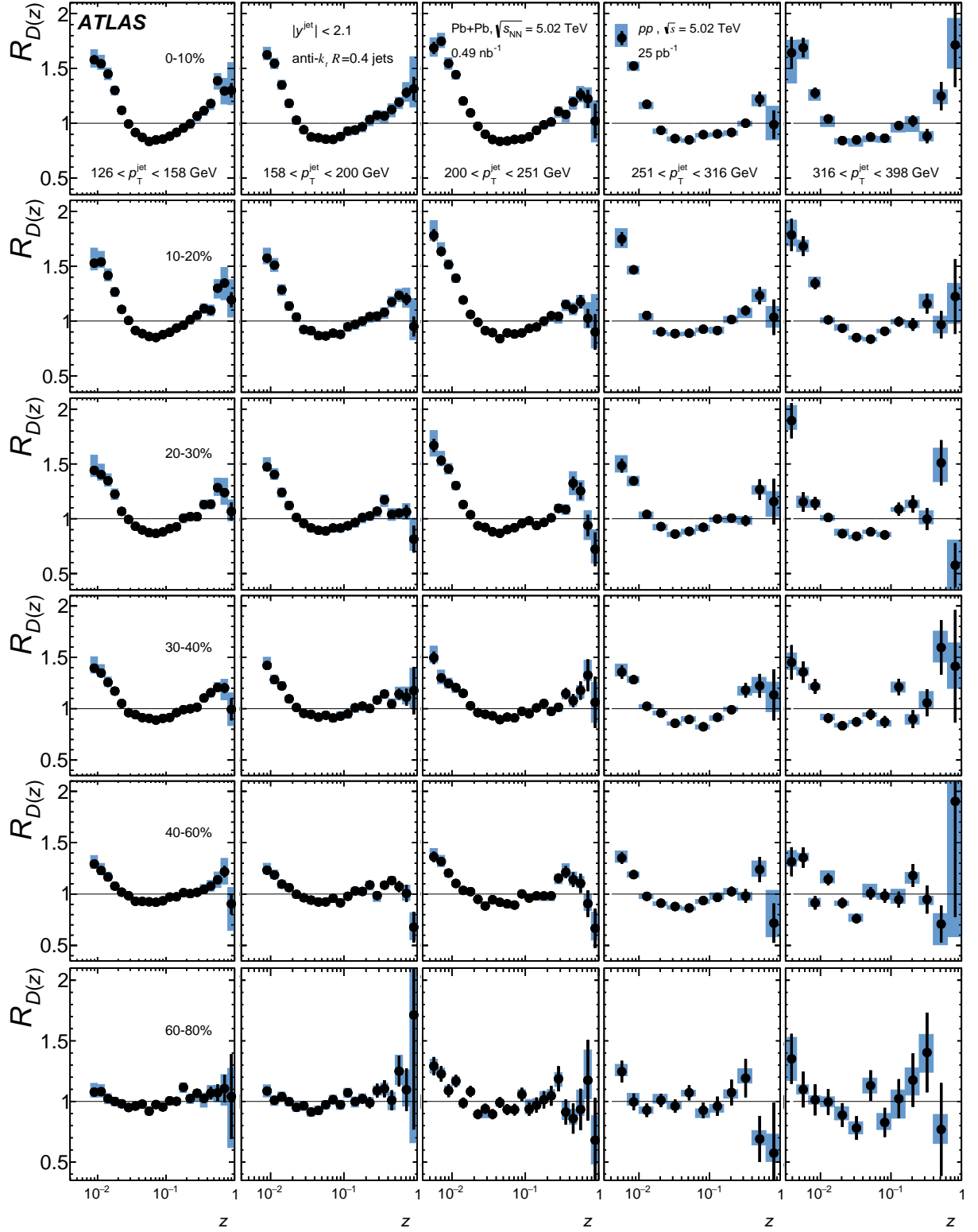
Figure 12: Ratios of $D(z)$ distributions in six centrality intervals of Pb+Pb collisions to pp collisions evaluated for five $p_{\mathrm{T}}^{\mathrm{jet}}$ ranges for jets with $|y^{\mathrm{jet}}| < 2.1$. The vertical bars on the data points indicate statistical uncertainties, while the shaded bands indicate systematic uncertainties. Centrality decreases from top to bottom panels and $p_{\mathrm{T}}^{\mathrm{jet}}$ increases from left to right panels.

Figure 13: Ratios of $D(p_T)$ distributions in six centrality intervals of Pb+Pb collisions to pp collisions evaluated for five p_T^{jet} ranges for jets with $|y^{jet}| < 2.1$. The vertical bars on the data points indicate statistical uncertainties, while the shaded bands indicate systematic uncertainties. Centrality decreases from top to bottom panels and p_T^{jet} increases from left to right panels.
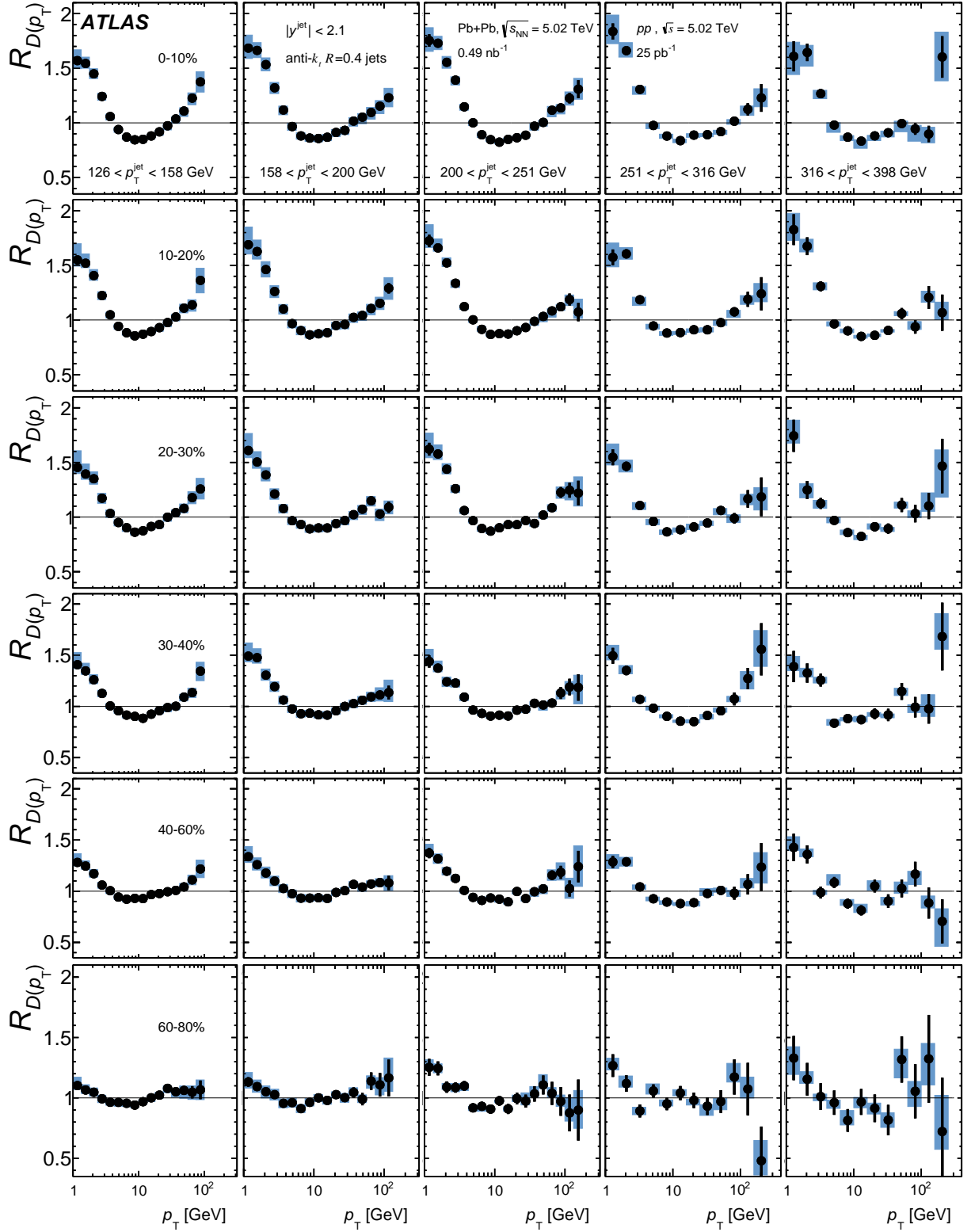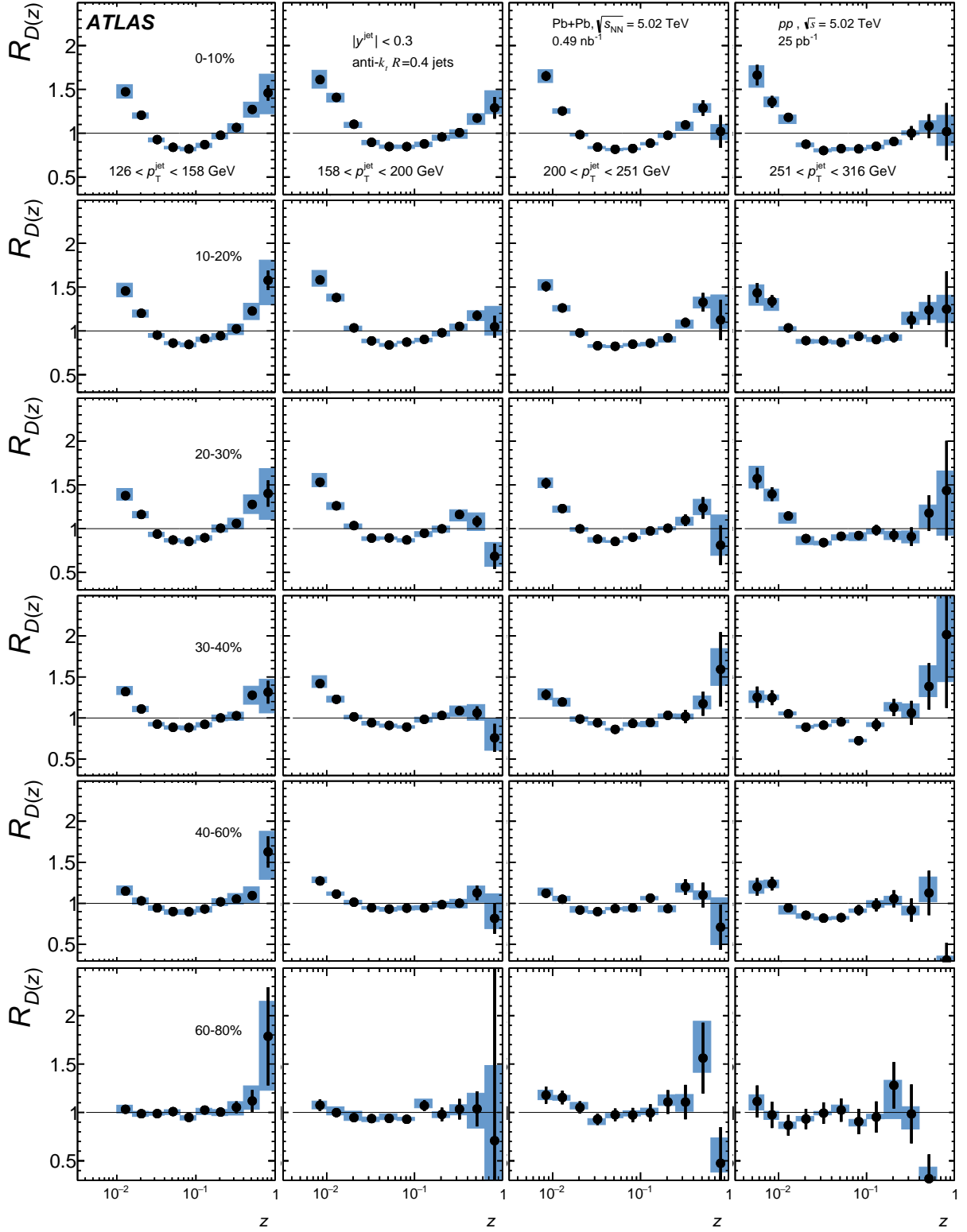
Figure 14: Ratios of $D(z)$ distributions in six centrality intervals of Pb+Pb collisions to pp collisions evaluated in four $p_{\mathrm{T}}^{\mathrm{jet}}$ ranges for jets with $|y^{\mathrm{jet}}| < 0.3$. The vertical bars on the data points indicate statistical uncertainties, while the shaded bands indicate systematic uncertainties. Centrality decreases from top to bottom panels and $p_{\mathrm{T}}^{\mathrm{jet}}$ increases from left to right panels.

Figure 15: Ratios of $D(z)$ distributions in six centrality intervals of Pb+Pb collisions to pp collisions evaluated in four $p_{\mathrm{T}}^{\mathrm{jet}}$ ranges for jets with $1.2 < |y^{\mathrm{jet}}| < 2.1$. The vertical bars on the data points indicate statistical uncertainties, while the shaded bands indicate systematic uncertainties. Centrality decreases from top to bottom panels and $p_{\mathrm{T}}^{\mathrm{jet}}$ increases from left to right panels.
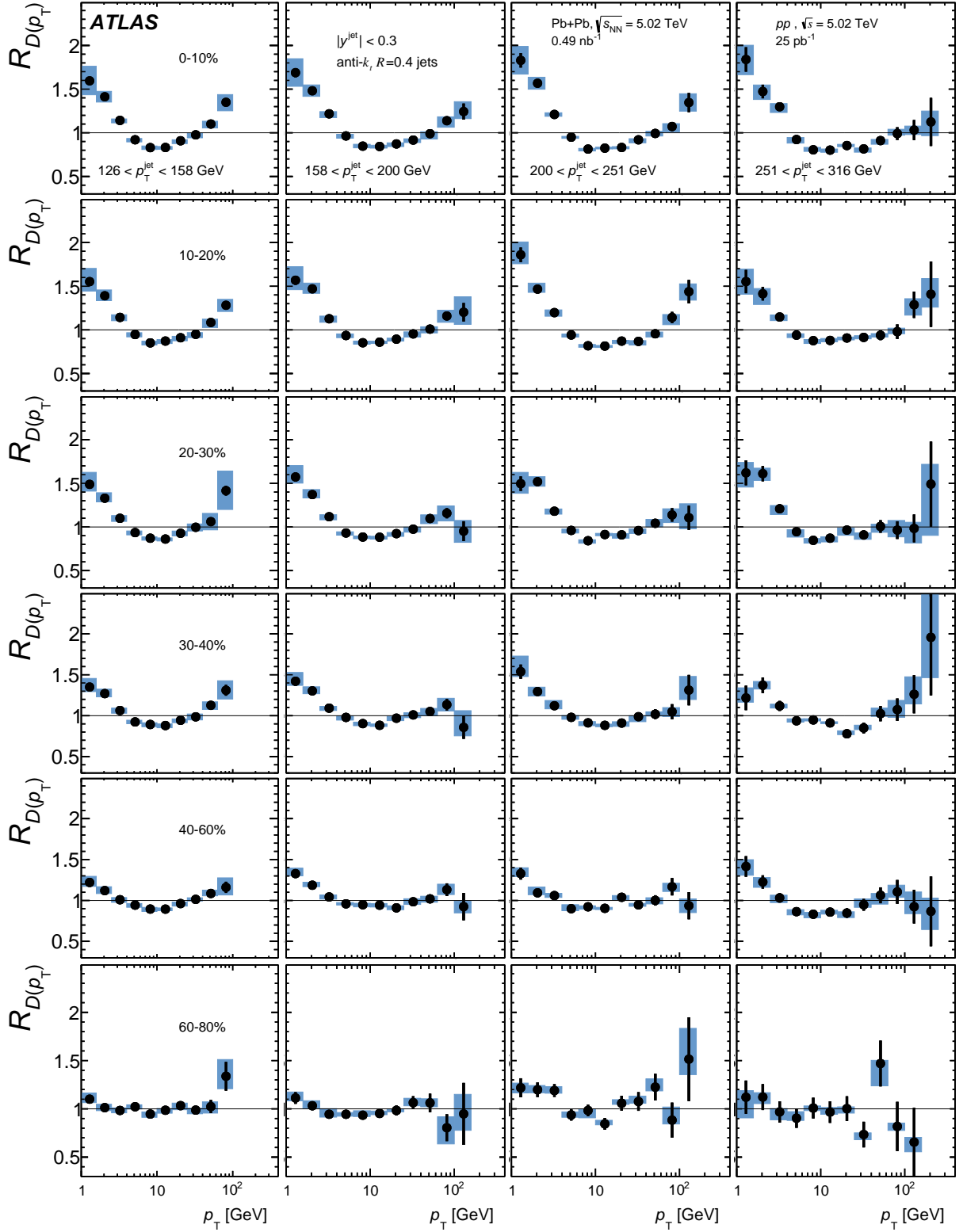
Figure 16: Ratios of $D(p_T)$ distributions in six centrality intervals of Pb+Pb collisions to pp collisions evaluated in four p_T^{jet} ranges for jets with $|y^{jet}| < 0.3$. The vertical bars on the data points indicate statistical uncertainties, while the shaded bands indicate systematic uncertainties. Centrality decreases from top to bottom panels and p_T^{jet} increases from left to right panels.
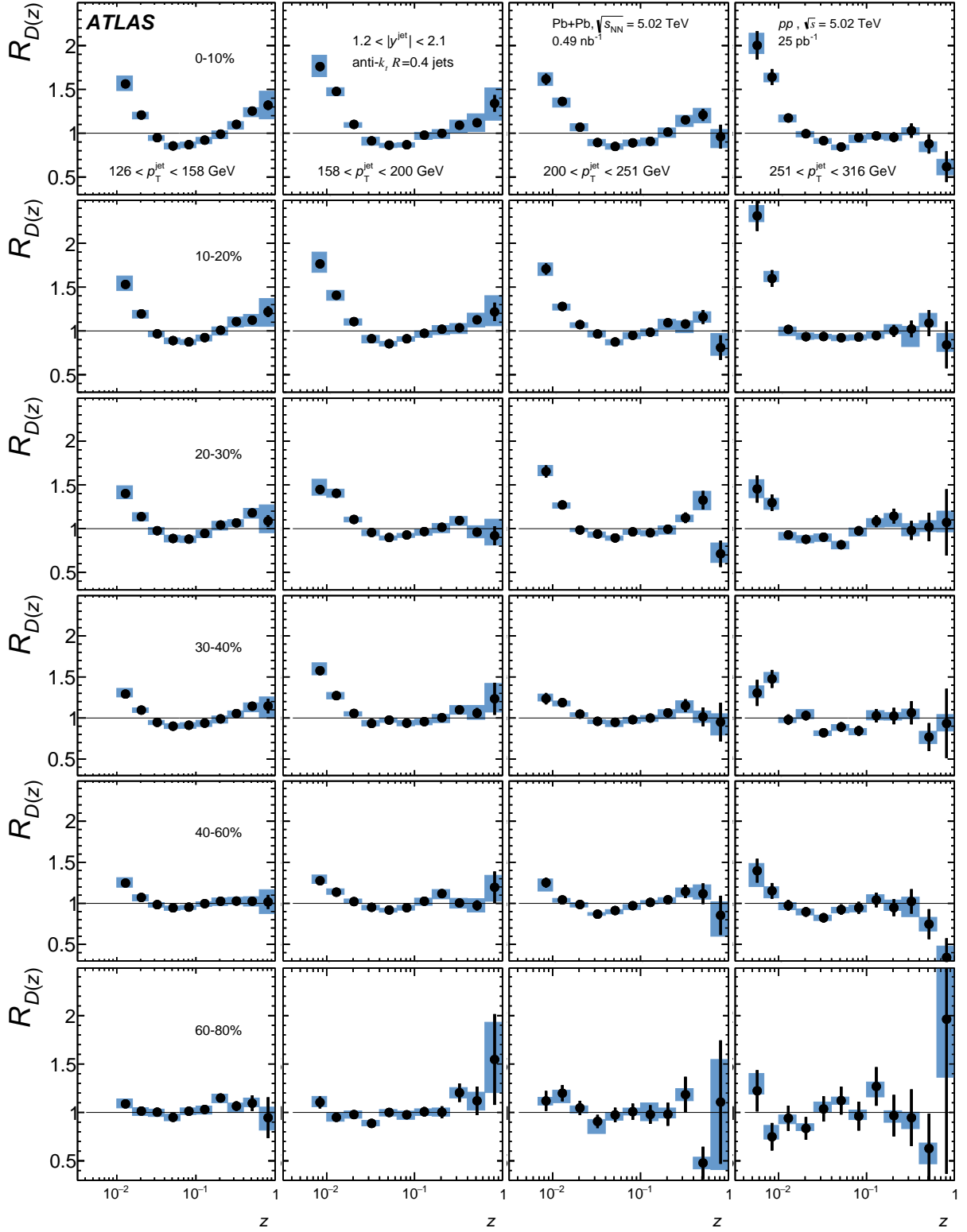
Figure 17: Ratios of $D(p_T)$ distributions in six centrality intervals of Pb+Pb collisions to pp collisions evaluated in four p_T^{jet} ranges for jets with $1.2 < |y^{jet}| < 2.1$. The vertical bars on the data points indicate statistical uncertainties, while the shaded bands indicate systematic uncertainties. Centrality decreases from top to bottom panels and p_T^{jet} increases from left to right panels.
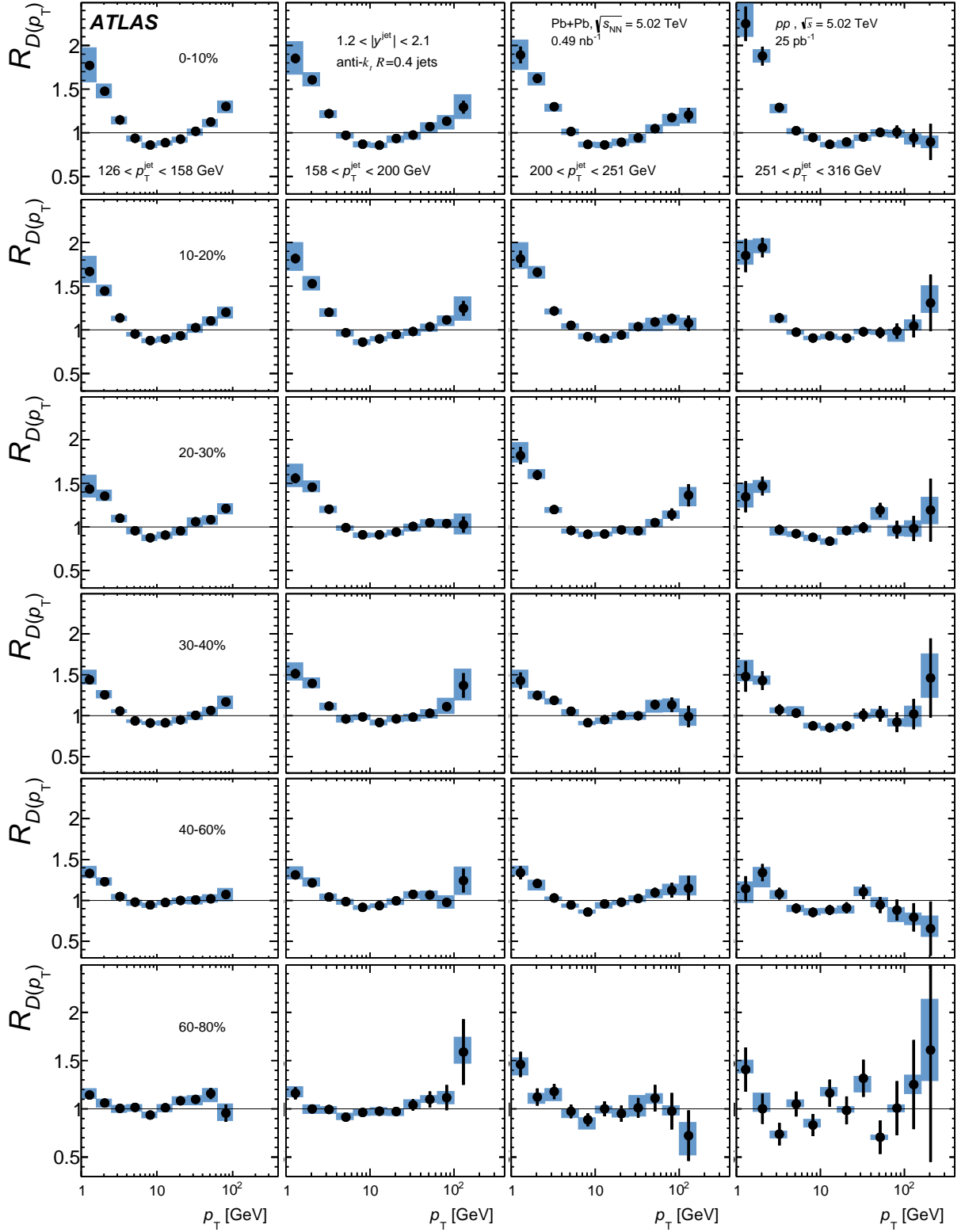
25

8 Discussion

In this section, the results from the previous section are further discussed and compared to theoretical models.

In order to make a direct comparison with measurements at 2.76 TeV, Figure 18 overlays the $R_{D(z)}$ and $R_{D(p_T)}$ distributions measured in 2.76 TeV collisions [16] on those obtained in this analysis at 5.02 TeV. The two measurements at the two collision energies quantitatively agree over the entire z and charged-particle p_T range of the measurement; no significant collision energy dependence is observed (the lowest point in the $D(p_T)$ ratios differs by less than two standard deviations when the statistical and systematic uncertainties are combined).
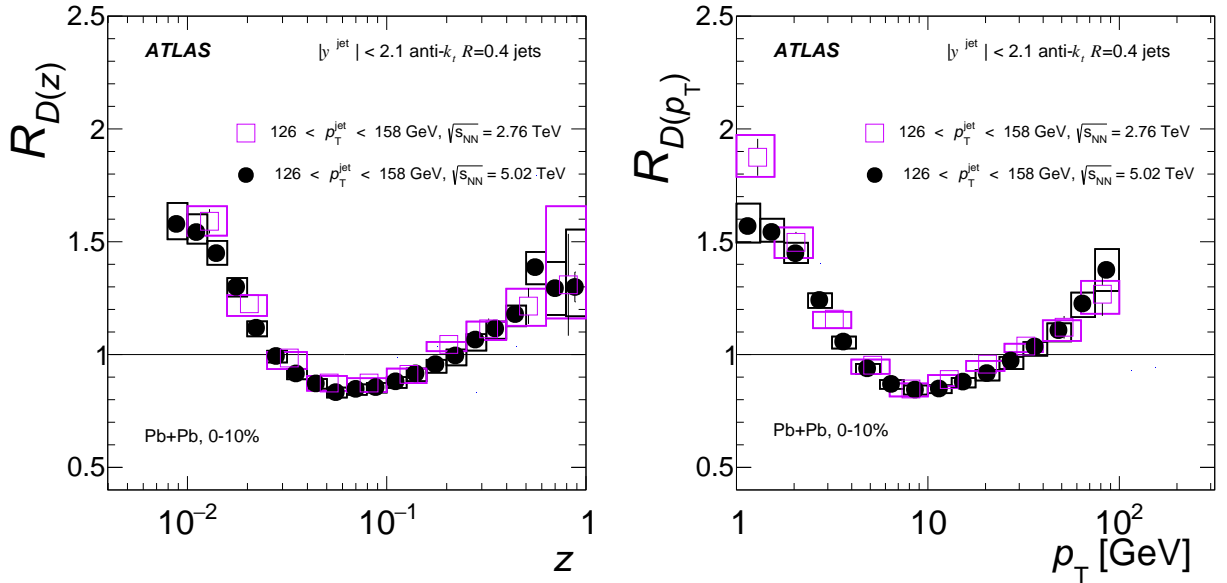

Figure 18: $R_{D(z)}$ (left) and $R_{D(p_T)}$ (right) for 126–158 GeV jets for collision energies of 5.02 TeV (this analysis) and 2.76 TeV [16]. The vertical bars on the data points indicate statistical uncertainties while the boxes indicate systematic uncertainties.

In order to determine how the fragmentation functions depend on p_T^{jet}, the fragmentation functions from three p_T^{jet} intervals are compared in Figure 19. The $D(p_T)$ and $D(z)$ distributions are closely related to each other, differing, primarily, in the normalization by p_T^{jet} in the definition of z (see Eq. (1)). Therefore, a comparison of the modifications of the fragmentation functions as a function of p_T^{jet} can show whether the size of modifications scales with charged-particle z or with p_T. The former would be expected for fragmentation effects, and the latter might indicate some scale in the QGP. The large p_T^{jet} range available in this measurement allows these two scenarios to be distinguished. Figure 19 shows that the excess of soft particles observed in central Pb+Pb collisions exhibits a much smaller p_T^{jet} dependence for the $D(p_T)$ ratios than for the $D(z)$ ratios; the transition from enhancement to suppression for soft fragments occurs at p_T around 4 GeV for all p_T^{jet} values investigated in this analysis. The same comparison can be made for the hard particles. In this case, Figure 19 shows that the enhancement of hard fragments with $z \gtrsim 0.3$ is nearly independent of p_T^{jet}.

The fragmentation functions have been calculated within a hybrid model of jet quenching, which uses

perturbative techniques for the high-Q^2 processes in jet evolution and strong coupling for the low momentum scales associated with the QGP [50, 51]. Within this model, there is a length scale, L_{res}, which can be interpreted as the minimum distance required to resolve a parton as separate from the others in the showering process when it occurs in the QGP medium. The scale L_{res} can be expressed in terms of the temperature of QGP, T, as $L_{res} = R_{res}/\pi T$ where R_{res} is a parameter of the model. The fragmentation functions measured here are compared with calculations from this model in Figure 20 for two values of R_{res}. The calculations with $R_{res} = 3$ are qualitatively consistent with the measurement at high z and p_T. At low z and p_T, the results of the calculations are below the data, in agreement with prior observations in comparisons to related observables [52]. Also shown in Figure 20 is a calculation from Ref. [21] which is a phenomenological model, the *Effective Quenching (EQ) Model*, incorporating energy-loss effects through two downward shifts in the p_T^{jet} spectrum: one for quark-initiated jets and a larger one for gluon-initiated jets. In this case, the jets fragment as in vacuum, but $R_{D(z)}$ differs from unity due to an increase in the fraction of quark jets in Pb+Pb collisions relative to pp collisions at a fixed p_T^{jet}. Since quark jets are more likely to produce high-z particles than gluon jets [53, 54] this causes $R_{D(z)} > 1$ at high z in the model predictions. The EQ model does not have a description of the soft processes from soft gluon radiation or the response of the hot QCD matter to the jet passing through it, so the comparison with data is only appropriate at $z > 0.1$.

Figure 21 shows a comparison between measured $R_{D(p_T)}$ and the hybrid model calculation with $R_{res} = 3$ for three p_T^{jet} intervals. The magnitude of the enhancement of high-p_T particles in the calculation agrees with the observations for p_T^{jet} in the ranges 126–158 GeVand 200–251 GeV. The $R_{D(z)}$ values are also compared in Figure 22 with a third model which uses calculations based on Soft Collinear Effective Theory (SCET) [55, 56]. This model well describes $R_{D(z)}$ in the low and intermediate z regions, but does not reproduce the enhancement in the high-z region observed in the data.
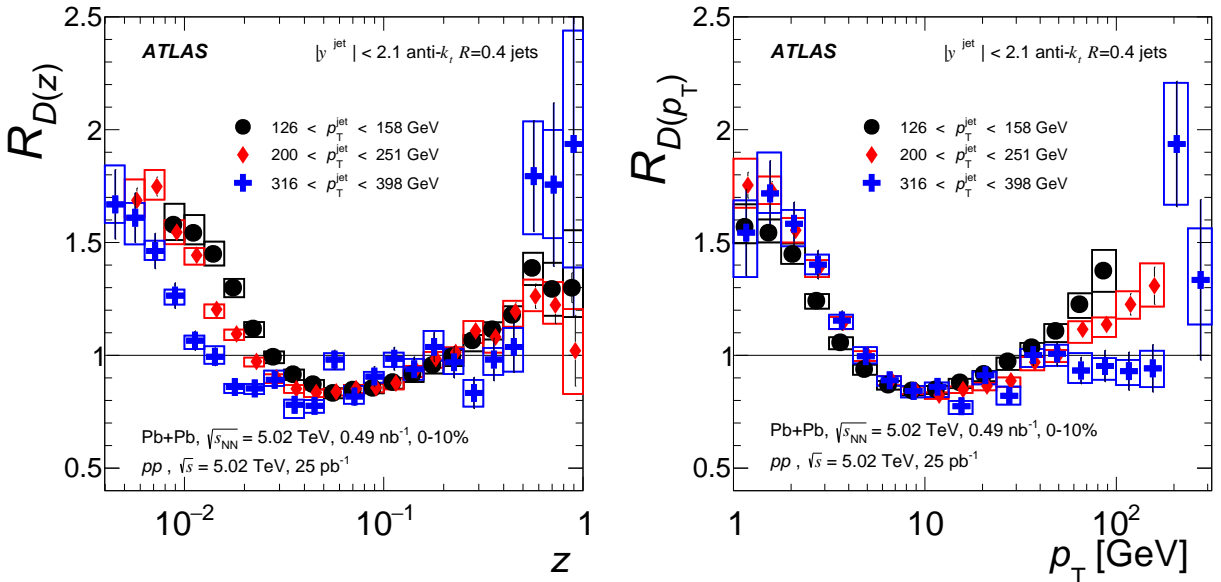

Figure 19: $R_{D(z)}$ (left) and $R_{D(p_T)}$ (right) ratios for three p_T^{jet} ranges: 126–158 GeV (circles), 200–251 GeV (diamonds) and 316–398 GeV (crosses). The statistical uncertainties are shown as bars and the systematic uncertainties as outlined boxes.

In order to quantify the magnitude of the low-p_T enhancement in the $D(p_T)$ distributions in Pb+Pb
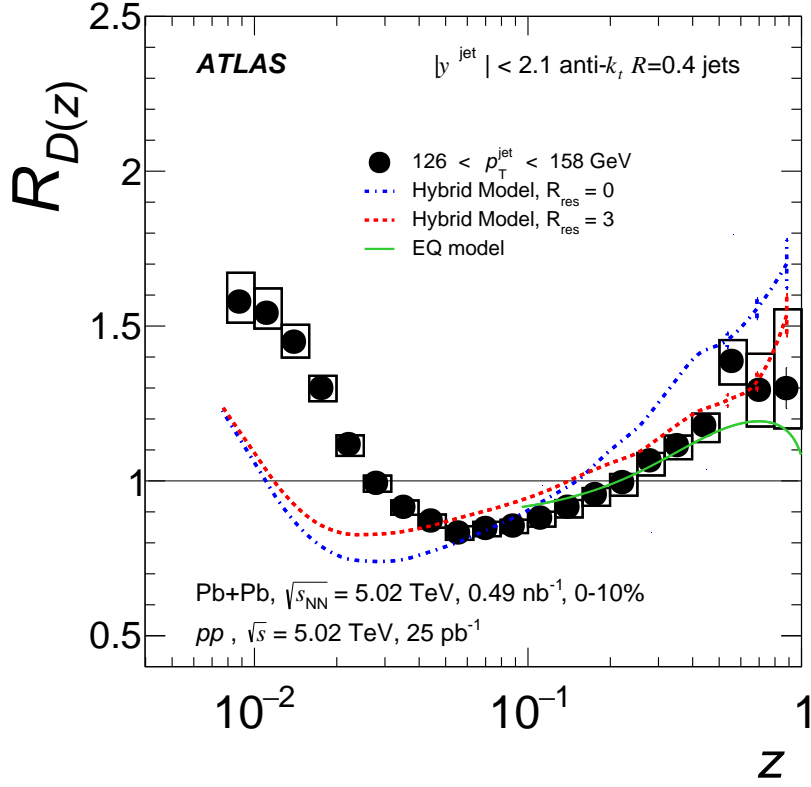
Figure 20: $R_{D(z)}$ for jets with $126 < p_T^{\text{jet}} < 158$ GeV compared with calculations from Ref. [51] (Hybrid model) for $R_{\text{res}} = 0$ (dot-dashed curve), $R_{\text{res}} = 3$ (dashed curve), and to calculations from Ref. [21] (EQ model).

collisions compared to pp collisions, the difference between the two distributions is evaluated for the p_T^{jet} and centrality intervals used in this analysis:

$$N^{\text{ch}}|_{\text{cent}} \equiv \int_{p_{\text{T,min}}}^{p_{\text{T,max}}} \left(D(p_T)|_{\text{cent}} - D(p_T)|_{pp} \right) dp_T,$$

where "cent" represents one of the six centrality intervals, and the values of $p_{\text{T,min}}$ and $p_{\text{T,max}}$ are boundaries of the low p_T enhancement region, chosen to be 1.0 and 4.2 GeV, respectively. In addition, the p_T-weighted difference between the same quantities is also computed:

$$P_T^{\text{ch}}|_{\text{cent}} \equiv \int_{p_{\text{T,min}}}^{p_{\text{T,max}}} \left(D(p_T)|_{\text{cent}} - D(p_T)|_{pp} \right) p_T dp_T.$$

The $P_T^{\text{ch}}|_{\text{cent}}$ represents the total transverse momentum carried by particles in the low p_T enhancement region. The dependence of $N^{\text{ch}}|_{\text{cent}}$ and $P_T^{\text{ch}}|_{\text{cent}}$ on p_T^{jet} and centrality is presented in Figure 23. Overall, both quantities are found to increase as a function of p_T^{jet} and collision centrality. In the most central collisions, N^{ch} increases from approximately 1.5 to 2.0 particles over the p_T^{jet} range of this measurement. The amount of transverse momentum carried by these particles increases from approximately 2.5 GeV to 4 GeV over the same p_T^{jet} range. In peripheral collisions, the number of particles contributing to the enhancement is much smaller, approximately 0.2 particles carrying less than 0.5 GeV of transverse
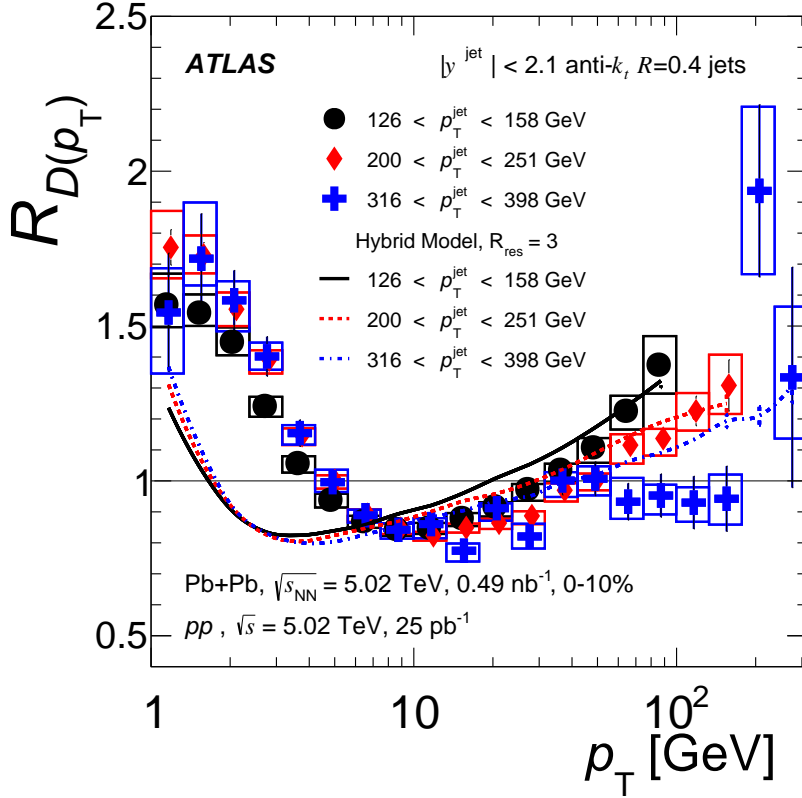
Figure 21: $R_{D(p_T)}$ ratios for three p_T^{jet} ranges: 126–158 GeV (circles), 200–251 GeV (diamonds) and 316–398 GeV (crosses) compared with calculations from the hybrid model [51] with $R_{res} = 3$.

momentum in the lowest p_T^{jet} range. These results are in qualitative agreement with measurements of the same quantities in $\sqrt{s_{NN}}$ = 2.76 TeV Pb+Pb collisions [16]; however, the p_T^{jet} ranges are not the same as used in this analysis and the p_T^{jet} dependence is not reported in that measurement.

In order to quantify the rapidity dependence, the ratio of $R_{D(z)}$ in the rapidity intervals 0.3–0.8, 0.8–1.2, and 1.2–2.1 to the $R_{D(z)}$ in $|y^{jet}| < 0.3$ is shown in Figure 24 for p_T^{jet} intervals of 126–158 GeV, 158–200 GeV, and 200–251 GeV and for 0–10%, 10–20%, and 20–30% central collisions. A similar quantity was reported in Ref. [16] for 100–398 GeV jets at 2.76 TeV. In that measurement, a small rapidity dependence for $R_{D(z)}$ is observed at high z for jets with $|y^{jet}| < 0.8$; however, no strong conclusion could be drawn due to the size of the uncertainties. The p_T^{jet} intervals used in the measurement presented here are selected to be similar to those used in the measurement of fragmentation functions at 2.76 TeV. Furthermore, jets populating the 200–251 GeV p_T^{jet} interval in collisions at 5.02 TeV have similar fractions of quark- and gluon-initiated jets as jets having p_T between 126 and 158 GeV in 2.76 TeV collisions. The ratios of $R_{D(z)}$ evaluated in various rapidity intervals to the most central rapidity $R_{D(z)}$ in different p_T^{jet} intervals suggest with a low significance a small enhancement of yields of fragments with low and intermediate z and reduction of yields of high-z fragments for more forward jets in the most central Pb+Pb collisions. However, the observation for high-z fragments is of limited significance due to the limited size of the available data sample. Figure 25 shows the same ratios for the 0–10% centrality interval compared with calculations from the Hybrid model [51] and the Effective Quenching model [21]. Both
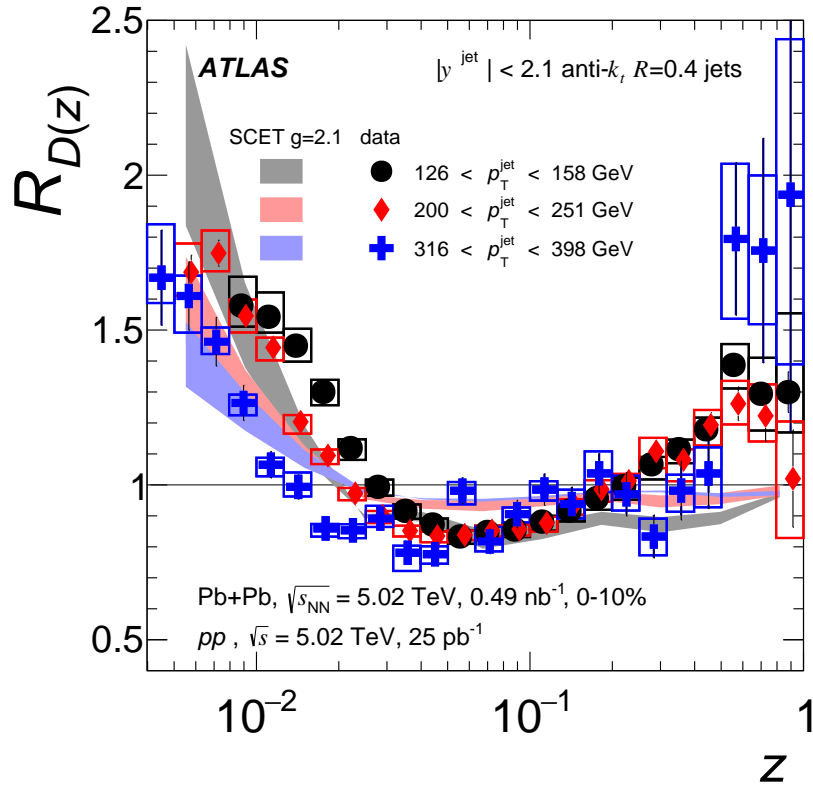
Figure 22: $R_{D(z)}$ for three p_T^{jet} ranges: 126–158 GeV (circles), 200–251 GeV (diamonds) and 316–398 GeV (crosses) compared with calculations from the SCET model [55, 56].

calculations are consistent with the data for jets with $|y^{jet}| < 1.2$ with larger deviations in rapidity interval $1.2 < |y^{jet}| < 2.1$.
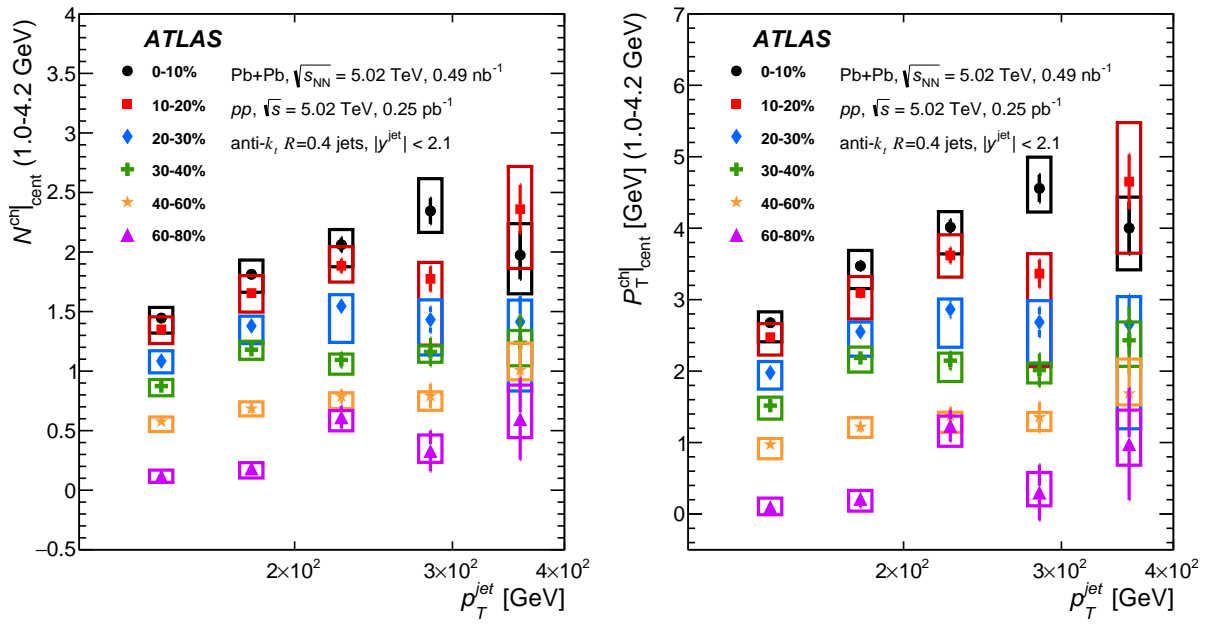
Figure 23: Difference between Pb+Pb collisions and *pp* collisions in the total yield of charged particles, $N^{\mathrm{ch}}|_{\mathrm{cent}}$, (left) and difference in the total transverse momentum carried by charged particles, $P_{\mathrm{T}}^{\mathrm{ch}}|_{\mathrm{cent}}$, (right) for particles with p_{T} from $1 < p_{\mathrm{T}} < 4.2$ GeV evaluated as a function of $p_{\mathrm{T}}^{\mathrm{jet}}$ for six centrality intervals. The vertical bars on the data points indicate statistical uncertainties while the boxes indicate systematic uncertainties.
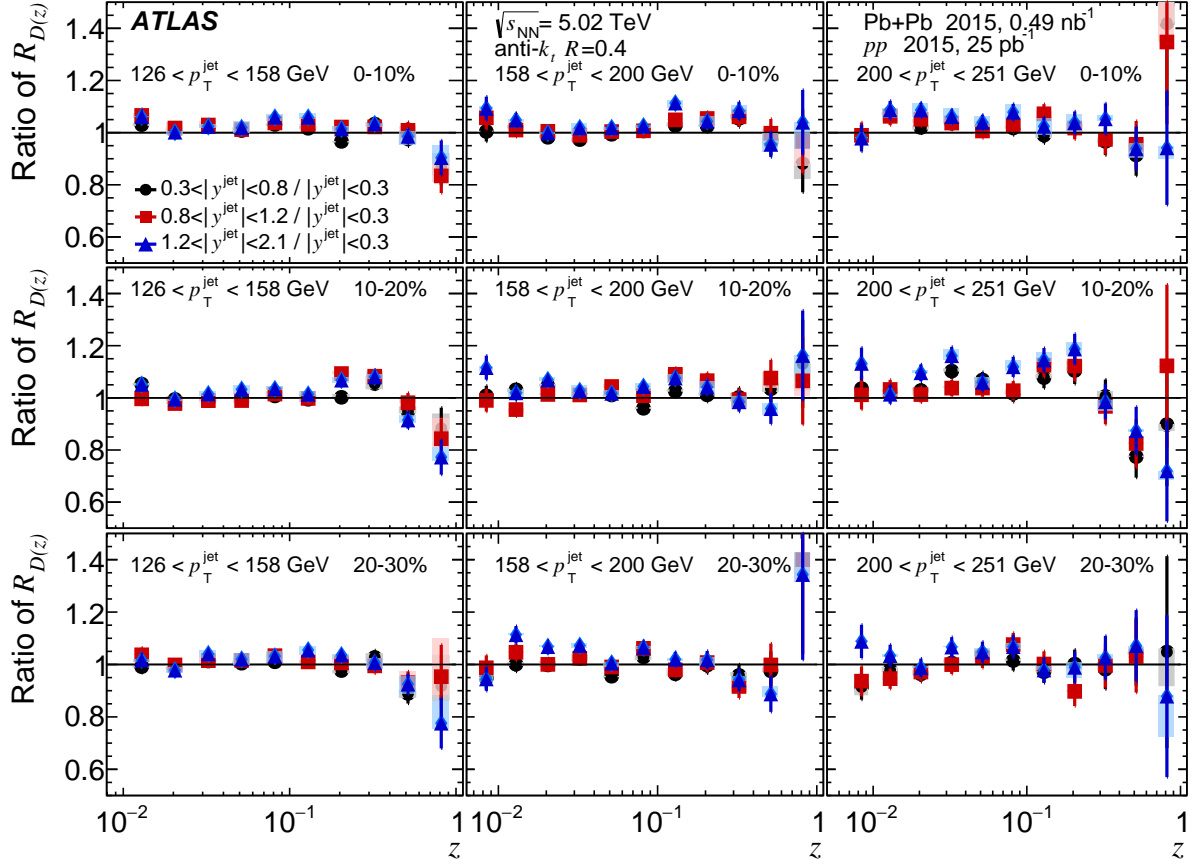
Figure 24: Ratio of the rapidity-selected $R_{D(z)}$ distributions to the $R_{D(z)}$ distributions measured in $|y^{\text{jet}}| < 0.3$ for three p_T^{jet} ranges and three centrality intervals. The vertical bars on the data points indicate statistical uncertainties while the shaded bands indicate systematic uncertainties.
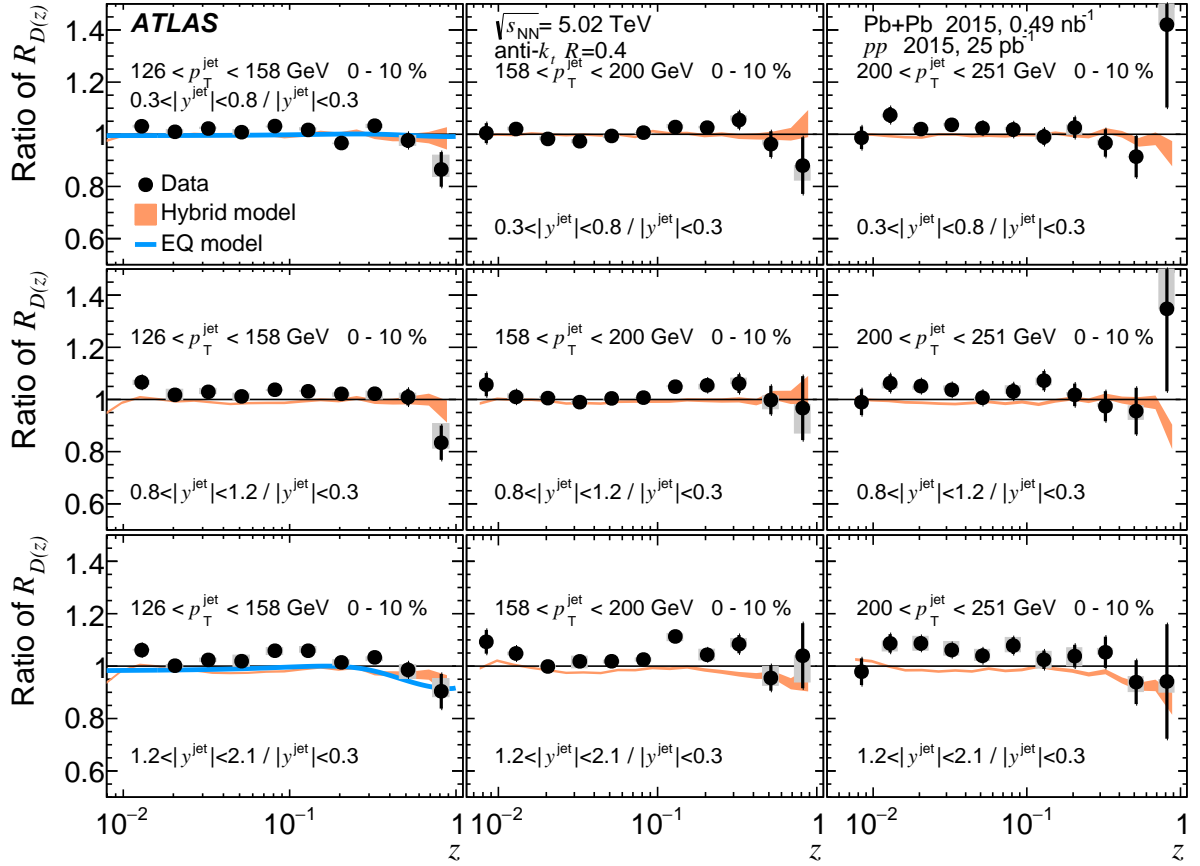
Figure 25: Comparison of the measured ratio of the rapidity-selected $R_{D(z)}$ distributions to the $R_{D(z)}$ distributions measured in $|y^{\mathrm{jet}}| < 0.3$ and the same quantity evaluated in the hybrid model [51] for $R_{\mathrm{res}} = 3$ and in the EQ model [21]. The comparison with the hybrid model is done for three $p_{\mathrm{T}}^{\mathrm{jet}}$ ranges in 0–10% central collisions. The comparison with the EQ model is shown for 126–158 GeV $p_{\mathrm{T}}^{\mathrm{jet}}$ interval. The vertical bars on the data points indicate statistical uncertainties while the shaded bars indicate systematic uncertainties. The band represents the statistical uncertainty of the calculations.

9 Summary

This paper presents an analysis of 0.49 nb^{-1} of Pb+Pb and 25 pb^{-1} of pp collisions at $\sqrt{s_{NN}}$ = 5.02 TeV using data collected with the ATLAS detector at the LHC in 2015. The analysis measures the fragmentation functions of jets into charged particles and the distributions of charged-particle transverse momenta within R = 0.4 anti-k_t jets with $|y^{jet}|$ <2.1 and with p_T^{jet} from 126 to 398 GeV. The studies are performed as a function of the event centrality, jet rapidity and jet transverse momentum for charged particles with transverse momentum greater than 1 GeV .

Centrality-dependent modifications to these fragmentation functions in Pb+Pb collisions are observed when compared with those measured in pp collisions. The magnitude of these modifications increases with increasing collision centrality. The ratios of fragmentation functions evaluated in Pb+Pb collisions to those in pp collisions exhibit enhancements both for transverse momentum less than 4 GeV and for $z \gtrsim 0.3$. Between these two enhancements there is a suppression of the fragmentation functions in Pb+Pb collisions compared to pp collisions. The enhancement of yields of low and high transverse momentum fragments is as large as 70% and 30%, respectively, in central collisions. The depletion of fragment yields with intermediate p_T and z is as large as 20%. The difference in charged-particle multiplicity and total transverse momentum in Pb+Pb compared to pp collisions for $1.0 < p_T < 4.2$ GeV range increases with increasing centrality and jet transverse momentum. No significant dependence of the high-z enhancement on the transverse momentum of the jet is observed. The SCET model describes the low p_T excess and the EQ and Hybrid models describe the high-z excess, but none of the models describes the modification of the full fragmentation functions. A small increase in the modification of yields of fragments with low and intermediate z is observed in forward jets compared to those at central rapidity. These measurements provide new information about the jet transverse momentum and rapidity dependence of the modifications to jet fragmentation in Pb+Pb collisions and, together with other jet measurements in heavy-ion collisions, will constrain models of jet quenching in the QGP created in heavy-ion collisions.

Acknowledgements

References

[1] G. Roland, K. Šafařík, and P. Steinberg, *Heavy-ion collisions at the LHC*, Prog. Part. Nucl. Phys. **77** (2014) 70.

[2] W. Busza, K. Rajagopal, and W. van der Schee, *Heavy Ion Collisions: The Big Picture, and the Big Questions*, (2018), arXiv: 1802.04801 [hep-ph].

[3] ALICE Collaboration, *Measurement of charged jet suppression in Pb-Pb collisions at $\sqrt{s_{NN}}$ = 2.76 TeV*, JHEP **03** (2014) 013, arXiv: 1311.0633 [nucl-ex].

[4] ATLAS Collaboration, *Measurements of the Nuclear Modification Factor for Jets in Pb+Pb Collisions at $\sqrt{s_{NN}}$ = 2.76 TeV with the ATLAS Detector*, Phys. Rev. Lett. **114** (2015) 072302, arXiv: 1411.2357 [hep-ex].

[5] CMS Collaboration,
Measurement of inclusive jet cross sections in pp and PbPb collisions at $\sqrt{s_{NN}}$ = 2.76 TeV,
Phys. Rev. C **96** (2017) 015202, arXiv: 1609.05383 [nucl-ex].

[6] ATLAS Collaboration, *Observation of a Centrality-Dependent Dijet Asymmetry in Lead-Lead
Collisions at $\sqrt{s_{NN}}$ = 2.77 TeV with the ATLAS Detector at the LHC*,
Phys. Rev. Lett. **105** (2010) 252303, arXiv: 1011.6182 [hep-ex].

[7] CMS Collaboration, *Observation and studies of jet quenching in PbPb collisions at
nucleon-nucleon center-of-mass energy = 2.76 TeV*, Phys. Rev. C **84** (2011) 024906,
arXiv: 1102.1957 [nucl-ex].

[8] ATLAS Collaboration, *Measurement of jet p_{T} correlations in Pb+Pb and pp collisions at $\sqrt{s_{NN}}$ =
2.76 TeV with the ATLAS detector*, Phys. Lett. B **774** (2017) 379, arXiv: 1706.09363 [hep-ex].

[9] CMS Collaboration, *Studies of jet quenching using isolated-photon+jet correlations in PbPb and
pp collisions at $\sqrt{s_{NN}}$ = 2.76 TeV*, Phys. Lett. B **718** (2013) 773, arXiv: 1205.0206 [nucl-ex].

[10] K. Adcox et al., *Suppression of hadrons with large transverse momentum in central Au+Au
collisions at $\sqrt{s_{NN}}$ = 130-GeV*, Phys. Rev. Lett. **88** (2002) 022301,
arXiv: nucl-ex/0109003 [nucl-ex].

[11] C. Adler et al., *Disappearance of back-to-back high p_T hadron correlations in central Au+Au
collisions at $\sqrt{s_{NN}}$ = 200-GeV*, Phys. Rev. Lett. **90** (2003) 082302,
arXiv: nucl-ex/0210033 [nucl-ex].

[12] B. I. Abelev et al., *Studying Parton Energy Loss in Heavy-Ion Collisions via Direct-Photon and
Charged-Particle Azimuthal Correlations*, Phys. Rev. **C82** (2010) 034909,
arXiv: 0912.1871 [nucl-ex].

[13] CMS Collaboration, *Modification of jet shapes in PbPb collisions at $\sqrt{s_{NN}}$ = 2.76 TeV*,
Phys. Lett. B **730** (2014) 243, arXiv: 1310.0878 [nucl-ex].

[14] ATLAS Collaboration, *Measurement of inclusive jet charged-particle fragmentation functions in
Pb+Pb collisions at $\sqrt{s_{NN}}$ = 2.76 TeV with the ATLAS detector*, Phys. Lett. B **739** (2014) 320,
arXiv: 1406.2979 [hep-ex].

[15] CMS Collaboration,
Measurement of jet fragmentation in PbPb and pp collisions at $\sqrt{s_{NN}}$ = 2.76 TeV,
Phys. Rev. C **90** (2014) 024908, arXiv: 1406.0932 [nucl-ex].

[16] ATLAS Collaboration, *Measurement of jet fragmentation in Pb+Pb and pp collisions at
$\sqrt{s_{\mathrm{NN}}}$ = 2.76 TeV with the ATLAS detector at the LHC*, Eur. Phys. J. C **77** (2017) 379,
arXiv: 1702.00674 [hep-ex].

[17] CMS Collaboration, *Decomposing transverse momentum balance contributions for quenched jets
in PbPb collisions at $\sqrt{s_{\mathrm{N\,N}}}$ = 2.76 TeV*, JHEP **11** (2016) 055, arXiv: 1609.02466 [nucl-ex].

[18] CMS Collaboration, *Jet properties in PbPb and pp collisions at $\sqrt{s_{\mathrm{NN}}}$ = 5.02 TeV*, (2018),
arXiv: 1803.00042 [nucl-ex].

[19] G.-Y. Qin and X.-N. Wang, *Jet quenching in high-energy heavy-ion collisions*,
Int. J. Mod. Phys. E **24** (2015) 1530014, arXiv: 1511.00790 [hep-ph].

[20] J.-P. Blaizot, Y. Mehtar-Tani, and M. A. C. Torres,
Angular structure of the in-medium QCD cascade, Phys. Rev. Lett. **114** (2015) 222002,
arXiv: 1407.0326 [hep-ph].

[21] M. Spousta and B. Cole, *Interpreting single jet measurements in Pb + Pb collisions at the LHC*, Eur. Phys. J. C **76** (2016) 50, arXiv: 1504.05169 [hep-ph].

[22] ATLAS Collaboration, *Measurement of jet fragmentation in 5.02 TeV proton–lead and proton–proton collisions with the ATLAS detector*, Nucl. Phys. A **978** (2018) 65, arXiv: 1706.02859 [hep-ex].

[23] ATLAS Collaboration, *Measurement of the charged-particle multiplicity inside jets from $\sqrt{s} = 8$ TeV pp collisions with the ATLAS detector*, Eur. Phys. J. C **76** (2016) 322, arXiv: 1602.00988 [hep-ex].

[24] M. Cacciari, G. P. Salam, and G. Soyez, *The anti-k_t jet clustering algorithm*, JHEP **04** (2008) 063, arXiv: 0802.1189 [hep-ph].

[25] ATLAS Collaboration, *The ATLAS Experiment at the CERN Large Hadron Collider*, JINST **3** (2008) S08003.

[26] ATLAS Collaboration, *ATLAS Insertable B-Layer Technical Design Report*, (2010), ATLAS-TDR-19, URL: http://cds.cern.ch/record/1291633.

[27] ATLAS Collaboration, *ATLAS Insertable B-Layer Technical Design Report Addendum*, (2012), ATLAS-TDR-19-ADD-1, URL: http://cds.cern.ch/record/1451888.

[28] ATLAS Collaboration, *Measurement of longitudinal flow de-correlations in Pb+Pb collisions at $\sqrt{s_{NN}} = 2.76$ and 5.02 TeV with the ATLAS detector*, Eur. Phys. J. C **78** (2018) 142, arXiv: 1709.02301 [nucl-ex].

[29] P. Nason, *A New method for combining NLO QCD with shower Monte Carlo algorithms*, JHEP **11** (2004) 040, arXiv: hep-ph/0409146 [hep-ph].

[30] T. Sjöstrand et al., *An introduction to PYTHIA 8.2*, Comput. Phys. Commun. **191** (2015) 159, arXiv: 1410.3012 [hep-ph].

[31] ATLAS Collaboration, *ATLAS Run 1 Pythia8 tunes*, (2014), ATLAS-PHYS-PUB-2014-021, URL: https://cds.cern.ch/record/1966419.

[32] R. D. Ball et al., *Parton distributions with LHC data*, Nucl. Phys. B **867** (2013) 244, arXiv: 1207.1303 [hep-ph].

[33] GEANT4 Collaboration, S. Agostinelli et al., *GEANT4 - a simulation toolkit*, Nucl. Instrum. Meth. A **506** (2003) 250.

[34] ATLAS Collaboration, *The ATLAS Simulation Infrastructure*, Eur. Phys. J. **C70** (2010) 823, arXiv: 1005.4568 [physics.ins-det].

[35] X.-N. Wang and M. Gyulassy, *HIJING: A Monte Carlo model for multiple jet production in pp, pA and AA collisions*, Phys. Rev. D **44** (1991) 3501.

[36] ATLAS Collaboration, *Measurement of the azimuthal anisotropy for charged particle production in $\sqrt{s_{NN}} = 2.76$ TeV lead-lead collisions with the ATLAS detector*, Phys. Rev. C **86** (2012) 014907, arXiv: 1203.3087 [hep-ex].

[37] ATLAS Collaboration, *Jet energy scale measurements and their systematic uncertainties in proton-proton collisions at $\sqrt{s} = 13$ TeV with the ATLAS detector*, Phys. Rev. D **96** (2017) 072002, arXiv: 1703.09665 [hep-ex].

[38] ATLAS Collaboration, *Properties of jets and inputs to jet reconstruction and calibration with the ATLAS detector using proton–proton collisions at $\sqrt{s}$ = 13 TeV*, ATL-PHYS-PUB-2015-036, 2015, URL: https://cds.cern.ch/record/2044564.

[39] ATLAS Collaboration, *Study of photon-jet momentum correlations in Pb+Pb and pp collisions at $\sqrt{s_{NN}}$ = 5.02 TeV with ATLAS*, ATLAS-CONF-2016-110, 2016, URL: https://cds.cern.ch/record/2220772.

[40] ATLAS Collaboration, *Performance of the ATLAS track reconstruction algorithms in dense environments in LHC Run 2*, Eur. Phys. J. C **77** (2017) 673, arXiv: 1704.07983 [hep-ex].

[41] ATLAS Collaboration, *Measurement of track reconstruction inefficiencies in the core of jets via pixel dE/dx with the ATLAS experiment using $\sqrt{s}$ = 13 TeV pp collision data*, ATL-PHYS-PUB-2016-007, 2016, URL: https://cds.cern.ch/record/2140460.

[42] G. D'Agostini, *A Multidimensional unfolding method based on Bayes' theorem*, Nucl. Instrum. Meth. A **362** (1995) 487.

[43] T. Adye, *Unfolding algorithms and tests using RooUnfold*, Proceedings of the PHYSTAT 2009 Workshop, CERN, Geneva, Switzerland, CERN-2011-006, pp 313 (2011), arXiv: 1105.1160 [physics.data-an].

[44] ATLAS Collaboration, *Jet energy measurement with the ATLAS detector in proton-proton collisions at $\sqrt{s}$ = 7 TeV*, Eur. Phys. J. C **73** (2013) 2304, arXiv: 1112.6426 [hep-ex].

[45] ATLAS Collaboration, *Jet energy scale and its uncertainty for jets reconstructed using the ATLAS heavy ion jet algorithm*, (2015), ATLAS-CONF-2015-016, URL: https://cds.cern.ch/record/2008677.

[46] ATLAS Collaboration, *Jet calibration and systematic uncertainties for jets reconstructed in the ATLAS detector at $\sqrt{s}$=13 TeV*, (2015), ATLAS-PHYS-PUB-2015-015, URL: https://cds.cern.ch/record/2037613.

[47] ATLAS Collaboration, *Jet energy resolution in proton-proton collisions at $\sqrt{s}$ = 7 TeV recorded in 2010 with the ATLAS detector*, Eur. Phys. J. C **73** (2013) 2306, arXiv: 1210.6210 [hep-ex].

[48] ATLAS Collaboration, *Data-driven determination of the energy scale and resolution of jets reconstructed in the ATLAS calorimeters using dijet and multijet events at $\sqrt{s}$ = 8 TeV*, (2015), ATLAS-CONF-2015-017, URL: https://cds.cern.ch/record/2008678.

[49] ATLAS Collaboration, *Early Inner Detector Tracking Performance in the 2015 Data at $\sqrt{s}$ = 13 TeV*, ATL-PHYS-PUB-2015-051, 2015, URL: https://cds.cern.ch/record/2110140.

[50] J. Casalderrey-Solana, D. C. Gulhan, J. G. Milhano, D. Pablos, and K. Rajagopal, *A Hybrid Strong/Weak Coupling Approach to Jet Quenching*, JHEP **10** (2014) 019, [Erratum: JHEP 09 (2015) 175], arXiv: 1405.3864 [hep-ph].

[51] Z. Hulcher, D. Pablos, and K. Rajagopal, *Resolution effects in the hybrid strong/weak coupling model*, JHEP **03** (2017) 010, arXiv: 1707.05245 [hep-ph].

[52] J. Casalderrey-Solana, D. C. Gulhan, J. G. Milhano, D. Pablos, and K. Rajagopal, *Angular structure of jet quenching within a hybrid strong/weak coupling model*, JHEP **03** (2017) 135, arXiv: 1609.05842 [hep-ph].

[53] ALEPH Collaboration, R. Barate et al.,
      Measurements of the structure of quark and gluon jets in hadronic Z decays,
      Eur. Phys. J. C **17** (2000) 1.

[54] OPAL Collaboration, G. Abbiendi et al.,
      Experimental properties of gluon and quark jets from a point source,
      Eur. Phys. J. C **11** (1999) 217, arXiv: `hep-ex/9903027 [hep-ex]`.

[55] Y.-T. Chien, A. Emerman, Z.-B. Kang, G. Ovanesyan, and I. Vitev,
      Jet quenching from QCD evolution, Phys. Rev. D **93** (2016) 074030,
      arXiv: `1509.02936 [hep-ph]`.

[56] Z.-B. Kang, F. Ringer, and I. Vitev,
      Inclusive production of small radius jets in heavy-ion collisions, Phys. Lett. B **769** (2017) 242,
      arXiv: `1701.05839 [hep-ph]`.

[57] ATLAS Collaboration, *ATLAS Computing Acknowledgements*, ATL-GEN-PUB-2016-002,
      URL: `https://cds.cern.ch/record/2202407`.

The ATLAS Collaboration

M. Aaboud[34d], G. Aad[99], B. Abbott[124], O. Abdinov[13,*], B. Abeloos[128], D.K. Abhayasinghe[91],
S.H. Abidi[164], O.S. AbouZeid[39], N.L. Abraham[153], H. Abramowicz[158], H. Abreu[157], Y. Abulaiti[6],
B.S. Acharya[64a,64b,n], S. Adachi[160], L. Adamczyk[81a], J. Adelman[119], M. Adersberger[112],
A. Adiguzel[12c,ag], T. Adye[141], A.A. Affolder[143], Y. Afik[157], C. Agheorghiesei[27c],
J.A. Aguilar-Saavedra[136f,136a], F. Ahmadov[77,ae], G. Aielli[71a,71b], S. Akatsuka[83], T.P.A. Åkesson[94],
E. Akilli[52], A.V. Akimov[108], G.L. Alberghi[23b,23a], J. Albert[173], P. Albicocco[49], M.J. Alconada Verzini[86],
S. Alderweireldt[117], M. Aleksa[35], I.N. Aleksandrov[77], C. Alexa[27b], T. Alexopoulos[10], M. Alhroob[124],
B. Ali[138], G. Alimonti[66a], J. Alison[36], S.P. Alkire[145], C. Allaire[128], B.M.M. Allbrooke[153], B.W. Allen[127],
P.P. Allport[21], A. Aloisio[67a,67b], A. Alonso[39], F. Alonso[86], C. Alpigiani[145], A.A. Alshehri[55],
M.I. Alstaty[99], B. Alvarez Gonzalez[35], D. Álvarez Piqueras[171], M.G. Alviggi[67a,67b], B.T. Amadio[18],
Y. Amaral Coutinho[78b], L. Ambroz[131], C. Amelung[26], D. Amidei[103], S.P. Amor Dos Santos[136a,136c],
S. Amoroso[44], C.S. Amrouche[52], C. Anastopoulos[146], L.S. Ancu[52], N. Andari[21], T. Andeen[11],
C.F. Anders[59b], J.K. Anders[20], K.J. Anderson[36], A. Andreazza[66a,66b], V. Andrei[59a], C.R. Anelli[173],
S. Angelidakis[37], I. Angelozzi[118], A. Angerami[38], A.V. Anisenkov[120b,120a], A. Annovi[69a], C. Antel[59a],
M.T. Anthony[146], M. Antonelli[49], D.J.A. Antrim[168], F. Anulli[70a], M. Aoki[79], L. Aperio Bella[35],
G. Arabidze[104], J.P. Araque[136a], V. Araujo Ferraz[78b], R. Araujo Pereira[78b], A.T.H. Arce[47], R.E. Ardell[91],
F.A. Arduh[86], J-F. Arguin[107], S. Argyropoulos[75], A.J. Armbruster[35], L.J. Armitage[90], A Armstrong[168],
O. Arnaez[164], H. Arnold[118], M. Arratia[31], O. Arslan[24], A. Artamonov[109,*], G. Artoni[131], S. Artz[97],
S. Asai[160], N. Asbah[44], A. Ashkenazi[158], E.M. Asimakopoulou[169], L. Asquith[153], K. Assamagan[29],
R. Astalos[28a], R.J. Atkin[32a], M. Atkinson[170], N.B. Atlay[148], K. Augsten[138], G. Avolio[35],
R. Avramidou[58a], M.K. Ayoub[15a], G. Azuelos[107,as], A.E. Baas[59a], M.J. Baca[21], H. Bachacou[142],
K. Bachas[65a,65b], M. Backes[131], P. Bagnaia[70a,70b], M. Bahmani[82], H. Bahrasemani[149], A.J. Bailey[171],
J.T. Baines[141], M. Bajic[39], C. Bakalis[10], O.K. Baker[180], P.J. Bakker[118], D. Bakshi Gupta[93],
E.M. Baldin[120b,120a], P. Balek[177], F. Balli[142], W.K. Balunas[133], J. Balz[97], E. Banas[82],
A. Bandyopadhyay[24], S. Banerjee[178,j], A.A.E. Bannoura[179], L. Barak[158], W.M. Barbe[37],
E.L. Barberio[102], D. Barberis[53b,53a], M. Barbero[99], T. Barillari[113], M-S. Barisits[35], J. Barkeloo[127],
T. Barklow[150], N. Barlow[31], R. Barnea[157], S.L. Barnes[58c], B.M. Barnett[141], R.M. Barnett[18],
Z. Barnovska-Blenessy[58a], A. Baroncelli[72a], G. Barone[26], A.J. Barr[131], L. Barranco Navarro[171],
F. Barreiro[96], J. Barreiro Guimarães da Costa[15a], R. Bartoldus[150], A.E. Barton[87], P. Bartos[28a],
A. Basalaev[134], A. Bassalat[128], R.L. Bates[55], S.J. Batista[164], S. Batlamous[34e], J.R. Batley[31],
M. Battaglia[143], M. Bauce[70a,70b], F. Bauer[142], K.T. Bauer[168], H.S. Bawa[150,l], J.B. Beacham[122],
M.D. Beattie[87], T. Beau[132], P.H. Beauchemin[167], P. Bechtle[24], H.C. Beck[51], H.P. Beck[20,q], K. Becker[50],
M. Becker[97], C. Becot[44], A. Beddall[12d], A.J. Beddall[12a], V.A. Bednyakov[77], M. Bedognetti[118],
C.P. Bee[152], T.A. Beermann[35], M. Begalli[78b], M. Begel[29], A. Behera[152], J.K. Behr[44], A.S. Bell[92],
G. Bella[158], L. Bellagamba[23b], A. Bellerive[33], M. Bellomo[157], P. Bellos[9], K. Belotskiy[110],
N.L. Belyaev[110], O. Benary[158,*], D. Benchekroun[34a], M. Bender[112], N. Benekos[10], Y. Benhammou[158],
E. Benhar Noccioli[180], J. Benitez[75], D.P. Benjamin[47], M. Benoit[52], J.R. Bensinger[26], S. Bentvelsen[118],
L. Beresford[131], M. Beretta[49], D. Berge[44], E. Bergeaas Kuutmann[169], N. Berger[5], L.J. Bergsten[26],
J. Beringer[18], S. Berlendis[7], N.R. Bernard[100], G. Bernardi[132], C. Bernius[150], F.U. Bernlochner[24],
T. Berry[91], P. Berta[97], C. Bertella[15a], G. Bertoli[43a,43b], I.A. Bertram[87], G.J. Besjes[39],
O. Bessidskaia Bylund[43a,43b], M. Bessner[44], N. Besson[142], A. Bethani[98], S. Bethke[113], A. Betti[24],
A.J. Bevan[90], J. Beyer[113], R.M.B. Bianchi[135], O. Biebel[112], D. Biedermann[19], R. Bielski[98],
K. Bierwagen[97], N.V. Biesuz[69a,69b], M. Biglietti[72a], T.R.V. Billoud[107], M. Bindi[51], A. Bingul[12d],
C. Bini[70a,70b], S. Biondi[23b,23a], M. Birman[177], T. Bisanz[51], J.P. Biswal[158], C. Bittrich[46],

D.M. Bjergaard[47], J.E. Black[150], K.M. Black[25], T. Blazek[28a], I. Bloch[44], C. Blocker[26], A. Blue[55], U. Blumenschein[90], Dr. Blunier[144a], G.J. Bobbink[118], V.S. Bobrovnikov[120b,120a], S.S. Bocchetta[94], A. Bocci[47], D. Boerner[179], D. Bogavac[112], A.G. Bogdanchikov[120b,120a], C. Bohm[43a], V. Boisvert[91], P. Bokan[169,x], T. Bold[81a], A.S. Boldyrev[111], A.E. Bolz[59b], M. Bomben[132], M. Bona[90], J.S. Bonilla[127], M. Boonekamp[142], A. Borisov[140], G. Borissov[87], J. Bortfeldt[35], D. Bortoletto[131], V. Bortolotto[71a,61b,61c,71b], D. Boscherini[23b], M. Bosman[14], J.D. Bossio Sola[30], K. Bouaouda[34a], J. Boudreau[135], E.V. Bouhova-Thacker[87], D. Boumediene[37], C. Bourdarios[128], S.K. Boutle[55], A. Boveia[122], J. Boyd[35], I.R. Boyko[77], A.J. Bozson[91], J. Bracinik[21], N. Brahimi[99], A. Brandt[8], G. Brandt[179], O. Brandt[59a], F. Braren[44], U. Bratzler[161], B. Brau[100], J.E. Brau[127], W.D. Breaden Madden[55], K. Brendlinger[44], A.J. Brennan[102], L. Brenner[44], R. Brenner[169], S. Bressler[177], B. Brickwedde[97], D.L. Briglin[21], D. Britton[55], D. Britzger[59b], I. Brock[24], R. Brock[104], G. Brooijmans[38], T. Brooks[91], W.K. Brooks[144b], E. Brost[119], J.H Broughton[21], P.A. Bruckman de Renstrom[82], D. Bruncko[28b], A. Bruni[23b], G. Bruni[23b], L.S. Bruni[118], S. Bruno[71a,71b], B.H. Brunt[31], M. Bruschi[23b], N. Bruscino[135], P. Bryant[36], L. Bryngemark[44], T. Buanes[17], Q. Buat[35], P. Buchholz[148], A.G. Buckley[55], I.A. Budagov[77], F. Buehrer[50], M.K. Bugge[130], O. Bulekov[110], D. Bullock[8], T.J. Burch[119], S. Burdin[88], C.D. Burgard[118], A.M. Burger[5], B. Burghgrave[119], K. Burka[82], S. Burke[141], I. Burmeister[45], J.T.P. Burr[131], D. Büscher[50], V. Büscher[97], E. Buschmann[51], P. Bussey[55], J.M. Butler[25], C.M. Buttar[55], J.M. Butterworth[92], P. Butti[35], W. Buttinger[35], A. Buzatu[155], A.R. Buzykaev[120b,120a], G. Cabras[23b,23a], S. Cabrera Urbán[171], D. Caforio[138], H. Cai[170], V.M.M. Cairo[2], O. Cakir[4a], N. Calace[52], P. Calafiura[18], A. Calandri[99], G. Calderini[132], P. Calfayan[63], G. Callea[40b,40a], L.P. Caloba[78b], S. Calvente Lopez[96], D. Calvet[37], S. Calvet[37], T.P. Calvet[152], M. Calvetti[69a,69b], R. Camacho Toro[132], S. Camarda[35], P. Camarri[71a,71b], D. Cameron[130], R. Caminal Armadans[100], C. Camincher[35], S. Campana[35], M. Campanelli[92], A. Camplani[39], A. Campoverde[148], V. Canale[67a,67b], M. Cano Bret[58c], J. Cantero[125], T. Cao[158], Y. Cao[170], M.D.M. Capeans Garrido[35], I. Caprini[27b], M. Caprini[27b], M. Capua[40b,40a], R.M. Carbone[38], R. Cardarelli[71a], F.C. Cardillo[50], I. Carli[139], T. Carli[35], G. Carlino[67a], B.T. Carlson[135], L. Carminati[66a,66b], R.M.D. Carney[43a,43b], S. Caron[117], E. Carquin[144b], S. Carrá[66a,66b], G.D. Carrillo-Montoya[35], D. Casadei[32b], M.P. Casado[14,f], A.F. Casha[164], M. Casolino[14], D.W. Casper[168], R. Castelijn[118], F.L. Castillo[171], V. Castillo Gimenez[171], N.F. Castro[136a,136e], A. Catinaccio[35], J.R. Catmore[130], A. Cattai[35], J. Caudron[24], V. Cavaliere[29], E. Cavallaro[14], D. Cavalli[66a], M. Cavalli-Sforza[14], V. Cavasinni[69a,69b], E. Celebi[12b], F. Ceradini[72a,72b], L. Cerda Alberich[171], A.S. Cerqueira[78a], A. Cerri[153], L. Cerrito[71a,71b], F. Cerutti[18], A. Cervelli[23b,23a], S.A. Cetin[12b], A. Chafaq[34a], D Chakraborty[119], S.K. Chan[57], W.S. Chan[118], Y.L. Chan[61a], J.D. Chapman[31], D.G. Charlton[21], C.C. Chau[33], C.A. Chavez Barajas[153], S. Che[122], A. Chegwidden[104], S. Chekanov[6], S.V. Chekulaev[165a], G.A. Chelkov[77,ar], M.A. Chelstowska[35], C. Chen[58a], C.H. Chen[76], H. Chen[29], J. Chen[58a], J. Chen[38], S. Chen[133], S.J. Chen[15c], X. Chen[15b,aq], Y. Chen[80], Y-H. Chen[44], H.C. Cheng[103], H.J. Cheng[15d], A. Cheplakov[77], E. Cheremushkina[140], R. Cherkaoui El Moursli[34e], E. Cheu[7], K. Cheung[62], L. Chevalier[142], V. Chiarella[49], G. Chiarelli[69a], G. Chiodini[65a], A.S. Chisholm[35], A. Chitan[27b], I. Chiu[160], Y.H. Chiu[173], M.V. Chizhov[77], K. Choi[63], A.R. Chomont[128], S. Chouridou[159], Y.S. Chow[118], V. Christodoulou[92], M.C. Chu[61a], J. Chudoba[137], A.J. Chuinard[101], J.J. Chwastowski[82], L. Chytka[126], D. Cinca[45], V. Cindro[89], I.A. Cioară[24], A. Ciocio[18], F. Cirotto[67a,67b], Z.H. Citron[177], M. Citterio[66a], A. Clark[52], M.R. Clark[38], P.J. Clark[48], C. Clement[43a,43b], Y. Coadou[99], M. Cobal[64a,64c], A. Coccaro[53b,53a], J. Cochran[76], A.E.C. Coimbra[177], L. Colasurdo[117], B. Cole[38], A.P. Colijn[118], J. Collot[56], P. Conde Muiño[136a,136b], E. Coniavitis[50], S.H. Connell[32b], I.A. Connelly[98], S. Constantinescu[27b], F. Conventi[67a,at], A.M. Cooper-Sarkar[131], F. Cormier[172], K.J.R. Cormier[164], M. Corradi[70a,70b], E.E. Corrigan[94], F. Corriveau[101,ac], A. Cortes-Gonzalez[35], M.J. Costa[171], D. Costanzo[146], G. Cottin[31], G. Cowan[91], B.E. Cox[98], J. Crane[98], K. Cranmer[121], S.J. Crawley[55], R.A. Creager[133], G. Cree[33], S. Crépé-Renaudin[56], F. Crescioli[132], M. Cristinziani[24], V. Croft[121],

41

G. Crosetti[40b,40a], A. Cueto[96], T. Cuhadar Donszelmann[146], A.R. Cukierman[150], J. Cúth[97], S. Czekierda[82], P. Czodrowski[35], M.J. Da Cunha Sargedas De Sousa[58b,136b], C. Da Via[98], W. Dabrowski[81a], T. Dado[28a,x], S. Dahbi[34e], T. Dai[103], F. Dallaire[107], C. Dallapiccola[100], M. Dam[39], G. D'amen[23b,23a], J. Damp[97], J.R. Dandoy[133], M.F. Daneri[30], N.P. Dang[178,j], N.D Dann[98], M. Danninger[172], V. Dao[35], G. Darbo[53b], S. Darmora[8], O. Dartsi[5], A. Dattagupta[127], T. Daubney[44], S. D'Auria[55], W. Davey[24], C. David[44], T. Davidek[139], D.R. Davis[47], E. Dawe[102], I. Dawson[146], K. De[8], R. De Asmundis[67a], A. De Benedetti[124], M. De Beurs[118], S. De Castro[23b,23a], S. De Cecco[70a,70b], N. De Groot[117], P. de Jong[118], H. De la Torre[104], F. De Lorenzi[76], A. De Maria[51,s], D. De Pedis[70a], A. De Salvo[70a], U. De Sanctis[71a,71b], A. De Santo[153], K. De Vasconcelos Corga[99], J.B. De Vivie De Regie[128], C. Debenedetti[143], D.V. Dedovich[77], N. Dehghanian[3], M. Del Gaudio[40b,40a], J. Del Peso[96], Y. Delabat Diaz[44], D. Delgove[128], F. Deliot[142], C.M. Delitzsch[7], M. Della Pietra[67a,67b], D. Della Volpe[52], A. Dell'Acqua[35], L. Dell'Asta[25], M. Delmastro[5], C. Delporte[128], P.A. Delsart[56], D.A. DeMarco[164], S. Demers[180], M. Demichev[77], S.P. Denisov[140], D. Denysiuk[118], L. D'Eramo[132], D. Derendarz[82], J.E. Derkaoui[34d], F. Derue[132], P. Dervan[88], K. Desch[24], C. Deterre[44], K. Dette[164], M.R. Devesa[30], P.O. Deviveiros[35], A. Dewhurst[141], S. Dhaliwal[26], F.A. Di Bello[52], A. Di Ciaccio[71a,71b], L. Di Ciaccio[5], W.K. Di Clemente[133], C. Di Donato[67a,67b], A. Di Girolamo[35], B. Di Micco[72a,72b], R. Di Nardo[100], K.F. Di Petrillo[57], A. Di Simone[50], R. Di Sipio[164], D. Di Valentino[33], C. Diaconu[99], M. Diamond[164], F.A. Dias[39], T. Dias Do Vale[136a], M.A. Diaz[144a], J. Dickinson[18], E.B. Diehl[103], J. Dietrich[19], S. Díez Cornell[44], A. Dimitrievska[18], J. Dingfelder[24], F. Dittus[35], F. Djama[99], T. Djobava[156b], J.I. Djuvsland[59a], M.A.B. Do Vale[78c], M. Dobre[27b], D. Dodsworth[26], C. Doglioni[94], J. Dolejsi[139], Z. Dolezal[139], M. Donadelli[78d], J. Donini[37], A. D'onofrio[90], M. D'Onofrio[88], J. Dopke[141], A. Doria[67a], M.T. Dova[86], A.T. Doyle[55], E. Drechsler[51], E. Dreyer[149], T. Dreyer[51], Y. Du[58b], J. Duarte-Campderros[158], F. Dubinin[108], M. Dubovsky[28a], A. Dubreuil[52], E. Duchovni[177], G. Duckeck[112], A. Ducourthial[132], O.A. Ducu[107,w], D. Duda[113], A. Dudarev[35], A.C. Dudder[97], E.M. Duffield[18], L. Duflot[128], M. Dührssen[35], C. Dülsen[179], M. Dumancic[177], A.E. Dumitriu[27b,d], A.K. Duncan[55], M. Dunford[59a], A. Duperrin[99], H. Duran Yildiz[4a], M. Düren[54], A. Durglishvili[156b], D. Duschinger[46], B. Dutta[44], D. Duvnjak[1], M. Dyndal[44], S. Dysch[98], B.S. Dziedzic[82], C. Eckardt[44], K.M. Ecker[113], R.C. Edgar[103], T. Eifert[35], G. Eigen[17], K. Einsweiler[18], T. Ekelof[169], M. El Kacimi[34c], R. El Kosseifi[99], V. Ellajosyula[99], M. Ellert[169], F. Ellinghaus[179], A.A. Elliot[90], N. Ellis[35], J. Elmsheuser[29], M. Elsing[35], D. Emeliyanov[141], Y. Enari[160], J.S. Ennis[175], M.B. Epland[47], J. Erdmann[45], A. Ereditato[20], S. Errede[170], M. Escalier[128], C. Escobar[171], O. Estrada Pastor[171], A.I. Etienvre[142], E. Etzion[158], H. Evans[63], A. Ezhilov[134], M. Ezzi[34e], F. Fabbri[55], L. Fabbri[23b,23a], V. Fabiani[117], G. Facini[92], R.M. Faisca Rodrigues Pereira[136a], R.M. Fakhrutdinov[140], S. Falciano[70a], P.J. Falke[5], S. Falke[5], J. Faltova[139], Y. Fang[15a], M. Fanti[66a,66b], A. Farbin[8], A. Farilla[72a], E.M. Farina[68a,68b], T. Farooque[104], S. Farrell[18], S.M. Farrington[175], P. Farthouat[35], F. Fassi[34e], P. Fassnacht[35], D. Fassouliotis[9], M. Faucci Giannelli[48], A. Favareto[53b,53a], W.J. Fawcett[52], L. Fayard[128], O.L. Fedin[134,p], W. Fedorko[172], M. Feickert[41], S. Feigl[130], L. Feligioni[99], C. Feng[58b], E.J. Feng[35], M. Feng[47], M.J. Fenton[55], A.B. Fenyuk[140], L. Feremenga[8], J. Ferrando[44], A. Ferrari[169], P. Ferrari[118], R. Ferrari[68a], D.E. Ferreira de Lima[59b], A. Ferrer[171], D. Ferrere[52], C. Ferretti[103], F. Fiedler[97], A. Filipčič[89], F. Filthaut[117], K.D. Finelli[25], M.C.N. Fiolhais[136a,136c,a], L. Fiorini[171], C. Fischer[14], W.C. Fisher[104], N. Flaschel[44], I. Fleck[148], P. Fleischmann[103], R.R.M. Fletcher[133], T. Flick[179], B.M. Flierl[112], L.M. Flores[133], L.R. Flores Castillo[61a], N. Fomin[17], G.T. Forcolin[98], A. Formica[142], F.A. Förster[14], A.C. Forti[98], A.G. Foster[21], D. Fournier[128], H. Fox[87], S. Fracchia[146], P. Francavilla[69a,69b], M. Franchini[23b,23a], S. Franchino[59a], D. Francis[35], L. Franconi[130], M. Franklin[57], M. Frate[168], M. Fraternali[68a,68b], D. Freeborn[92], S.M. Fressard-Batraneanu[35], B. Freund[107], W.S. Freund[78b], D. Froidevaux[35], J.A. Frost[131], C. Fukunaga[161], E. Fullana Torregrosa[171], T. Fusayasu[114], J. Fuster[171], O. Gabizon[157], A. Gabrielli[23b,23a], A. Gabrielli[18], G.P. Gach[81a], S. Gadatsch[52], P. Gadow[113],

G. Gagliardi[53b,53a], L.G. Gagnon[107], C. Galea[27b], B. Galhardo[136a,136c], E.J. Gallas[131], B.J. Gallop[141], P. Gallus[138], G. Galster[39], R. Gamboa Goni[90], K.K. Gan[122], S. Ganguly[177], Y. Gao[88], Y.S. Gao[150,l], C. García[171], J.E. García Navarro[171], J.A. García Pascual[15a], M. Garcia-Sciveres[18], R.W. Gardner[36], N. Garelli[150], V. Garonne[130], K. Gasnikova[44], A. Gaudiello[53b,53a], G. Gaudio[68a], I.L. Gavrilenko[108], A. Gavrilyuk[109], C. Gay[172], G. Gaycken[24], E.N. Gazis[10], C.N.P. Gee[141], J. Geisen[51], M. Geisen[97], M.P. Geisler[59a], K. Gellerstedt[43a,43b], C. Gemme[53b], M.H. Genest[56], C. Geng[103], S. Gentile[70a,70b], C. Gentsos[159], S. George[91], D. Gerbaudo[14], G. Gessner[45], S. Ghasemi[148], M. Ghasemi Bostanabad[173], M. Ghneimat[24], B. Giacobbe[23b], S. Giagu[70a,70b], N. Giangiacomi[23b,23a], P. Giannetti[69a], A. Giannini[67a,67b], S.M. Gibson[91], M. Gignac[143], D. Gillberg[33], G. Gilles[179], D.M. Gingrich[3,as], M.P. Giordani[64a,64c], F.M. Giorgi[23b], P.F. Giraud[142], P. Giromini[57], G. Giugliarelli[64a,64c], D. Giugni[66a], F. Giuli[131], M. Giulini[59b], S. Gkaitatzis[159], I. Gkialas[9,i], E.L. Gkougkousis[14], P. Gkountoumis[10], L.K. Gladilin[111], C. Glasman[96], J. Glatzer[14], P.C.F. Glaysher[44], A. Glazov[44], M. Goblirsch-Kolb[26], J. Godlewski[82], S. Goldfarb[102], T. Golling[52], D. Golubkov[140], A. Gomes[136a,136b,136d], R. Goncalves Gama[78a], R. Gonçalo[136a], G. Gonella[50], L. Gonella[21], A. Gongadze[77], F. Gonnella[21], J.L. Gonski[57], S. González de la Hoz[171], S. Gonzalez-Sevilla[52], L. Goossens[35], P.A. Gorbounov[109], H.A. Gordon[29], B. Gorini[35], E. Gorini[65a,65b], A. Gorišek[89], A.T. Goshaw[47], C. Gössling[45], M.I. Gostkin[77], C.A. Gottardo[24], C.R. Goudet[128], D. Goujdami[34c], A.G. Goussiou[145], N. Govender[32b,b], C. Goy[5], E. Gozani[157], I. Grabowska-Bold[81a], P.O.J. Gradin[169], E.C. Graham[88], J. Gramling[168], E. Gramstad[130], S. Grancagnolo[19], V. Gratchev[134], P.M. Gravila[27f], C. Gray[55], H.M. Gray[18], Z.D. Greenwood[93,ai], C. Grefe[24], K. Gregersen[92], I.M. Gregor[44], P. Grenier[150], K. Grevtsov[44], J. Griffiths[8], A.A. Grillo[143], K. Grimm[150], S. Grinstein[14,y], Ph. Gris[37], J.-F. Grivaz[128], S. Groh[97], E. Gross[177], J. Grosse-Knetter[51], G.C. Grossi[93], Z.J. Grout[92], C. Grud[103], A. Grummer[116], L. Guan[103], W. Guan[178], J. Guenther[35], A. Guerguichon[128], F. Guescini[165a], D. Guest[168], R. Gugel[50], B. Gui[122], T. Guillemin[5], S. Guindon[35], U. Gul[55], C. Gumpert[35], J. Guo[58c], W. Guo[103], Y. Guo[58a,r], Z. Guo[99], R. Gupta[41], S. Gurbuz[12c], G. Gustavino[124], B.J. Gutelman[157], P. Gutierrez[124], C. Gutschow[92], C. Guyot[142], M.P. Guzik[81a], C. Gwenlan[131], C.B. Gwilliam[88], A. Haas[121], C. Haber[18], H.K. Hadavand[8], N. Haddad[34e], A. Hadef[58a], S. Hageböck[24], M. Hagihara[166], H. Hakobyan[181,*], M. Haleem[174], J. Haley[125], G. Halladjian[104], G.D. Hallewell[99], K. Hamacher[179], P. Hamal[126], K. Hamano[173], A. Hamilton[32a], G.N. Hamity[146], K. Han[58a,ah], L. Han[58a], S. Han[15d], K. Hanagaki[79,u], M. Hance[143], D.M. Handl[112], B. Haney[133], R. Hankache[132], P. Hanke[59a], E. Hansen[94], J.B. Hansen[39], J.D. Hansen[39], M.C. Hansen[24], P.H. Hansen[39], K. Hara[166], A.S. Hard[178], T. Harenberg[179], S. Harkusha[105], P.F. Harrison[175], N.M. Hartmann[112], Y. Hasegawa[147], A. Hasib[48], S. Hassani[142], S. Haug[20], R. Hauser[104], L. Hauswald[46], L.B. Havener[38], M. Havranek[138], C.M. Hawkes[21], R.J. Hawkings[35], D. Hayden[104], C. Hayes[152], C.P. Hays[131], J.M. Hays[90], H.S. Hayward[88], S.J. Haywood[141], M.P. Heath[48], V. Hedberg[94], L. Heelan[8], S. Heer[24], K.K. Heidegger[50], J. Heilman[33], S. Heim[44], T. Heim[18], B. Heinemann[44,an], J.J. Heinrich[112], L. Heinrich[121], C. Heinz[54], J. Hejbal[137], L. Helary[35], A. Held[172], S. Hellesund[130], S. Hellman[43a,43b], C. Helsens[35], R.C.W. Henderson[87], Y. Heng[178], S. Henkelmann[172], A.M. Henriques Correia[35], G.H. Herbert[19], H. Herde[26], V. Herget[174], Y. Hernández Jiménez[32c], H. Herr[97], M.G. Herrmann[112], G. Herten[50], R. Hertenberger[112], L. Hervas[35], T.C. Herwig[133], G.G. Hesketh[92], N.P. Hessey[165a], J.W. Hetherly[41], S. Higashino[79], E. Higón-Rodriguez[171], K. Hildebrand[36], E. Hill[173], J.C. Hill[31], K.K. Hill[29], K.H. Hiller[44], S.J. Hillier[21], M. Hils[46], I. Hinchliffe[18], M. Hirose[129], D. Hirschbuehl[179], B. Hiti[89], O. Hladik[137], D.R. Hlaluku[32c], X. Hoad[48], J. Hobbs[152], N. Hod[165a], M.C. Hodgkinson[146], A. Hoecker[35], M.R. Hoeferkamp[116], F. Hoenig[112], D. Hohn[24], D. Hohov[128], T.R. Holmes[36], M. Holzbock[112], M. Homann[45], S. Honda[166], T. Honda[79], T.M. Hong[135], A. Hönle[113], B.H. Hooberman[170], W.H. Hopkins[127], Y. Horii[115], P. Horn[46], A.J. Horton[149], L.A. Horyn[36], J-Y. Hostachy[56], A. Hostiuc[145], S. Hou[155], A. Hoummada[34a], J. Howarth[98], J. Hoya[86], M. Hrabovsky[126], J. Hrdinka[35], I. Hristova[19], J. Hrivnac[128], A. Hrynevich[106],

T. Hryn'ova[5], P.J. Hsu[62], S.-C. Hsu[145], Q. Hu[29], S. Hu[58c], Y. Huang[15a], Z. Hubacek[138], F. Hubaut[99], M. Huebner[24], F. Huegging[24], T.B. Huffman[131], E.W. Hughes[38], M. Huhtinen[35], R.F.H. Hunter[33], P. Huo[152], A.M. Hupe[33], N. Huseynov[77,ae], J. Huston[104], J. Huth[57], R. Hyneman[103], G. Iacobucci[52], G. Iakovidis[29], I. Ibragimov[148], L. Iconomidou-Fayard[128], Z. Idrissi[34e], P. Iengo[35], R. Ignazzi[39], O. Igonkina[118,aa], R. Iguchi[160], T. Iizawa[52], Y. Ikegami[79], M. Ikeno[79], D. Iliadis[159], N. Ilic[150], F. Iltzsche[46], G. Introzzi[68a,68b], M. Iodice[72a], K. Iordanidou[38], V. Ippolito[70a,70b], M.F. Isacson[169], N. Ishijima[129], M. Ishino[160], M. Ishitsuka[162], W. Islam[125], C. Issever[131], S. Istin[12c,am], F. Ito[166], J.M. Iturbe Ponce[61a], R. Iuppa[73a,73b], A. Ivina[177], H. Iwasaki[79], J.M. Izen[42], V. Izzo[67a], S. Jabbar[3], P. Jacka[137], P. Jackson[1], R.M. Jacobs[24], V. Jain[2], G. Jäkel[179], K.B. Jakobi[97], K. Jakobs[50], S. Jakobsen[74], T. Jakoubek[137], D.O. Jamin[125], D.K. Jana[93], R. Jansky[52], J. Janssen[24], M. Janus[51], P.A. Janus[81a], G. Jarlskog[94], N. Javadov[77,ae], T. Javůrek[50], M. Javurkova[50], F. Jeanneau[142], L. Jeanty[18], J. Jejelava[156a,af], A. Jelinskas[175], P. Jenni[50,c], J. Jeong[44], S. Jézéquel[5], H. Ji[178], J. Jia[152], H. Jiang[76], Y. Jiang[58a], Z. Jiang[150], S. Jiggins[50], F.A. Jimenez Morales[37], J. Jimenez Pena[171], S. Jin[15c], A. Jinaru[27b], O. Jinnouchi[162], H. Jivan[32c], P. Johansson[146], K.A. Johns[7], C.A. Johnson[63], W.J. Johnson[145], K. Jon-And[43a,43b], R.W.L. Jones[87], S.D. Jones[153], S. Jones[7], T.J. Jones[88], J. Jongmanns[59a], P.M. Jorge[136a,136b], J. Jovicevic[165a], X. Ju[178], J.J. Junggeburth[113], A. Juste Rozas[14,y], A. Kaczmarska[82], M. Kado[128], H. Kagan[122], M. Kagan[150], T. Kaji[176], E. Kajomovitz[157], C.W. Kalderon[94], A. Kaluza[97], S. Kama[41], A. Kamenshchikov[140], L. Kanjir[89], Y. Kano[160], V.A. Kantserov[110], J. Kanzaki[79], B. Kaplan[121], L.S. Kaplan[178], D. Kar[32c], M.J. Kareem[165b], E. Karentzos[10], S.N. Karpov[77], Z.M. Karpova[77], V. Kartvelishvili[87], A.N. Karyukhin[140], K. Kasahara[166], L. Kashif[178], R.D. Kass[122], A. Kastanas[151], Y. Kataoka[160], C. Kato[160], J. Katzy[44], K. Kawade[80], K. Kawagoe[85], T. Kawamoto[160], G. Kawamura[51], E.F. Kay[88], V.F. Kazanin[120b,120a], R. Keeler[173], R. Kehoe[41], J.S. Keller[33], E. Kellermann[94], J.J. Kempster[21], J. Kendrick[21], O. Kepka[137], S. Kersten[179], B.P. Kerševan[89], R.A. Keyes[101], M. Khader[170], F. Khalil-Zada[13], A. Khanov[125], A.G. Kharlamov[120b,120a], T. Kharlamova[120b,120a], A. Khodinov[163], T.J. Khoo[52], E. Khramov[77], J. Khubua[156b], S. Kido[80], M. Kiehn[52], C.R. Kilby[91], S.H. Kim[166], Y.K. Kim[36], N. Kimura[64a,64c], O.M. Kind[19], B.T. King[88], D. Kirchmeier[46], J. Kirk[141], A.E. Kiryunin[113], T. Kishimoto[160], D. Kisielewska[81a], V. Kitali[44], O. Kivernyk[5], E. Kladiva[28b], T. Klapdor-Kleingrothaus[50], M.H. Klein[103], M. Klein[88], U. Klein[88], K. Kleinknecht[97], P. Klimek[119], A. Klimentov[29], R. Klingenberg[45,*], T. Klingl[24], T. Klioutchnikova[35], F.F. Klitzner[112], P. Kluit[118], S. Kluth[113], E. Kneringer[74], E.B.F.G. Knoops[99], A. Knue[50], A. Kobayashi[160], D. Kobayashi[85], T. Kobayashi[160], M. Kobel[46], M. Kocian[150], P. Kodys[139], T. Koffas[33], E. Koffeman[118], N.M. Köhler[113], T. Koi[150], M. Kolb[59b], I. Koletsou[5], T. Kondo[79], N. Kondrashova[58c], K. Köneke[50], A.C. König[117], T. Kono[79], R. Konoplich[121,aj], V. Konstantinides[92], N. Konstantinidis[92], B. Konya[94], R. Kopeliansky[63], S. Koperny[81a], K. Korcyl[82], K. Kordas[159], A. Korn[92], I. Korolkov[14], E.V. Korolkova[146], O. Kortner[113], S. Kortner[113], T. Kosek[139], V.V. Kostyukhin[24], A. Kotwal[47], A. Koulouris[10], A. Kourkoumeli-Charalampidi[68a,68b], C. Kourkoumelis[9], E. Kourlitis[146], V. Kouskoura[29], A.B. Kowalewska[82], R. Kowalewski[173], T.Z. Kowalski[81a], C. Kozakai[160], W. Kozanecki[142], A.S. Kozhin[140], V.A. Kramarenko[111], G. Kramberger[89], D. Krasnopevtsev[110], M.W. Krasny[132], A. Krasznahorkay[35], D. Krauss[113], J.A. Kremer[81a], J. Kretzschmar[88], P. Krieger[164], K. Krizka[18], K. Kroeninger[45], H. Kroha[113], J. Kroll[137], J. Kroll[133], J. Krstic[16], U. Kruchonak[77], H. Krüger[24], N. Krumnack[76], M.C. Kruse[47], T. Kubota[102], S. Kuday[4b], J.T. Kuechler[179], S. Kuehn[35], A. Kugel[59a], F. Kuger[174], T. Kuhl[44], V. Kukhtin[77], R. Kukla[99], Y. Kulchitsky[105], S. Kuleshov[144b], Y.P. Kulinich[170], M. Kuna[56], T. Kunigo[83], A. Kupco[137], T. Kupfer[45], O. Kuprash[158], H. Kurashige[80], L.L. Kurchaninov[165a], Y.A. Kurochkin[105], M.G. Kurth[15d], E.S. Kuwertz[173], M. Kuze[162], J. Kvita[126], T. Kwan[101], A. La Rosa[113], J.L. La Rosa Navarro[78d], L. La Rotonda[40b,40a], F. La Ruffa[40b,40a], C. Lacasta[171], F. Lacava[70a,70b], J. Lacey[44], D.P.J. Lack[98], H. Lacker[19], D. Lacour[132], E. Ladygin[77], R. Lafaye[5], B. Laforge[132], T. Lagouri[32c], S. Lai[51], S. Lammers[63], W. Lampl[7], E. Lançon[29],

44

U. Landgraf[50], M.P.J. Landon[90], M.C. Lanfermann[52], V.S. Lang[44], J.C. Lange[14], R.J. Langenberg[35], A.J. Lankford[168], F. Lanni[29], K. Lantzsch[24], A. Lanza[68a], A. Lapertosa[53b,53a], S. Laplace[132], J.F. Laporte[142], T. Lari[66a], F. Lasagni Manghi[23b,23a], M. Lassnig[35], T.S. Lau[61a], A. Laudrain[128], M. Lavorgna[67a,67b], A.T. Law[143], P. Laycock[88], M. Lazzaroni[66a,66b], B. Le[102], O. Le Dortz[132], E. Le Guirriec[99], E.P. Le Quilleuc[142], M. LeBlanc[7], T. LeCompte[6], F. Ledroit-Guillon[56], C.A. Lee[29], G.R. Lee[144a], L. Lee[57], S.C. Lee[155], B. Lefebvre[101], M. Lefebvre[173], F. Legger[112], C. Leggett[18], N. Lehmann[179], G. Lehmann Miotto[35], W.A. Leight[44], A. Leisos[159,v], M.A.L. Leite[78d], R. Leitner[139], D. Lellouch[177], B. Lemmer[51], K.J.C. Leney[92], T. Lenz[24], B. Lenzi[35], R. Leone[7], S. Leone[69a], C. Leonidopoulos[48], G. Lerner[153], C. Leroy[107], R. Les[164], A.A.J. Lesage[142], C.G. Lester[31], M. Levchenko[134], J. Levêque[5], D. Levin[103], L.J. Levinson[177], D. Lewis[90], B. Li[103], C-Q. Li[58a], H. Li[58b], L. Li[58c], Q. Li[15d], Q.Y. Li[58a], S. Li[58d,58c], X. Li[58c], Y. Li[148], Z. Liang[15a], B. Liberti[71a], A. Liblong[164], K. Lie[61c], S. Liem[118], A. Limosani[154], C.Y. Lin[31], K. Lin[104], T.H. Lin[97], R.A. Linck[63], B.E. Lindquist[152], A.L. Lionti[52], E. Lipeles[133], A. Lipniacka[17], M. Lisovyi[59b], T.M. Liss[170,ap], A. Lister[172], A.M. Litke[143], J.D. Little[8], B. Liu[76], B.L Liu[6], H.B. Liu[29], H. Liu[103], J.B. Liu[58a], J.K.K. Liu[131], K. Liu[132], M. Liu[58a], P. Liu[18], Y. Liu[15a], Y.L. Liu[58a], Y.W. Liu[58a], M. Livan[68a,68b], A. Lleres[56], J. Llorente Merino[15a], S.L. Lloyd[90], C.Y. Lo[61b], F. Lo Sterzo[41], E.M. Lobodzinska[44], P. Loch[7], A. Loesle[50], K.M. Loew[26], T. Lohse[19], K. Lohwasser[146], M. Lokajicek[137], B.A. Long[25], J.D. Long[170], R.E. Long[87], L. Longo[65a,65b], K.A. Looper[122], J.A. Lopez[144b], I. Lopez Paz[14], A. Lopez Solis[146], J. Lorenz[112], N. Lorenzo Martinez[5], M. Losada[22], P.J. Lösel[112], X. Lou[44], X. Lou[15a], A. Lounis[128], J. Love[6], P.A. Love[87], J.J. Lozano Bahilo[171], H. Lu[61a], M. Lu[58a], N. Lu[103], Y.J. Lu[62], H.J. Lubatti[145], C. Luci[70a,70b], A. Lucotte[56], C. Luedtke[50], F. Luehring[63], I. Luise[132], W. Lukas[74], L. Luminari[70a], B. Lund-Jensen[151], M.S. Lutz[100], P.M. Luzi[132], D. Lynn[29], R. Lysak[137], E. Lytken[94], F. Lyu[15a], V. Lyubushkin[77], H. Ma[29], L.L. Ma[58b], Y. Ma[58b], G. Maccarrone[49], A. Macchiolo[113], C.M. Macdonald[146], J. Machado Miguens[133,136b], D. Madaffari[171], R. Madar[37], W.F. Mader[46], A. Madsen[44], N. Madysa[46], J. Maeda[80], K. Maekawa[160], S. Maeland[17], T. Maeno[29], A.S. Maevskiy[111], V. Magerl[50], C. Maidantchik[78b], T. Maier[112], A. Maio[136a,136b,136d], O. Majersky[28a], S. Majewski[127], Y. Makida[79], N. Makovec[128], B. Malaescu[132], Pa. Malecki[82], V.P. Maleev[134], F. Malek[56], U. Mallik[75], D. Malon[6], C. Malone[31], S. Maltezos[10], S. Malyukov[35], J. Mamuzic[171], G. Mancini[49], I. Mandić[89], J. Maneira[136a], L. Manhaes de Andrade Filho[78a], J. Manjarres Ramos[46], K.H. Mankinen[94], A. Mann[112], A. Manousos[74], B. Mansoulie[142], J.D. Mansour[15a], M. Mantoani[51], S. Manzoni[66a,66b], G. Marceca[30], L. March[52], L. Marchese[131], G. Marchiori[132], M. Marcisovsky[137], C.A. Marin Tobon[35], M. Marjanovic[37], D.E. Marley[103], F. Marroquim[78b], Z. Marshall[18], M.U.F Martensson[169], S. Marti-Garcia[171], C.B. Martin[122], T.A. Martin[175], V.J. Martin[48], B. Martin dit Latour[17], M. Martinez[14,y], V.I. Martinez Outschoorn[100], S. Martin-Haugh[141], V.S. Martoiu[27b], A.C. Martyniuk[92], A. Marzin[35], L. Masetti[97], T. Mashimo[160], R. Mashinistov[108], J. Masik[98], A.L. Maslennikov[120b,120a], L.H. Mason[102], L. Massa[71a,71b], P. Mastrandrea[5], A. Mastroberardino[40b,40a], T. Masubuchi[160], P. Mättig[179], J. Maurer[27b], B. Maček[89], S.J. Maxfield[88], D.A. Maximov[120b,120a], R. Mazini[155], I. Maznas[159], S.M. Mazza[143], N.C. Mc Fadden[116], G. Mc Goldrick[164], S.P. Mc Kee[103], A. McCarn[103], T.G. McCarthy[113], L.I. McClymont[92], E.F. McDonald[102], J.A. Mcfayden[35], G. Mchedlidze[51], M.A. McKay[41], K.D. McLean[173], S.J. McMahon[141], P.C. McNamara[102], C.J. McNicol[175], R.A. McPherson[173,ac], J.E. Mdhluli[32c], Z.A. Meadows[100], S. Meehan[145], T. Megy[50], S. Mehlhase[112], A. Mehta[88], T. Meideck[56], B. Meirose[42], D. Melini[171,g], B.R. Mellado Garcia[32c], J.D. Mellenthin[51], M. Melo[28a], F. Meloni[44], A. Melzer[24], S.B. Menary[98], E.D. Mendes Gouveia[136a], L. Meng[88], X.T. Meng[103], A. Mengarelli[23b,23a], S. Menke[113], E. Meoni[40b,40a], S. Mergelmeyer[19], C. Merlassino[20], P. Mermod[52], L. Merola[67a,67b], C. Meroni[66a], F.S. Merritt[36], A. Messina[70a,70b], J. Metcalfe[6], A.S. Mete[168], C. Meyer[133], J. Meyer[157], J-P. Meyer[142], H. Meyer Zu Theenhausen[59a], F. Miano[153], R.P. Middleton[141], L. Mijović[48], G. Mikenberg[177], M. Mikestikova[137], M. Mikuž[89], M. Milesi[102],

A. Milic[164], D.A. Millar[90], D.W. Miller[36], A. Milov[177], D.A. Milstead[43a,43b], A.A. Minaenko[140],
M. Miñano Moya[171], I.A. Minashvili[156b], A.I. Mincer[121], B. Mindur[81a], M. Mineev[77], Y. Minegishi[160],
Y. Ming[178], L.M. Mir[14], A. Mirto[65a,65b], K.P. Mistry[133], T. Mitani[176], J. Mitrevski[112], V.A. Mitsou[171],
A. Miucci[20], P.S. Miyagawa[146], A. Mizukami[79], J.U. Mjörnmark[94], T. Mkrtchyan[181], M. Mlynarikova[139],
T. Moa[43a,43b], K. Mochizuki[107], P. Mogg[50], S. Mohapatra[38], S. Molander[43a,43b], R. Moles-Valls[24],
M.C. Mondragon[104], K. Mönig[44], J. Monk[39], E. Monnier[99], A. Montalbano[149], J. Montejo Berlingen[35],
F. Monticelli[86], S. Monzani[66a], R.W. Moore[3], N. Morange[128], D. Moreno[22], M. Moreno Llácer[35],
P. Morettini[53b], M. Morgenstern[118], S. Morgenstern[46], D. Mori[149], T. Mori[160], M. Morii[57],
M. Morinaga[176], V. Morisbak[130], A.K. Morley[35], G. Mornacchi[35], A.P. Morris[92], J.D. Morris[90],
L. Morvaj[152], P. Moschovakos[10], M. Mosidze[156b], H.J. Moss[146], J. Moss[150,m], K. Motohashi[162],
R. Mount[150], E. Mountricha[35], E.J.W. Moyse[100], S. Muanza[99], F. Mueller[113], J. Mueller[135],
R.S.P. Mueller[112], D. Muenstermann[87], P. Mullen[55], G.A. Mullier[20], F.J. Munoz Sanchez[98], P. Murin[28b],
W.J. Murray[175,141], A. Murrone[66a,66b], M. Muškinja[89], C. Mwewa[32a], A.G. Myagkov[140,ak], J. Myers[127],
M. Myska[138], B.P. Nachman[18], O. Nackenhorst[45], K. Nagai[131], K. Nagano[79], Y. Nagasaka[60],
K. Nagata[166], M. Nagel[50], E. Nagy[99], A.M. Nairz[35], Y. Nakahama[115], K. Nakamura[79], T. Nakamura[160],
I. Nakano[123], H. Nanjo[129], F. Napolitano[59a], R.F. Naranjo Garcia[44], R. Narayan[11], D.I. Narrias Villar[59a],
I. Naryshkin[134], T. Naumann[44], G. Navarro[22], R. Nayyar[7], H.A. Neal[103], P.Y. Nechaeva[108], T.J. Neep[142],
A. Negri[68a,68b], M. Negrini[23b], S. Nektarijevic[117], C. Nellist[51], M.E. Nelson[131], S. Nemecek[137],
P. Nemethy[121], M. Nessi[35,e], M.S. Neubauer[170], M. Neumann[179], P.R. Newman[21], T.Y. Ng[61c], Y.S. Ng[19],
H.D.N. Nguyen[99], T. Nguyen Manh[107], E. Nibigira[37], R.B. Nickerson[131], R. Nicolaidou[142],
J. Nielsen[143], N. Nikiforou[11], V. Nikolaenko[140,ak], I. Nikolic-Audit[132], K. Nikolopoulos[21], P. Nilsson[29],
Y. Ninomiya[79], A. Nisati[70a], N. Nishu[58c], R. Nisius[113], I. Nitsche[45], T. Nitta[176], T. Nobe[160],
Y. Noguchi[83], M. Nomachi[129], I. Nomidis[132], M.A. Nomura[29], T. Nooney[90], M. Nordberg[35],
N. Norjoharuddeen[131], T. Novak[89], O. Novgorodova[46], R. Novotny[138], L. Nozka[126], K. Ntekas[168],
E. Nurse[92], F. Nuti[102], F.G. Oakham[33,as], H. Oberlack[113], T. Obermann[24], J. Ocariz[132], A. Ochi[80],
I. Ochoa[38], J.P. Ochoa-Ricoux[144a], K. O'Connor[26], S. Oda[85], S. Odaka[79], S. Oerdek[51], A. Oh[98],
S.H. Oh[47], C.C. Ohm[151], H. Oide[53b,53a], H. Okawa[166], Y. Okazaki[83], Y. Okumura[160], T. Okuyama[79],
A. Olariu[27b], L.F. Oleiro Seabra[136a], S.A. Olivares Pino[144a], D. Oliveira Damazio[29], J.L. Oliver[1],
M.J.R. Olsson[36], A. Olszewski[82], J. Olszowska[82], D.C. O'Neil[149], A. Onofre[136a,136e], K. Onogi[115],
P.U.E. Onyisi[11], H. Oppen[130], M.J. Oreglia[36], Y. Oren[158], D. Orestano[72a,72b], E.C. Orgill[98],
N. Orlando[61b], A.A. O'Rourke[44], R.S. Orr[164], B. Osculati[53b,53a,*], V. O'Shea[55], R. Ospanov[58a],
G. Otero y Garzon[30], H. Otono[85], M. Ouchrif[34d], F. Ould-Saada[130], A. Ouraou[142], Q. Ouyang[15a],
M. Owen[55], R.E. Owen[21], V.E. Ozcan[12c], N. Ozturk[8], J. Pacalt[126], H.A. Pacey[31], K. Pachal[149],
A. Pacheco Pages[14], L. Pacheco Rodriguez[142], C. Padilla Aranda[14], S. Pagan Griso[18], M. Paganini[180],
G. Palacino[63], S. Palazzo[40b,40a], S. Palestini[35], M. Palka[81b], D. Pallin[37], I. Panagoulias[10], C.E. Pandini[35],
J.G. Panduro Vazquez[91], P. Pani[35], G. Panizzo[64a,64c], L. Paolozzi[52], T.D. Papadopoulou[10],
K. Papageorgiou[9,i], A. Paramonov[6], D. Paredes Hernandez[61b], S.R. Paredes Saenz[131], B. Parida[58c],
A.J. Parker[87], K.A. Parker[44], M.A. Parker[31], F. Parodi[53b,53a], J.A. Parsons[38], U. Parzefall[50],
V.R. Pascuzzi[164], J.M.P. Pasner[143], E. Pasqualucci[70a], S. Passaggio[53b], F. Pastore[91], P. Pasuwan[43a,43b],
S. Pataraia[97], J.R. Pater[98], A. Pathak[178,j], T. Pauly[35], B. Pearson[113], M. Pedersen[130], L. Pedraza Diaz[117],
R. Pedro[136a,136b], S.V. Peleganchuk[120b,120a], O. Penc[137], C. Peng[15d], H. Peng[58a], B.S. Peralva[78a],
M.M. Perego[142], A.P. Pereira Peixoto[136a], D.V. Perepelitsa[29], F. Peri[19], L. Perini[66a,66b], H. Pernegger[35],
S. Perrella[67a,67b], V.D. Peshekhonov[77,*], K. Peters[44], R.F.Y. Peters[98], B.A. Petersen[35], T.C. Petersen[39],
E. Petit[56], A. Petridis[1], C. Petridou[159], P. Petroff[128], E. Petrolo[70a], M. Petrov[131], F. Petrucci[72a,72b],
M. Pettee[180], N.E. Pettersson[100], A. Peyaud[142], R. Pezoa[144b], T. Pham[102], F.H. Phillips[104],
P.W. Phillips[141], G. Piacquadio[152], E. Pianori[18], A. Picazio[100], M.A. Pickering[131], R. Piegaia[30],
J.E. Pilcher[36], A.D. Pilkington[98], M. Pinamonti[71a,71b], J.L. Pinfold[3], M. Pitt[177], M-A. Pleier[29],

V. Pleskot[139], E. Plotnikova[77], D. Pluth[76], P. Podberezko[120b,120a], R. Poettgen[94], R. Poggi[52],
L. Poggioli[128], I. Pogrebnyak[104], D. Pohl[24], I. Pokharel[51], G. Polesello[68a], A. Poley[44],
A. Policicchio[40b,40a], R. Polifka[35], A. Polini[23b], C.S. Pollard[44], V. Polychronakos[29], D. Ponomarenko[110],
L. Pontecorvo[70a], G.A. Popeneciu[27d], D.M. Portillo Quintero[132], S. Pospisil[138], K. Potamianos[44],
I.N. Potrap[77], C.J. Potter[31], H. Potti[11], T. Poulsen[94], J. Poveda[35], T.D. Powell[146],
M.E. Pozo Astigarraga[35], P. Pralavorio[99], S. Prell[76], D. Price[98], M. Primavera[65a], S. Prince[101],
N. Proklova[110], K. Prokofiev[61c], F. Prokoshin[144b], S. Protopopescu[29], J. Proudfoot[6], M. Przybycien[81a],
A. Puri[170], P. Puzo[128], J. Qian[103], Y. Qin[98], A. Quadt[51], M. Queitsch-Maitland[44], A. Qureshi[1],
P. Rados[102], F. Ragusa[66a,66b], G. Rahal[95], J.A. Raine[98], S. Rajagopalan[29], A. Ramirez Morales[90],
T. Rashid[128], S. Raspopov[5], M.G. Ratti[66a,66b], D.M. Rauch[44], F. Rauscher[112], S. Rave[97], B. Ravina[146],
I. Ravinovich[177], J.H. Rawling[98], M. Raymond[35], A.L. Read[130], N.P. Readioff[56], M. Reale[65a,65b],
D.M. Rebuzzi[68a,68b], A. Redelbach[174], G. Redlinger[29], R. Reece[143], R.G. Reed[32c], K. Reeves[42],
L. Rehnisch[19], J. Reichert[133], A. Reiss[97], C. Rembser[35], H. Ren[15d], M. Rescigno[70a], S. Resconi[66a],
E.D. Resseguie[133], S. Rettie[172], E. Reynolds[21], O.L. Rezanova[120b,120a], P. Reznicek[139], R. Richter[113],
S. Richter[92], E. Richter-Was[81b], O. Ricken[24], M. Ridel[132], P. Rieck[113], C.J. Riegel[179], O. Rifki[44],
M. Rijssenbeek[152], A. Rimoldi[68a,68b], M. Rimoldi[20], L. Rinaldi[23b], G. Ripellino[151], B. Ristić[87],
E. Ritsch[35], I. Riu[14], J.C. Rivera Vergara[144a], F. Rizatdinova[125], E. Rizvi[90], C. Rizzi[14], R.T. Roberts[98],
S.H. Robertson[101,ac], A. Robichaud-Veronneau[101], D. Robinson[31], J.E.M. Robinson[44], A. Robson[55],
E. Rocco[97], C. Roda[69a,69b], Y. Rodina[99], S. Rodriguez Bosca[171], A. Rodriguez Perez[14],
D. Rodriguez Rodriguez[171], A.M. Rodríguez Vera[165b], S. Roe[35], C.S. Rogan[57], O. Røhne[130],
R. Röhrig[113], C.P.A. Roland[63], J. Roloff[57], A. Romaniouk[110], M. Romano[23b,23a], N. Rompotis[88],
M. Ronzani[121], L. Roos[132], S. Rosati[70a], K. Rosbach[50], P. Rose[143], N-A. Rosien[51], E. Rossi[67a,67b],
L.P. Rossi[53b], L. Rossini[66a,66b], J.H.N. Rosten[31], R. Rosten[14], M. Rotaru[27b], J. Rothberg[145],
D. Rousseau[128], D. Roy[32c], A. Rozanov[99], Y. Rozen[157], X. Ruan[32c], F. Rubbo[150], F. Rühr[50],
A. Ruiz-Martinez[171], Z. Rurikova[50], N.A. Rusakovich[77], H.L. Russell[101], J.P. Rutherfoord[7],
E.M. Rüttinger[44,k], Y.F. Ryabov[134], M. Rybar[170], G. Rybkin[128], S. Ryu[6], A. Ryzhov[140], G.F. Rzehorz[51],
P. Sabatini[51], G. Sabato[118], S. Sacerdoti[128], H.F-W. Sadrozinski[143], R. Sadykov[77], F. Safai Tehrani[70a],
P. Saha[119], M. Sahinsoy[59a], A. Sahu[179], M. Saimpert[44], M. Saito[160], T. Saito[160], H. Sakamoto[160],
A. Sakharov[121,aj], D. Salamani[52], G. Salamanna[72a,72b], J.E. Salazar Loyola[144b], D. Salek[118],
P.H. Sales De Bruin[169], D. Salihagic[113], A. Salnikov[150], J. Salt[171], D. Salvatore[40b,40a], F. Salvatore[153],
A. Salvucci[61a,61b,61c], A. Salzburger[35], J. Samarati[35], D. Sammel[50], D. Sampsonidis[159],
D. Sampsonidou[159], J. Sánchez[171], A. Sanchez Pineda[64a,64c], H. Sandaker[130], C.O. Sander[44],
M. Sandhoff[179], C. Sandoval[22], D.P.C. Sankey[141], M. Sannino[53b,53a], Y. Sano[115], A. Sansoni[49],
C. Santoni[37], H. Santos[136a], I. Santoyo Castillo[153], A. Sapronov[77], J.G. Saraiva[136a,136d], O. Sasaki[79],
K. Sato[166], E. Sauvan[5], P. Savard[164,as], N. Savic[113], R. Sawada[160], C. Sawyer[141], L. Sawyer[93,ai],
C. Sbarra[23b], A. Sbrizzi[23b,23a], T. Scanlon[92], J. Schaarschmidt[145], P. Schacht[113], B.M. Schachtner[112],
D. Schaefer[36], L. Schaefer[133], J. Schaeffer[97], S. Schaepe[35], U. Schäfer[97], A.C. Schaffer[128], D. Schaile[112],
R.D. Schamberger[152], N. Scharmberg[98], V.A. Schegelsky[134], D. Scheirich[139], F. Schenck[19],
M. Schernau[168], C. Schiavi[53b,53a], S. Schier[143], L.K. Schildgen[24], Z.M. Schillaci[26], E.J. Schioppa[35],
M. Schioppa[40b,40a], K.E. Schleicher[50], S. Schlenker[35], K.R. Schmidt-Sommerfeld[113], K. Schmieden[35],
C. Schmitt[97], S. Schmitt[44], S. Schmitz[97], U. Schnoor[50], L. Schoeffel[142], A. Schoening[59b], E. Schopf[24],
M. Schott[97], J.F.P. Schouwenberg[117], J. Schovancova[35], S. Schramm[52], A. Schulte[97],
H-C. Schultz-Coulon[59a], M. Schumacher[50], B.A. Schumm[143], Ph. Schune[142], A. Schwartzman[150],
T.A. Schwarz[103], H. Schweiger[98], Ph. Schwemling[142], R. Schwienhorst[104], A. Sciandra[24], G. Sciolla[26],
M. Scornajenghi[40b,40a], F. Scuri[69a], F. Scutti[102], L.M. Scyboz[113], J. Searcy[103], C.D. Sebastiani[70a,70b],
P. Seema[24], S.C. Seidel[116], A. Seiden[143], T. Seiss[36], J.M. Seixas[78b], G. Sekhniaidze[67a], K. Sekhon[103],
S.J. Sekula[41], N. Semprini-Cesari[23b,23a], S. Sen[47], S. Senkin[37], C. Serfon[130], L. Serin[128], L. Serkin[64a,64b],

47

M. Sessa[72a,72b], H. Severini[124], F. Sforza[167], A. Sfyrla[52], E. Shabalina[51], J.D. Shahinian[143],
N.W. Shaikh[43a,43b], L.Y. Shan[15a], R. Shang[170], J.T. Shank[25], M. Shapiro[18], A.S. Sharma[1], A. Sharma[131],
P.B. Shatalov[109], K. Shaw[153], S.M. Shaw[98], A. Shcherbakova[134], Y. Shen[124], N. Sherafati[33],
A.D. Sherman[25], P. Sherwood[92], L. Shi[155,ao], S. Shimizu[80], C.O. Shimmin[180], M. Shimojima[114],
I.P.J. Shipsey[131], S. Shirabe[85], M. Shiyakova[77], J. Shlomi[177], A. Shmeleva[108], D. Shoaleh Saadi[107],
M.J. Shochet[36], S. Shojaii[102], D.R. Shope[124], S. Shrestha[122], E. Shulga[110], P. Sicho[137], A.M. Sickles[170],
P.E. Sidebo[151], E. Sideras Haddad[32c], O. Sidiropoulou[174], A. Sidoti[23b,23a], F. Siegert[46], Dj. Sijacki[16],
J. Silva[136a], M. Silva Jr.[178], M.V. Silva Oliveira[78a], S.B. Silverstein[43a], L. Simic[77], S. Simion[128],
E. Simioni[97], M. Simon[97], R. Simoniello[97], P. Sinervo[164], N.B. Sinev[127], M. Sioli[23b,23a], G. Siragusa[174],
I. Siral[103], S.Yu. Sivoklokov[111], J. Sjölin[43a,43b], M.B. Skinner[87], P. Skubic[124], M. Slater[21], T. Slavicek[138],
M. Slawinska[82], K. Sliwa[167], R. Slovak[139], V. Smakhtin[177], B.H. Smart[5], J. Smiesko[28a], N. Smirnov[110],
S.Yu. Smirnov[110], Y. Smirnov[110], L.N. Smirnova[111], O. Smirnova[94], J.W. Smith[51], M.N.K. Smith[38],
R.W. Smith[38], M. Smizanska[87], K. Smolek[138], A.A. Snesarev[108], I.M. Snyder[127], S. Snyder[29],
R. Sobie[173,ac], A.M. Soffa[168], A. Soffer[158], A. Søgaard[48], D.A. Soh[155], G. Sokhrannyi[89],
C.A. Solans Sanchez[35], M. Solar[138], E.Yu. Soldatov[110], U. Soldevila[171], A.A. Solodkov[140],
A. Soloshenko[77], O.V. Solovyanov[140], V. Solovyev[134], P. Sommer[146], H. Son[167], W. Song[141],
A. Sopczak[138], F. Sopkova[28b], D. Sosa[59b], C.L. Sotiropoulou[69a,69b], S. Sottocornola[68a,68b],
R. Soualah[64a,64c,h], A.M. Soukharev[120b,120a], D. South[44], B.C. Sowden[91], S. Spagnolo[65a,65b],
M. Spalla[113], M. Spangenberg[175], F. Spanò[91], D. Sperlich[19], F. Spettel[113], T.M. Spieker[59a], R. Spighi[23b],
G. Spigo[35], L.A. Spiller[102], D.P. Spiteri[55], M. Spousta[139], A. Stabile[66a,66b], R. Stamen[59a], S. Stamm[19],
E. Stanecka[82], R.W. Stanek[6], C. Stanescu[72a], B. Stanislaus[131], M.M. Stanitzki[44], B. Stapf[118],
S. Stapnes[130], E.A. Starchenko[140], G.H. Stark[36], J. Stark[56], S.H Stark[39], P. Staroba[137], P. Starovoitov[59a],
S. Stärz[35], R. Staszewski[82], M. Stegler[44], P. Steinberg[29], B. Stelzer[149], H.J. Stelzer[35],
O. Stelzer-Chilton[165a], H. Stenzel[54], T.J. Stevenson[90], G.A. Stewart[55], M.C. Stockton[127], G. Stoicea[27b],
P. Stolte[51], S. Stonjek[113], A. Straessner[46], J. Strandberg[151], S. Strandberg[43a,43b], M. Strauss[124],
P. Strizenec[28b], R. Ströhmer[174], D.M. Strom[127], R. Stroynowski[41], A. Strubig[48], S.A. Stucci[29],
B. Stugu[17], J. Stupak[124], N.A. Styles[44], D. Su[150], J. Su[135], S. Suchek[59a], Y. Sugaya[129], M. Suk[138],
V.V. Sulin[108], D.M.S. Sultan[52], S. Sultansoy[4c], T. Sumida[83], S. Sun[103], X. Sun[3], K. Suruliz[153],
C.J.E. Suster[154], M.R. Sutton[153], S. Suzuki[79], M. Svatos[137], M. Swiatlowski[36], S.P. Swift[2],
A. Sydorenko[97], I. Sykora[28a], T. Sykora[139], D. Ta[97], K. Tackmann[44,z], J. Taenzer[158], A. Taffard[168],
R. Tafirout[165a], E. Tahirovic[90], N. Taiblum[158], H. Takai[29], R. Takashima[84], E.H. Takasugi[113],
K. Takeda[80], T. Takeshita[147], Y. Takubo[79], M. Talby[99], A.A. Talyshev[120b,120a], J. Tanaka[160],
M. Tanaka[162], R. Tanaka[128], R. Tanioka[80], B.B. Tannenwald[122], S. Tapia Araya[144b], S. Tapprogge[97],
A. Tarek Abouelfadl Mohamed[132], S. Tarem[157], G. Tarna[27b,d], G.F. Tartarelli[66a], P. Tas[139],
M. Tasevsky[137], T. Tashiro[83], E. Tassi[40b,40a], A. Tavares Delgado[136a,136b], Y. Tayalati[34e], A.C. Taylor[116],
A.J. Taylor[48], G.N. Taylor[102], P.T.E. Taylor[102], W. Taylor[165b], A.S. Tee[87], P. Teixeira-Dias[91],
H. Ten Kate[35], P.K. Teng[155], J.J. Teoh[118], F. Tepel[179], S. Terada[79], K. Terashi[160], J. Terron[96], S. Terzo[14],
M. Testa[49], R.J. Teuscher[164,ac], S.J. Thais[180], T. Theveneaux-Pelzer[44], F. Thiele[39], J.P. Thomas[21],
A.S. Thompson[55], P.D. Thompson[21], L.A. Thomsen[180], E. Thomson[133], Y. Tian[38], R.E. Ticse Torres[51],
V.O. Tikhomirov[108,al], Yu.A. Tikhonov[120b,120a], S. Timoshenko[110], P. Tipton[180], S. Tisserant[99],
K. Todome[162], S. Todorova-Nova[5], S. Todt[46], J. Tojo[85], S. Tokár[28a], K. Tokushuku[79], E. Tolley[122],
K.G. Tomiwa[32c], M. Tomoto[115], L. Tompkins[150], K. Toms[116], B. Tong[57], P. Tornambe[50], E. Torrence[127],
H. Torres[46], E. Torró Pastor[145], C. Tosciri[131], J. Toth[99,ab], F. Touchard[99], D.R. Tovey[146], C.J. Treado[121],
T. Trefzger[174], F. Tresoldi[153], A. Tricoli[29], I.M. Trigger[165a], S. Trincaz-Duvoid[132], M.F. Tripiana[14],
W. Trischuk[164], B. Trocmé[56], A. Trofymov[128], C. Troncon[66a], M. Trovatelli[173], F. Trovato[153],
L. Truong[32b], M. Trzebinski[82], A. Trzupek[82], F. Tsai[44], J.C-L. Tseng[131], P.V. Tsiareshka[105],
N. Tsirintanis[9], V. Tsiskaridze[152], E.G. Tskhadadze[156a], I.I. Tsukerman[109], V. Tsulaia[18], S. Tsuno[79],

D. Tsybychev[152], Y. Tu[61b], A. Tudorache[27b], V. Tudorache[27b], T.T. Tulbure[27a], A.N. Tuna[57],
S. Turchikhin[77], D. Turgeman[177], I. Turk Cakir[4b,t], R. Turra[66a], P.M. Tuts[38], E. Tzovara[97],
G. Ucchielli[23b,23a], I. Ueda[79], M. Ughetto[43a,43b], F. Ukegawa[166], G. Unal[35], A. Undrus[29], G. Unel[168],
F.C. Ungaro[102], Y. Unno[79], K. Uno[160], J. Urban[28b], P. Urquijo[102], P. Urrejola[97], G. Usai[8], J. Usui[79],
L. Vacavant[99], V. Vacek[138], B. Vachon[101], K.O.H. Vadla[130], A. Vaidya[92], C. Valderanis[112],
E. Valdes Santurio[43a,43b], M. Valente[52], S. Valentinetti[23b,23a], A. Valero[171], L. Valéry[44], R.A. Vallance[21],
A. Vallier[5], J.A. Valls Ferrer[171], T.R. Van Daalen[14], W. Van Den Wollenberg[118], H. Van der Graaf[118],
P. Van Gemmeren[6], J. Van Nieuwkoop[149], I. Van Vulpen[118], M. Vanadia[71a,71b], W. Vandelli[35],
A. Vaniachine[163], P. Vankov[118], R. Vari[70a], E.W. Varnes[7], C. Varni[53b,53a], T. Varol[41], D. Varouchas[128],
K.E. Varvell[154], G.A. Vasquez[144b], J.G. Vasquez[180], F. Vazeille[37], D. Vazquez Furelos[14],
T. Vazquez Schroeder[101], J. Veatch[51], V. Vecchio[72a,72b], L.M. Veloce[164], F. Veloso[136a,136c],
S. Veneziano[70a], A. Ventura[65a,65b], M. Venturi[173], N. Venturi[35], V. Vercesi[68a], M. Verducci[72a,72b],
C.M. Vergel Infante[76], W. Verkerke[118], A.T. Vermeulen[118], J.C. Vermeulen[118], M.C. Vetterli[149,as],
N. Viaux Maira[144b], M. Vicente Barreto Pinto[52], I. Vichou[170,*], T. Vickey[146], O.E. Vickey Boeriu[146],
G.H.A. Viehhauser[131], S. Viel[18], L. Vigani[131], M. Villa[23b,23a], M. Villaplana Perez[66a,66b], E. Vilucchi[49],
M.G. Vincter[33], V.B. Vinogradov[77], A. Vishwakarma[44], C. Vittori[23b,23a], I. Vivarelli[153], S. Vlachos[10],
M. Vogel[179], P. Vokac[138], G. Volpi[14], S.E. von Buddenbrock[32c], E. Von Toerne[24], V. Vorobel[139],
K. Vorobev[110], M. Vos[171], J.H. Vossebeld[88], N. Vranjes[16], M. Vranjes Milosavljevic[16], V. Vrba[138],
M. Vreeswijk[118], T. Šfiligoj[89], R. Vuillermet[35], I. Vukotic[36], T. Ženiš[28a], L. Živković[16], P. Wagner[24],
W. Wagner[179], J. Wagner-Kuhr[112], H. Wahlberg[86], S. Wahrmund[46], K. Wakamiya[80], V.M. Walbrecht[113],
J. Walder[87], R. Walker[112], W. Walkowiak[148], V. Wallangen[43a,43b], A.M. Wang[57], C. Wang[58b,d],
F. Wang[178], H. Wang[18], H. Wang[3], J. Wang[154], J. Wang[59b], P. Wang[41], Q. Wang[124], R.-J. Wang[132],
R. Wang[58a], R. Wang[6], S.M. Wang[155], W.T. Wang[58a], W. Wang[155,o], W.X. Wang[58a,ad], Y. Wang[58a],
Z. Wang[58c], C. Wanotayaroj[44], A. Warburton[101], C.P. Ward[31], D.R. Wardrope[92], A. Washbrook[48],
P.M. Watkins[21], A.T. Watson[21], M.F. Watson[21], G. Watts[145], S. Watts[98], B.M. Waugh[92], A.F. Webb[11],
S. Webb[97], C. Weber[180], M.S. Weber[20], S.A. Weber[33], S.M. Weber[59a], J.S. Webster[6], A.R. Weidberg[131],
B. Weinert[63], J. Weingarten[51], M. Weirich[97], C. Weiser[50], P.S. Wells[35], T. Wenaus[29], T. Wengler[35],
S. Wenig[35], N. Wermes[24], M.D. Werner[76], P. Werner[35], M. Wessels[59a], T.D. Weston[20], K. Whalen[127],
N.L. Whallon[145], A.M. Wharton[87], A.S. White[103], A. White[8], M.J. White[1], R. White[144b],
D. Whiteson[168], B.W. Whitmore[87], F.J. Wickens[141], W. Wiedenmann[178], M. Wielers[141],
C. Wiglesworth[39], L.A.M. Wiik-Fuchs[50], A. Wildauer[113], F. Wilk[98], H.G. Wilkens[35], L.J. Wilkins[91],
H.H. Williams[133], S. Williams[31], C. Willis[104], S. Willocq[100], J.A. Wilson[21], I. Wingerter-Seez[5],
E. Winkels[153], F. Winklmeier[127], O.J. Winston[153], B.T. Winter[24], M. Wittgen[150], M. Wobisch[93],
A. Wolf[97], T.M.H. Wolf[118], R. Wolff[99], M.W. Wolter[82], H. Wolters[136a,136c], V.W.S. Wong[172],
N.L. Woods[143], S.D. Worm[21], B.K. Wosiek[82], K.W. Woźniak[82], K. Wraight[55], M. Wu[36], S.L. Wu[178],
X. Wu[52], Y. Wu[58a], T.R. Wyatt[98], B.M. Wynne[48], S. Xella[39], Z. Xi[103], L. Xia[175], D. Xu[15a], H. Xu[58a],
L. Xu[29], T. Xu[142], W. Xu[103], B. Yabsley[154], S. Yacoob[32a], K. Yajima[129], D.P. Yallup[92], D. Yamaguchi[162],
Y. Yamaguchi[162], A. Yamamoto[79], T. Yamanaka[160], F. Yamane[80], M. Yamatani[160], T. Yamazaki[160],
Y. Yamazaki[80], Z. Yan[25], H.J. Yang[58c,58d], H.T. Yang[18], S. Yang[75], Y. Yang[160], Z. Yang[17], W-M. Yao[18],
Y.C. Yap[44], Y. Yasu[79], E. Yatsenko[58c,58d], J. Ye[41], S. Ye[29], I. Yeletskikh[77], E. Yigitbasi[25], E. Yildirim[97],
K. Yorita[176], K. Yoshihara[133], C.J.S. Young[35], C. Young[150], J. Yu[8], J. Yu[76], X. Yue[59a], S.P.Y. Yuen[24],
B. Zabinski[82], G. Zacharis[10], E. Zaffaroni[52], R. Zaidan[14], A.M. Zaitsev[140,ak], N. Zakharchuk[44],
J. Zalieckas[17], S. Zambito[57], D. Zanzi[35], D.R. Zaripovas[55], S.V. Zeißner[45], C. Zeitnitz[179],
G. Zemaityte[131], J.C. Zeng[170], Q. Zeng[150], O. Zenin[140], D. Zerwas[128], M. Zgubič[131], D.F. Zhang[58b],
D. Zhang[103], F. Zhang[178], G. Zhang[58a], H. Zhang[15c], J. Zhang[6], L. Zhang[15c], L. Zhang[58a], M. Zhang[170],
P. Zhang[15c], R. Zhang[58a], R. Zhang[24], X. Zhang[58b], Y. Zhang[15d], Z. Zhang[128], X. Zhao[41],
Y. Zhao[58b,128,ah], Z. Zhao[58a], A. Zhemchugov[77], B. Zhou[103], C. Zhou[178], L. Zhou[41], M.S. Zhou[15d],

M. Zhou[152], N. Zhou[58c], Y. Zhou[7], C.G. Zhu[58b], H.L. Zhu[58a], H. Zhu[15a], J. Zhu[103], Y. Zhu[58a], X. Zhuang[15a], K. Zhukov[108], V. Zhulanov[120b,120a], A. Zibell[174], D. Zieminska[63], N.I. Zimine[77], S. Zimmermann[50], Z. Zinonos[113], M. Zinser[97], M. Ziolkowski[148], G. Zobernig[178], A. Zoccoli[23b,23a], K. Zoch[51], T.G. Zorbas[146], R. Zou[36], M. Zur Nedden[19], L. Zwalinski[35].

[1]Department of Physics, University of Adelaide, Adelaide; Australia.

[2]Physics Department, SUNY Albany, Albany NY; United States of America.

[3]Department of Physics, University of Alberta, Edmonton AB; Canada.

[4][(a)]Department of Physics, Ankara University, Ankara;[(b)]Istanbul Aydin University, Istanbul;[(c)]Division of Physics, TOBB University of Economics and Technology, Ankara; Turkey.

[5]LAPP, Université Grenoble Alpes, Université Savoie Mont Blanc, CNRS/IN2P3, Annecy; France.

[6]High Energy Physics Division, Argonne National Laboratory, Argonne IL; United States of America.

[7]Department of Physics, University of Arizona, Tucson AZ; United States of America.

[8]Department of Physics, University of Texas at Arlington, Arlington TX; United States of America.

[9]Physics Department, National and Kapodistrian University of Athens, Athens; Greece.

[10]Physics Department, National Technical University of Athens, Zografou; Greece.

[11]Department of Physics, University of Texas at Austin, Austin TX; United States of America.

[12][(a)]Bahcesehir University, Faculty of Engineering and Natural Sciences, Istanbul;[(b)]Istanbul Bilgi University, Faculty of Engineering and Natural Sciences, Istanbul;[(c)]Department of Physics, Bogazici University, Istanbul;[(d)]Department of Physics Engineering, Gaziantep University, Gaziantep; Turkey.

[13]Institute of Physics, Azerbaijan Academy of Sciences, Baku; Azerbaijan.

[14]Institut de Física d'Altes Energies (IFAE), Barcelona Institute of Science and Technology, Barcelona; Spain.

[15][(a)]Institute of High Energy Physics, Chinese Academy of Sciences, Beijing;[(b)]Physics Department, Tsinghua University, Beijing;[(c)]Department of Physics, Nanjing University, Nanjing;[(d)]University of Chinese Academy of Science (UCAS), Beijing; China.

[16]Institute of Physics, University of Belgrade, Belgrade; Serbia.

[17]Department for Physics and Technology, University of Bergen, Bergen; Norway.

[18]Physics Division, Lawrence Berkeley National Laboratory and University of California, Berkeley CA; United States of America.

[19]Institut für Physik, Humboldt Universität zu Berlin, Berlin; Germany.

[20]Albert Einstein Center for Fundamental Physics and Laboratory for High Energy Physics, University of Bern, Bern; Switzerland.

[21]School of Physics and Astronomy, University of Birmingham, Birmingham; United Kingdom.

[22]Centro de Investigaciónes, Universidad Antonio Nariño, Bogota; Colombia.

[23][(a)]Dipartimento di Fisica e Astronomia, Università di Bologna, Bologna;[(b)]INFN Sezione di Bologna; Italy.

[24]Physikalisches Institut, Universität Bonn, Bonn; Germany.

[25]Department of Physics, Boston University, Boston MA; United States of America.

[26]Department of Physics, Brandeis University, Waltham MA; United States of America.

[27][(a)]Transilvania University of Brasov, Brasov;[(b)]Horia Hulubei National Institute of Physics and Nuclear Engineering, Bucharest;[(c)]Department of Physics, Alexandru Ioan Cuza University of Iasi, Iasi;[(d)]National Institute for Research and Development of Isotopic and Molecular Technologies, Physics Department, Cluj-Napoca;[(e)]University Politehnica Bucharest, Bucharest;[(f)]West University in Timisoara, Timisoara; Romania.

[28][(a)]Faculty of Mathematics, Physics and Informatics, Comenius University, Bratislava;[(b)]Department of Subnuclear Physics, Institute of Experimental Physics of the Slovak Academy of Sciences, Kosice;

Slovak Republic.

[29]Physics Department, Brookhaven National Laboratory, Upton NY; United States of America.

[30]Departamento de Física, Universidad de Buenos Aires, Buenos Aires; Argentina.

[31]Cavendish Laboratory, University of Cambridge, Cambridge; United Kingdom.

[32][a]Department of Physics, University of Cape Town, Cape Town;[b]Department of Mechanical Engineering Science, University of Johannesburg, Johannesburg;[c]School of Physics, University of the Witwatersrand, Johannesburg; South Africa.

[33]Department of Physics, Carleton University, Ottawa ON; Canada.

[34][a]Faculté des Sciences Ain Chock, Réseau Universitaire de Physique des Hautes Energies - Université Hassan II, Casablanca;[b]Centre National de l'Energie des Sciences Techniques Nucleaires (CNESTEN), Rabat;[c]Faculté des Sciences Semlalia, Université Cadi Ayyad, LPHEA-Marrakech;[d]Faculté des Sciences, Université Mohamed Premier and LPTPM, Oujda;[e]Faculté des sciences, Université Mohammed V, Rabat; Morocco.

[35]CERN, Geneva; Switzerland.

[36]Enrico Fermi Institute, University of Chicago, Chicago IL; United States of America.

[37]LPC, Université Clermont Auvergne, CNRS/IN2P3, Clermont-Ferrand; France.

[38]Nevis Laboratory, Columbia University, Irvington NY; United States of America.

[39]Niels Bohr Institute, University of Copenhagen, Copenhagen; Denmark.

[40][a]Dipartimento di Fisica, Università della Calabria, Rende;[b]INFN Gruppo Collegato di Cosenza, Laboratori Nazionali di Frascati; Italy.

[41]Physics Department, Southern Methodist University, Dallas TX; United States of America.

[42]Physics Department, University of Texas at Dallas, Richardson TX; United States of America.

[43][a]Department of Physics, Stockholm University;[b]Oskar Klein Centre, Stockholm; Sweden.

[44]Deutsches Elektronen-Synchrotron DESY, Hamburg and Zeuthen; Germany.

[45]Lehrstuhl für Experimentelle Physik IV, Technische Universität Dortmund, Dortmund; Germany.

[46]Institut für Kern- und Teilchenphysik, Technische Universität Dresden, Dresden; Germany.

[47]Department of Physics, Duke University, Durham NC; United States of America.

[48]SUPA - School of Physics and Astronomy, University of Edinburgh, Edinburgh; United Kingdom.

[49]INFN e Laboratori Nazionali di Frascati, Frascati; Italy.

[50]Physikalisches Institut, Albert-Ludwigs-Universität Freiburg, Freiburg; Germany.

[51]II. Physikalisches Institut, Georg-August-Universität Göttingen, Göttingen; Germany.

[52]Département de Physique Nucléaire et Corpusculaire, Université de Genève, Genève; Switzerland.

[53][a]Dipartimento di Fisica, Università di Genova, Genova;[b]INFN Sezione di Genova; Italy.

[54]II. Physikalisches Institut, Justus-Liebig-Universität Giessen, Giessen; Germany.

[55]SUPA - School of Physics and Astronomy, University of Glasgow, Glasgow; United Kingdom.

[56]LPSC, Université Grenoble Alpes, CNRS/IN2P3, Grenoble INP, Grenoble; France.

[57]Laboratory for Particle Physics and Cosmology, Harvard University, Cambridge MA; United States of America.

[58][a]Department of Modern Physics and State Key Laboratory of Particle Detection and Electronics, University of Science and Technology of China, Hefei;[b]Institute of Frontier and Interdisciplinary Science and Key Laboratory of Particle Physics and Particle Irradiation (MOE), Shandong University, Qingdao;[c]School of Physics and Astronomy, Shanghai Jiao Tong University, KLPPAC-MoE, SKLPPC, Shanghai;[d]Tsung-Dao Lee Institute, Shanghai; China.

[59][a]Kirchhoff-Institut für Physik, Ruprecht-Karls-Universität Heidelberg, Heidelberg;[b]Physikalisches Institut, Ruprecht-Karls-Universität Heidelberg, Heidelberg; Germany.

[60]Faculty of Applied Information Science, Hiroshima Institute of Technology, Hiroshima; Japan.

[61][a]Department of Physics, Chinese University of Hong Kong, Shatin, N.T., Hong Kong;[b]Department

of Physics, University of Hong Kong, Hong Kong;[(c)]Department of Physics and Institute for Advanced Study, Hong Kong University of Science and Technology, Clear Water Bay, Kowloon, Hong Kong; China.

[62]Department of Physics, National Tsing Hua University, Hsinchu; Taiwan.

[63]Department of Physics, Indiana University, Bloomington IN; United States of America.

[64(a)]INFN Gruppo Collegato di Udine, Sezione di Trieste, Udine;[(b)]ICTP, Trieste;[(c)]Dipartimento di Chimica, Fisica e Ambiente, Università di Udine, Udine; Italy.

[65(a)]INFN Sezione di Lecce;[(b)]Dipartimento di Matematica e Fisica, Università del Salento, Lecce; Italy.

[66(a)]INFN Sezione di Milano;[(b)]Dipartimento di Fisica, Università di Milano, Milano; Italy.

[67(a)]INFN Sezione di Napoli;[(b)]Dipartimento di Fisica, Università di Napoli, Napoli; Italy.

[68(a)]INFN Sezione di Pavia;[(b)]Dipartimento di Fisica, Università di Pavia, Pavia; Italy.

[69(a)]INFN Sezione di Pisa;[(b)]Dipartimento di Fisica E. Fermi, Università di Pisa, Pisa; Italy.

[70(a)]INFN Sezione di Roma;[(b)]Dipartimento di Fisica, Sapienza Università di Roma, Roma; Italy.

[71(a)]INFN Sezione di Roma Tor Vergata;[(b)]Dipartimento di Fisica, Università di Roma Tor Vergata, Roma; Italy.

[72(a)]INFN Sezione di Roma Tre;[(b)]Dipartimento di Matematica e Fisica, Università Roma Tre, Roma; Italy.

[73(a)]INFN-TIFPA;[(b)]Università degli Studi di Trento, Trento; Italy.

[74]Institut für Astro- und Teilchenphysik, Leopold-Franzens-Universität, Innsbruck; Austria.

[75]University of Iowa, Iowa City IA; United States of America.

[76]Department of Physics and Astronomy, Iowa State University, Ames IA; United States of America.

[77]Joint Institute for Nuclear Research, Dubna; Russia.

[78(a)]Departamento de Engenharia Elétrica, Universidade Federal de Juiz de Fora (UFJF), Juiz de Fora;[(b)]Universidade Federal do Rio De Janeiro COPPE/EE/IF, Rio de Janeiro;[(c)]Universidade Federal de São João del Rei (UFSJ), São João del Rei;[(d)]Instituto de Física, Universidade de São Paulo, São Paulo; Brazil.

[79]KEK, High Energy Accelerator Research Organization, Tsukuba; Japan.

[80]Graduate School of Science, Kobe University, Kobe; Japan.

[81(a)]AGH University of Science and Technology, Faculty of Physics and Applied Computer Science, Krakow;[(b)]Marian Smoluchowski Institute of Physics, Jagiellonian University, Krakow; Poland.

[82]Institute of Nuclear Physics Polish Academy of Sciences, Krakow; Poland.

[83]Faculty of Science, Kyoto University, Kyoto; Japan.

[84]Kyoto University of Education, Kyoto; Japan.

[85]Research Center for Advanced Particle Physics and Department of Physics, Kyushu University, Fukuoka ; Japan.

[86]Instituto de Física La Plata, Universidad Nacional de La Plata and CONICET, La Plata; Argentina.

[87]Physics Department, Lancaster University, Lancaster; United Kingdom.

[88]Oliver Lodge Laboratory, University of Liverpool, Liverpool; United Kingdom.

[89]Department of Experimental Particle Physics, Jožef Stefan Institute and Department of Physics, University of Ljubljana, Ljubljana; Slovenia.

[90]School of Physics and Astronomy, Queen Mary University of London, London; United Kingdom.

[91]Department of Physics, Royal Holloway University of London, Egham; United Kingdom.

[92]Department of Physics and Astronomy, University College London, London; United Kingdom.

[93]Louisiana Tech University, Ruston LA; United States of America.

[94]Fysiska institutionen, Lunds universitet, Lund; Sweden.

[95]Centre de Calcul de l'Institut National de Physique Nucléaire et de Physique des Particules (IN2P3), Villeurbanne; France.

[96]Departamento de Física Teorica C-15 and CIAFF, Universidad Autónoma de Madrid, Madrid; Spain.

[97]Institut für Physik, Universität Mainz, Mainz; Germany.

[98]School of Physics and Astronomy, University of Manchester, Manchester; United Kingdom.

[99]CPPM, Aix-Marseille Université, CNRS/IN2P3, Marseille; France.

[100]Department of Physics, University of Massachusetts, Amherst MA; United States of America.

[101]Department of Physics, McGill University, Montreal QC; Canada.

[102]School of Physics, University of Melbourne, Victoria; Australia.

[103]Department of Physics, University of Michigan, Ann Arbor MI; United States of America.

[104]Department of Physics and Astronomy, Michigan State University, East Lansing MI; United States of America.

[105]B.I. Stepanov Institute of Physics, National Academy of Sciences of Belarus, Minsk; Belarus.

[106]Research Institute for Nuclear Problems of Byelorussian State University, Minsk; Belarus.

[107]Group of Particle Physics, University of Montreal, Montreal QC; Canada.

[108]P.N. Lebedev Physical Institute of the Russian Academy of Sciences, Moscow; Russia.

[109]Institute for Theoretical and Experimental Physics (ITEP), Moscow; Russia.

[110]National Research Nuclear University MEPhI, Moscow; Russia.

[111]D.V. Skobeltsyn Institute of Nuclear Physics, M.V. Lomonosov Moscow State University, Moscow; Russia.

[112]Fakultät für Physik, Ludwig-Maximilians-Universität München, München; Germany.

[113]Max-Planck-Institut für Physik (Werner-Heisenberg-Institut), München; Germany.

[114]Nagasaki Institute of Applied Science, Nagasaki; Japan.

[115]Graduate School of Science and Kobayashi-Maskawa Institute, Nagoya University, Nagoya; Japan.

[116]Department of Physics and Astronomy, University of New Mexico, Albuquerque NM; United States of America.

[117]Institute for Mathematics, Astrophysics and Particle Physics, Radboud University Nijmegen/Nikhef, Nijmegen; Netherlands.

[118]Nikhef National Institute for Subatomic Physics and University of Amsterdam, Amsterdam; Netherlands.

[119]Department of Physics, Northern Illinois University, DeKalb IL; United States of America.

[120][(a)]Budker Institute of Nuclear Physics, SB RAS, Novosibirsk;[(b)]Novosibirsk State University Novosibirsk; Russia.

[121]Department of Physics, New York University, New York NY; United States of America.

[122]Ohio State University, Columbus OH; United States of America.

[123]Faculty of Science, Okayama University, Okayama; Japan.

[124]Homer L. Dodge Department of Physics and Astronomy, University of Oklahoma, Norman OK; United States of America.

[125]Department of Physics, Oklahoma State University, Stillwater OK; United States of America.

[126]Palacký University, RCPTM, Joint Laboratory of Optics, Olomouc; Czech Republic.

[127]Center for High Energy Physics, University of Oregon, Eugene OR; United States of America.

[128]LAL, Université Paris-Sud, CNRS/IN2P3, Université Paris-Saclay, Orsay; France.

[129]Graduate School of Science, Osaka University, Osaka; Japan.

[130]Department of Physics, University of Oslo, Oslo; Norway.

[131]Department of Physics, Oxford University, Oxford; United Kingdom.

[132]LPNHE, Sorbonne Université, Paris Diderot Sorbonne Paris Cité, CNRS/IN2P3, Paris; France.

[133]Department of Physics, University of Pennsylvania, Philadelphia PA; United States of America.

[134]Konstantinov Nuclear Physics Institute of National Research Centre "Kurchatov Institute", PNPI, St. Petersburg; Russia.

[135]Department of Physics and Astronomy, University of Pittsburgh, Pittsburgh PA; United States of America.

[136](a)Laboratório de Instrumentação e Física Experimental de Partículas - LIP;(b)Departamento de Física, Faculdade de Ciências, Universidade de Lisboa, Lisboa;(c)Departamento de Física, Universidade de Coimbra, Coimbra;(d)Centro de Física Nuclear da Universidade de Lisboa, Lisboa;(e)Departamento de Física, Universidade do Minho, Braga;(f)Departamento de Física Teorica y del Cosmos, Universidad de Granada, Granada (Spain);(g)Dep Física and CEFITEC of Faculdade de Ciências e Tecnologia, Universidade Nova de Lisboa, Caparica; Portugal.

[137]Institute of Physics, Academy of Sciences of the Czech Republic, Prague; Czech Republic.

[138]Czech Technical University in Prague, Prague; Czech Republic.

[139]Charles University, Faculty of Mathematics and Physics, Prague; Czech Republic.

[140]State Research Center Institute for High Energy Physics, NRC KI, Protvino; Russia.

[141]Particle Physics Department, Rutherford Appleton Laboratory, Didcot; United Kingdom.

[142]IRFU, CEA, Université Paris-Saclay, Gif-sur-Yvette; France.

[143]Santa Cruz Institute for Particle Physics, University of California Santa Cruz, Santa Cruz CA; United States of America.

[144](a)Departamento de Física, Pontificia Universidad Católica de Chile, Santiago;(b)Departamento de Física, Universidad Técnica Federico Santa María, Valparaíso; Chile.

[145]Department of Physics, University of Washington, Seattle WA; United States of America.

[146]Department of Physics and Astronomy, University of Sheffield, Sheffield; United Kingdom.

[147]Department of Physics, Shinshu University, Nagano; Japan.

[148]Department Physik, Universität Siegen, Siegen; Germany.

[149]Department of Physics, Simon Fraser University, Burnaby BC; Canada.

[150]SLAC National Accelerator Laboratory, Stanford CA; United States of America.

[151]Physics Department, Royal Institute of Technology, Stockholm; Sweden.

[152]Departments of Physics and Astronomy, Stony Brook University, Stony Brook NY; United States of America.

[153]Department of Physics and Astronomy, University of Sussex, Brighton; United Kingdom.

[154]School of Physics, University of Sydney, Sydney; Australia.

[155]Institute of Physics, Academia Sinica, Taipei; Taiwan.

[156](a)E. Andronikashvili Institute of Physics, Iv. Javakhishvili Tbilisi State University, Tbilisi;(b)High Energy Physics Institute, Tbilisi State University, Tbilisi; Georgia.

[157]Department of Physics, Technion, Israel Institute of Technology, Haifa; Israel.

[158]Raymond and Beverly Sackler School of Physics and Astronomy, Tel Aviv University, Tel Aviv; Israel.

[159]Department of Physics, Aristotle University of Thessaloniki, Thessaloniki; Greece.

[160]International Center for Elementary Particle Physics and Department of Physics, University of Tokyo, Tokyo; Japan.

[161]Graduate School of Science and Technology, Tokyo Metropolitan University, Tokyo; Japan.

[162]Department of Physics, Tokyo Institute of Technology, Tokyo; Japan.

[163]Tomsk State University, Tomsk; Russia.

[164]Department of Physics, University of Toronto, Toronto ON; Canada.

[165](a)TRIUMF, Vancouver BC;(b)Department of Physics and Astronomy, York University, Toronto ON; Canada.

[166]Division of Physics and Tomonaga Center for the History of the Universe, Faculty of Pure and Applied Sciences, University of Tsukuba, Tsukuba; Japan.

[167]Department of Physics and Astronomy, Tufts University, Medford MA; United States of America.

[168]Department of Physics and Astronomy, University of California Irvine, Irvine CA; United States of

America.

[169]Department of Physics and Astronomy, University of Uppsala, Uppsala; Sweden.

[170]Department of Physics, University of Illinois, Urbana IL; United States of America.

[171]Instituto de Física Corpuscular (IFIC), Centro Mixto Universidad de Valencia - CSIC, Valencia; Spain.

[172]Department of Physics, University of British Columbia, Vancouver BC; Canada.

[173]Department of Physics and Astronomy, University of Victoria, Victoria BC; Canada.

[174]Fakultät für Physik und Astronomie, Julius-Maximilians-Universität Würzburg, Würzburg; Germany.

[175]Department of Physics, University of Warwick, Coventry; United Kingdom.

[176]Waseda University, Tokyo; Japan.

[177]Department of Particle Physics, Weizmann Institute of Science, Rehovot; Israel.

[178]Department of Physics, University of Wisconsin, Madison WI; United States of America.

[179]Fakultät für Mathematik und Naturwissenschaften, Fachgruppe Physik, Bergische Universität Wuppertal, Wuppertal; Germany.

[180]Department of Physics, Yale University, New Haven CT; United States of America.

[181]Yerevan Physics Institute, Yerevan; Armenia.

[a] Also at Borough of Manhattan Community College, City University of New York, NY; United States of America.

[b] Also at Centre for High Performance Computing, CSIR Campus, Rosebank, Cape Town; South Africa.

[c] Also at CERN, Geneva; Switzerland.

[d] Also at CPPM, Aix-Marseille Université, CNRS/IN2P3, Marseille; France.

[e] Also at Département de Physique Nucléaire et Corpusculaire, Université de Genève, Genève; Switzerland.

[f] Also at Departament de Fisica de la Universitat Autonoma de Barcelona, Barcelona; Spain.

[g] Also at Departamento de Física Teorica y del Cosmos, Universidad de Granada, Granada (Spain); Spain.

[h] Also at Department of Applied Physics and Astronomy, University of Sharjah, Sharjah; United Arab Emirates.

[i] Also at Department of Financial and Management Engineering, University of the Aegean, Chios; Greece.

[j] Also at Department of Physics and Astronomy, University of Louisville, Louisville, KY; United States of America.

[k] Also at Department of Physics and Astronomy, University of Sheffield, Sheffield; United Kingdom.

[l] Also at Department of Physics, California State University, Fresno CA; United States of America.

[m] Also at Department of Physics, California State University, Sacramento CA; United States of America.

[n] Also at Department of Physics, King's College London, London; United Kingdom.

[o] Also at Department of Physics, Nanjing University, Nanjing; China.

[p] Also at Department of Physics, St. Petersburg State Polytechnical University, St. Petersburg; Russia.

[q] Also at Department of Physics, University of Fribourg, Fribourg; Switzerland.

[r] Also at Department of Physics, University of Michigan, Ann Arbor MI; United States of America.

[s] Also at Dipartimento di Fisica E. Fermi, Università di Pisa, Pisa; Italy.

[t] Also at Giresun University, Faculty of Engineering, Giresun; Turkey.

[u] Also at Graduate School of Science, Osaka University, Osaka; Japan.

[v] Also at Hellenic Open University, Patras; Greece.

[w] Also at Horia Hulubei National Institute of Physics and Nuclear Engineering, Bucharest; Romania.

[x] Also at II. Physikalisches Institut, Georg-August-Universität Göttingen, Göttingen; Germany.

[y] Also at Institucio Catalana de Recerca i Estudis Avancats, ICREA, Barcelona; Spain.

[z] Also at Institut für Experimentalphysik, Universität Hamburg, Hamburg; Germany.

^{aa} Also at Institute for Mathematics, Astrophysics and Particle Physics, Radboud University Nijmegen/Nikhef, Nijmegen; Netherlands.

^{ab} Also at Institute for Particle and Nuclear Physics, Wigner Research Centre for Physics, Budapest; Hungary.

^{ac} Also at Institute of Particle Physics (IPP); Canada.

^{ad} Also at Institute of Physics, Academia Sinica, Taipei; Taiwan.

^{ae} Also at Institute of Physics, Azerbaijan Academy of Sciences, Baku; Azerbaijan.

^{af} Also at Institute of Theoretical Physics, Ilia State University, Tbilisi; Georgia.

^{ag} Also at Istanbul University, Dept. of Physics, Istanbul; Turkey.

^{ah} Also at LAL, Université Paris-Sud, CNRS/IN2P3, Université Paris-Saclay, Orsay; France.

^{ai} Also at Louisiana Tech University, Ruston LA; United States of America.

^{aj} Also at Manhattan College, New York NY; United States of America.

^{ak} Also at Moscow Institute of Physics and Technology State University, Dolgoprudny; Russia.

^{al} Also at National Research Nuclear University MEPhI, Moscow; Russia.

^{am} Also at Near East University, Nicosia, North Cyprus, Mersin; Turkey.

^{an} Also at Physikalisches Institut, Albert-Ludwigs-Universität Freiburg, Freiburg; Germany.

^{ao} Also at School of Physics, Sun Yat-sen University, Guangzhou; China.

^{ap} Also at The City College of New York, New York NY; United States of America.

^{aq} Also at The Collaborative Innovation Center of Quantum Matter (CICQM), Beijing; China.

^{ar} Also at Tomsk State University, Tomsk, and Moscow Institute of Physics and Technology State University, Dolgoprudny; Russia.

^{as} Also at TRIUMF, Vancouver BC; Canada.

^{at} Also at Universita di Napoli Parthenope, Napoli; Italy.

* Deceased